

Assessment of Pollutants in Water and Sediment in Urban River Environment

March 2024

Graduate School of Fisheries and Environmental Sciences

Nagasaki University, Japan

Md. Shahidul Islam

Table of contents

Chapter 1.....	1
General introduction.....	1
1.1 Background.....	1
1.2 Treatise structure and contents.....	3
Chapter 2.....	5
Spatial distribution and source identification of water quality parameters of an industrial seaport riverbank area in Bangladesh.....	5
2.1 Introduction.....	5
2.2 Materials and Method.....	7
2.2.1 Study area.....	7
2.2.2 Methods.....	9
2.2.3 Water Quality Index (<i>WQI</i>).....	10
2.2.4 Comprehensive Pollution Index (<i>CPI</i>).....	11
2.2.5 Metal Index (<i>MI</i>).....	11
2.2.6 Statistical Analysis.....	12
2.3 Results and Discussion.....	12
2.3.1 Water Quality Guidelines.....	12
2.3.2 Water Quality Indices.....	17
2.3.3 Spatial Distribution of Water Quality Indices.....	17
2.3.4 Multivariate Analysis.....	21
2.3.4.1 Pearson's Correlation Matrix.....	21
2.3.4.2 Principal Component Analyses.....	22
2.3.4.3 Hierarchical Cluster Analysis (<i>HCA</i>).....	23
2.4 Conclusions.....	26
Chapter 3.....	28
Toxicity and source identification of pollutants in an urban river in Bangladesh.....	28
3.1 Introduction.....	28
3.2 Materials and Methods.....	30
3.2.1 Study area.....	30

3.2.2	Sample collection, preparation, and analysis.....	31
3.2.3	Data reliability	32
3.3	Water quality assessment methods.....	33
3.3.1	Water quality index (<i>WQI</i>)	33
3.3.2	Heavy Metal Evaluation Index (<i>HEI</i>).....	34
3.3.3	Degree of Contamination (<i>C_d</i>)	34
3.4	Sediment assessment methods.....	35
3.4.1	Potential Ecological Risk Index (<i>PERI</i>).....	35
3.4.2	Enrichment Factor (<i>EF</i>)	35
3.4.3	Geo-accumulation Index (<i>I_{geo}</i>).....	36
3.4.4	Pollution Load Index (<i>PLI</i>).....	36
3.4.5	Statistical analysis	36
3.5	Results and Discussion.....	37
3.5.1	Water pollutants.....	37
3.5.2	Metal distribution in sediment	41
3.5.3	Water and sediment pollution indices	44
3.5.3.1	Water pollution indices.....	44
3.5.3.2	Sediment pollution indices.....	47
3.5.4	Pearson correlation	48
3.5.5	Principal component (PCA) and hierarchical cluster analysis (HCA)	50
3.6	Conclusion.....	55
Chapter 4.....		57
	Coprostanol adsorption behavior in agricultural soil, riverbed sediment, and sand.....	57
4.1	Introduction	57
4.2	Materials and methods.....	59
4.2.1	Samples.....	59
4.2.2	Chemicals	59
4.2.3	Methods	60
4.2.4	Batch adsorption experiments.....	61
4.2.5	Adsorption model and data analysis.....	62

4.3	Results and discussion.....	64
4.3.1	Physicochemical characteristics of samples	64
4.3.2	Adsorption isotherm	64
4.4	Conclusions	72
Chapter 5.....		73
	Summary and conclusions	73
	References	76
	Acknowledgements.....	99

Chapter 1

General introduction

1.1 Background

Most of the civilizations of the world originated and developed intimately linked with rivers. It is a very important water resources for industry, agriculture, households, and an important source of food. But, due to the rapid development of urbanization with heavy industry, and agricultural activities, the deterioration of river water and sediment quality has become a great concern worldwide (Qin et al., 2020; Zhang et al., 2022). Recently, effective technologies and national strategies have been taken to ensure safe water by many developed countries such as Japan, USA, and South Korea. Moreover, according to SDG (Sustainable Development Goals) 6.3 set by United Nations, to improve water quality by reducing pollution, eliminating dumping, and minimizing the release of hazardous chemicals, by halving the proportion of untreated wastewater; and hence proper management of water resources are very important for the accomplishment of the SDGs target (Colla et al., 2023; Rampley et. al., 2020; United Nations, 2023).

Generally, developing countries associate with severe water supply problems due to the absence of proper water resource administration. The water quality may deteriorate by anthropogenic activities, and water is going to be unsuitable for uses (Nasiruddin et al., 2023). Basically, huge amounts of waste materials from industries and urban sewage have been releasing directly into the river and the river becoming more polluted because of unplanned urbanization and industrialization (Arefin et al., 2018; Sarkar et al., 2019). Additionally, farmers apply extreme doses of insecticides, herbicide, pesticides, and inorganic fertilizers which are mixed with river water due to storm water runoff. During rainy season, soluble and insoluble waste materials have come to the adjoining rivers after mixing with water (Uddin et al., 2021). Moreover, large amounts of untreated sewage discharge, industrial effluent, and surrounding agricultural storm water runoff containing toxic elements lead to critical challenges for river environments. Trace elements accumulate in sediments by precipitation and release back into water due to the influence of hydrodynamic conditions. Consequently, sediments act as sink for heavy metal pollution and potential secondary source of trace elements (Cai et al., 2023; Mookan et al., 2023). Heavy metals can also be bioaccumulated in biological systems of marine organisms and biomagnified along the food chain leading to high ecological risks due to toxic effects (Bawa-Allah, 2023).

The neighboring population uses the river water for washing, cooking, bathing, and other everyday activities. However, the river is also an exhaustive fishing area, and the local population eats stuck in the river. Different diseases such as disorders at nervous system, cancer, liver damage, hematological and reproductive effects, cardiovascular diseases, health problems in lung, and kidney

damage can cause due to consume fish contaminated by trace metals (Kalipci et al., 2023). Therefore, it is utmost important to assess the degree of pollution and recognize the potential source of contaminants in river water and sediments, which can help researchers establish priorities for pollution control effectively and protect the river environment.

Currently, comprehensive, and single-factor evaluation methods have been widely used for the evaluation of river environmental quality. The Comprehensive evaluation methods such as Water Quality Index (*WQI*), Metal Index (*MI*), Contamination Index (*C_d*), Comprehensive Pollution Index (*CPI*), Heavy metal Evaluation Index (*HEI*), for water (Omeka and Egbueri, 2023; Sangaré et al., 2023; Varol et al., 2022); and potential ecological risk index (*PERI*), enrichment factors (*EFs*), geo-accumulation indices (*I_{geo}*), pollution load indices (*PLIs*), and contamination factors (*CFs*), for sediment sample (Bawa-Allah, 2023; Duodu et al., 2016; Omwene et al., 2018; Proshad et al., 2023) can display the overall pollution status and influence of multiple pollutants by counting individual values mathematically. Moreover, multivariate statistical methods, such as correlation analysis (CoA), cluster analysis (CA), and principal component analysis (PCA), have been extensively applied in the interpretation of complex monitoring of water and sediment quality data to elucidate the spatiotemporal characteristics and factors influencing environmental quality by extracting potential data (Aditya et al., 2023; Ding et al., 2023; Fentahun et al., 2023). Therefore, they are effective at dealing with multiple varying parameters by providing an overall quality assessment and identifying possible sources affecting water and sediment quality. However, these methods have been used for evaluating the degree of pollution and source identification in the urban riverine system.

Urban rivers as well as ground and surface water have also been associated with fecal contamination problems (Whaley-Martin et al., 2017; Islam et al., 2017; Hasan et al., 2019; Parvin et al., 2022; Geen et al., 2011; Hossain et al., 2021). Rapid unplanned urbanization, poor sanitation and sewerage systems, inefficient solid waste management, and frequent flooding may be responsible for fecal pollution. According to literature review 80% of fecal sludge in Bangladesh from on-site pit latrines is not safely controlled (Amin et al., 2019). Meanwhile, Fecal sterols are a worldwide complementary approach to evaluate sewage discharge and accumulation in rivers and water environments (Frena et al., 2016a; Frena et al., 2016b; Vane et al., 2010), and sterol profile of humans and livestock are mostly governed by coprostanol sterol. Coprostanol is incorporated into riverbed sediments after association with particulate matter in sewage effluent. Therefore, groundwater is not free from the hazard of fecal pollution and can be affected by fecal origin. It could generate severe environmental pollution risks by transporting and reaching to the groundwater system through riverbed sediment.

In the current research, I have predominantly discussed three topics based on the preservation and sustainable utilization of urban river environment related to surface and groundwater resources. The first two topics are how the urban riverine system is influenced by unplanned rapid urbanization,

industrialization and agricultural activities based on different land-used types. In this study, I have determined physicochemical and toxicological parameters including different environmental evaluation indices with spatial distribution of the pollutants for evaluating the degree of pollution of the respective riverine environment. Finally, the multivariate analysis method was used to identify the source of pollutants including trace and heavy metal contamination. In the third topic, I have evaluated for the first-time sorption behavior of a fecal pollution marker named coprostanol in urban riverbed sediment and an estimation of its fate, and transport mechanism. Then, I compared the results with agricultural soil and sand samples to estimate which geologic media is more responsible for leaching the fecal pollutants that migrate to groundwater and posing potential risks to the groundwater system.

1.2 Treatise structure and contents

The thesis consists of five chapters as follows.

The existing problem with urban river environment including surface water deterioration, and riverbed sediment depletion due to discharging of untreated sewage, industrial effluents, and stormwater runoff from agricultural field by rapid unplanned urbanization, industrialization and agricultural activities were described in chapter 1. Meanwhile, measuring the quality parameters is not only sufficient but also needs to identify the sources of pollutants for controlling this pollution. There are many methods, techniques, and measures that have been performed to solve this problem in many countries throughout the world. Then, the contents of our research were illustrated.

Chapter 2 described the spatial distribution and source identification of water quality parameters in Pasur river by using water quality evaluation indices. It is a vital reservoir of surface water along the mangrove forest of Sundarbans area in Bangladesh. Geospatial analysis and mapping of water pollutant distribution were performed to assess the physicochemical and toxicological situation in the study area. I used different water quality indices such as weighted arithmetic water quality index method (*WQI*), comprehensive pollution index (*CPI*), and metal index (*MI*) to improve the understanding of pollution distribution and processes determining the quality of river water. Based on these data, the changes of river water chemistry have been interpreted by influences of discharges from urban areas, heavy industries, and agricultural activities.

Chapter 3 discussed the investigated physicochemical and toxicological parameters of water and riverbed sediment of the urban Shitalakshaya River, Bangladesh, using multivariate approaches. In this research, I determined the physicochemical variables such as temperature, pH, electrical conductivity (EC), total dissolved solids (TDS), total suspended solids (TSS), chloride, alkalinity, total hardness (TH), and chemical oxygen demand (COD) of water, and toxicological parameters such as iron (Fe), manganese (Mn), cadmium (Cd), cobalt (Co), chromium (Cr), copper (Cu), lead (Pb), nickel (Ni), and zinc (Zn) of water and sediment including spatial distribution of the pollutants in the

Shitalakshaya River. The risks posed by heavy metals in water and sediment were investigated using water quality index (*WQI*), heavy metal evaluation index (*HEI*), and contamination index (C_d) for water, and sediment quality guidelines (*SQGs*), potential ecological risk index (*PERI*), geo-accumulation indices (I_{geo}), enrichment factors (*EFs*), contamination factors (*CFs*), and pollution load indices (*PLIs*) for sediment to obtain more robust outcomes. Pearson correlation matrix, principal component analysis (*PCA*), and hierarchical cluster analysis (*HCA*) were used to determine the sources of water and sediment pollutants in the study area.

In Chapter 4 the sorption behavior of a fecal pollution indicator was evaluated in the urban riverbed sediment, and then compared with that in agricultural soil and sand samples using different isotherm models such as Henry (linear) (K_D), Langmuir (K_L), and Freundlich (K_F) model. I experimentally determined the maximum sorption capacity and distribution coefficients (K_D , K_L , and K_F) of coprostanol with different adsorption influencing factors such as particle size distribution (clay, silt, and sand), cation exchange capacity (*CEC*), pH, EC, and organic matter (*OM*) content in urban riverbed sediment, soil, and sand samples. In addition, I have assessed the leaching properties of coprostanol and improved the understanding of transport processes in different geologic media. The adsorption parameters (K_D , and K_F) indicated that the fecal pollution risks may be more severe in riverbed sediments and sands than in soil due to low content of adsorption influencing parameters. Thus, the migration pattern of coprostanol in the environment can be better described to reduce the risks of environmental and public health issues due to fecal pollutants.

Chapter 5 summarized the obtained conclusions from this study. The evaluation data of water and sediment by multivariate approaches and sorption mechanism indicated that urban river environment and related groundwater system have been polluted by unplanned urbanization, rapid industrialization, and agricultural activities.

Chapter 2

Spatial distribution and source identification of water quality parameters of an industrial seaport riverbank area in Bangladesh

2.1 Introduction

According to the United Nations, about one-third of the world's population drinks contaminated water (Yeh et al., 2021). Clean water is essential for human health, aquatic and terrestrial ecosystems, and life-supporting activities. However, industrial, urban, and agricultural activities release untreated effluents into surface water, creating an alarming water pollution situation in Bangladesh (Proshad et al., 2021). Pathogenic bacteria (total coliform and fecal coliform) gradually degrade water quality. In the oil refinery industry, conventional oil, gas, and coal bed methane are often accompanied by large volumes of contaminated water (Pichtel, 2016). These industries give a high load of organic pollutants such as phenols, which are potentially dangerous for the environment and human health. Industrial wastewater also contains nitrogen, phosphorus, and heavy metals such as Fe, Cr, Ni, Cd, Zn, and Mn (Pavlidou et al., 2014). Geogenic sources may also contribute to the pollution load in river water systems. These sources include rock–water weathering, biological activity, sediment erosion, benthic distress, and riverine system flow regime changes (Apollaro et al., 2022; Smedley and Kinniburgh, 2002). Iron and manganese exist naturally in rivers; they may also be released to water from natural geologic deposits. The Earth's crust is a major source of Mn to the atmosphere, soil, and water.

Exposure to heavy metal pollution is a significant threat to the environment and public health worldwide and especially in the developing world (Lin et al., 2016). Heavy metals enter the food chain through biomagnification and eventually affect human health (Aradpour et al., 2021). The discharge of heavy metal waste into receiving waters may result in many physical, chemical, and biological disorders such as damaged DNA and gene expression changes (Sorlini et al., 2013). Heavy metals in effluents are moderately soluble in water depending on pH and may affect the total and effective exposure to humans and accumulation in soils and plants (Mahmoud and Ghoneim, 2016). Fly ash from thermal power plants and the cement industry is either discarded as dry disposal in landfills or discharged into natural drainage systems such as rivers. These disposal methods result in metal contamination of surface and ground-water resources that eventually will turn up in the food chain (Ramachandra et al., 2012). Polluted water is the main reason for several diseases such as cancer, congenital disabilities, and skin, lung, brain, kidney, and liver conditions are several times more prevalent in the investigated area than elsewhere in the country. Waterborne diseases, such as hepatitis

(A, B, and C), cholera, typhoid, dysentery, and diarrhea, are also caused by polluted water (Khan et al., 2021). To control geogenic and anthropogenic sources of pollution and prevent them from growing to levels detrimental to human beings, programs to monitor pollutants in the river water and sediments are necessary (Zereen et al., 2011).

The Pasur River is one of the most important waterways for economic growth in Bangladesh. It passes through the Mongla Seaport and the Mongla shantytown of the Bagerhat district in Bangladesh. Mongla is the second largest seaport in Bangladesh. It consists of the Pasur channel beside the Sundarban mangrove forest (Hossain et al., 2016). The Sundarban mangrove forest is the largest remaining tract of mangrove in the world. Beside the river lies the coal-based Rampal power plant station. This study was carried out on the Pasur River in the Mongla port area. A significant site of oil refinery (petroleum and vegetable oil), cement, dye and paint, leather, and shipbreaking industries is established near the Pasur River. The industry directly dis-charges poorly or untreated toxic effluent into the Pasur River that becomes increasingly polluted (Environment Review Report, 2014). The river water is used for different functions such as industrial purposes, household activities, bathing, irrigation of fields, and cooking foods by the adjacent rural populations. In some cases, in the dry season, when the drinking water is at crisis level, local rural people use the river water for drinking purposes after boiling. The river was once an important freshwater source for drinking and domestic uses, fisheries, and agricultural irrigation. The river is still used for fishing, and fishermen use smaller or larger boats for fishing. Polluted fish is another crucial reason to assess and monitor the surface water of this river.

Given the above, this study focused on assessing the Pasur River water quality by using water quality evaluation indices such as Water Quality Index (*WQI*) (Chowdhury et al., 2012; Tabrez et al., 2022), Comprehensive Pollution Index (*CPI*) (Xiong et al., 2021; Yan et al., 2015), and the Metal Index (*MI*) (Bakan et al., 2010; Goher et al., 2014). Though some research has been conducted for this river (Ali et al., 2018), there are still no systematic studies focusing on both physicochemical parameters and toxic metal pollution and pollution source determination in the concerned area. Assessment of pollution status is, thus, insufficient in this area. It is also essential to identify the pollution sources. For this purpose, I used multivariate analysis to indicate sources of water pollutants, including metals (Algul and Beyhan, 2020; Krishna et al., 2019). Therefore, the objectives of this study were (i) to determine the water quality parameters of the Pasur River by using physicochemical and toxicological parameters, (ii) to use water quality indices such as *WQI*, *CPI*, and *MI* for assessing the physico-chemical and toxicological properties with spatial distribution for the Pasur River, and (iii) to identify the source of pollutants including metal contamination in water by using multivariate analysis methods.

2.2 Materials and Method

2.2.1 Study area

The Pasur is the largest river in the Sundarban (Mangrove Forest) region, located at 89°30'0" E and 21°45'0" N. This river is known as Rupsha in Khulna. To the north of Khulna in the Jashore region, the river is known as Bhairab River, and to the south of Khulna, from the Chalna area, it is named Pasur River, and this location is known as Mongla Upazila. Mongla Port Municipality is the second largest seaport of the country, export processing zone, and fishing industry area on the shore of the Pasur River. The study was conducted in the Pasur River at Mongla Port Municipality area in Mongla Upazila of Bagherhat District in Khulna, Bangladesh. It is located about 55 km south of Khulna City and 131 km north of the Bay of Bengal.

Land use is concentrated in manufacturing industries, forests, upland fields, and urban areas. The geology is mainly constituted by tidal deltaic deposits but the northern and western area by marsh clay and peat deposits. The southern region also contains mangrove swamp deposits and north-eastern area deltaic silt deposits (**Fig. 2-1d**). The western and central area of the eastern region of the study area are constituted by agricultural areas and the eastern and northern area is constituted by industry mixed with urban areas (**Fig. 2-1**). Mongla Port was established in 1954 on the Pasur and Mongla River junction bank, where 1280 cargo ships were handled in the fiscal year 2019–2020. According to Bangladesh 2011 census, the municipality area is 19.4 km² with a population of about 40,000 (Mongla Municipality in Khulna Division, 2011).

The location of the present study was 22°47' N and 22°60' N and 89°60' E and 89°52' E. The river passes through the right side of the Trikona and Dubla islands and discharges into the Bay of Bengal. The river is deep, so big ships can enter the Mongla Port year-round. The river width varies. It is about 460 m wide at Rupsha, 790 m at Bajuyan, and 2.44 km at Pasur-Shibsha. The river is about 142 km long. The Pasur River and all its tributaries are tidal channels. The river is now also an effluent channel as it receives more than 80% of the wastewater generated from urban areas and industrial sites.

More than 49 small and large manufacturing and processing industries are located in the study area that discharge waste and wastewater into the river without proper treatment. Jute processing, cement manufacturing, fertilizer manufacturing, oil refinery industry, construction materials, and automobile oil storage activities are included in this area (Ali et al., 2018). The sampling points were selected based on assumed representative connections between the river and pollution sources. The study area location and samplings points are shown in **Fig. 2-1**.

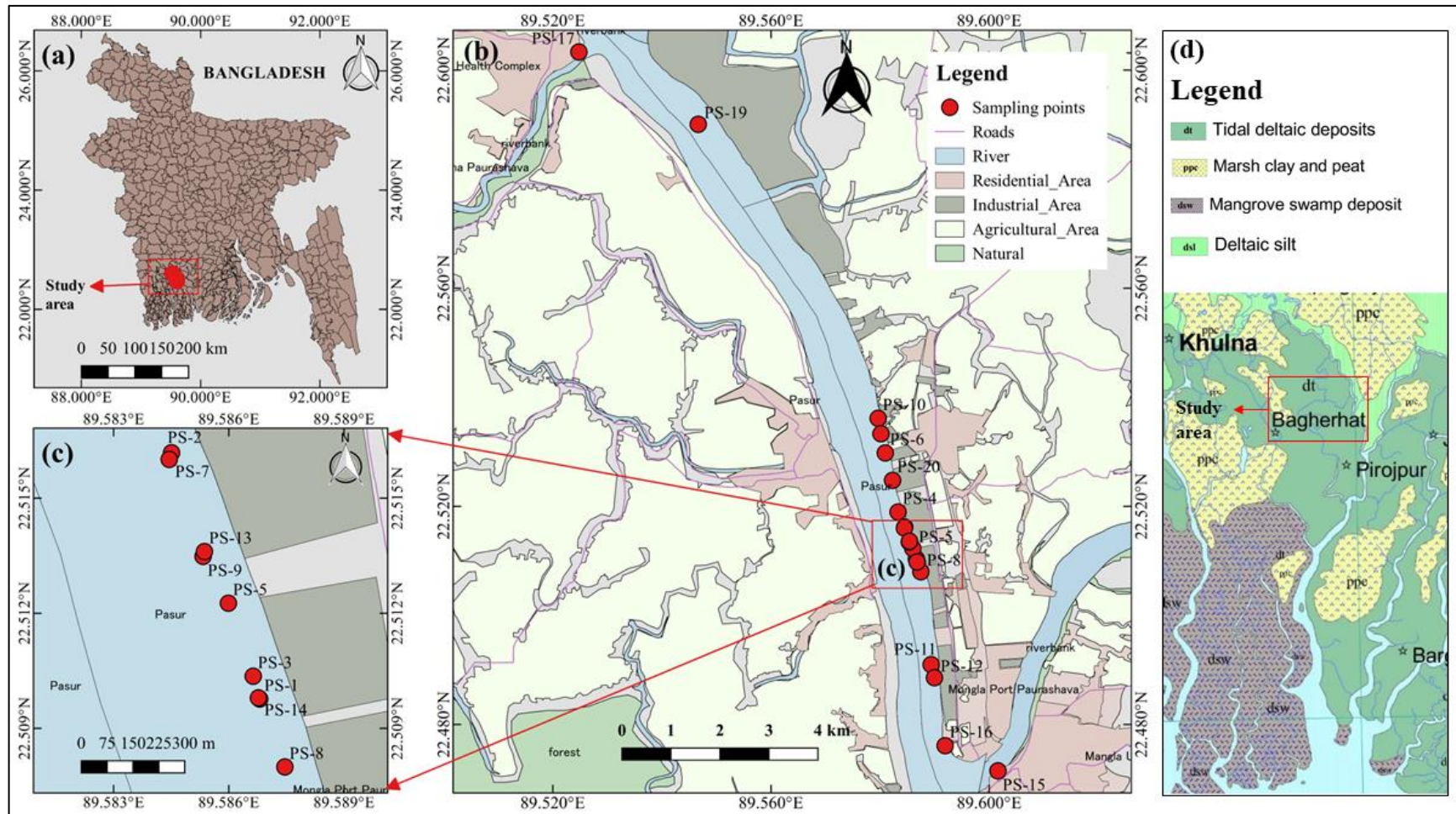


Fig. 2-1 Location of (a) study area; (b, c) sampling points; and (d) geological map (Persits et al., 2001); of the study area.

2.2.2 Methods

The surface water quality varies with rainfall. During the rainy season, due to increased rain, the concentration of pollutants in surface water can either be decreased by dilution or increase due to surface runoff due to first flush (Ling et al., 2017). The present research collected water samples during the rainy season at 20 sampling points. Sampling sites were selected based on functional area, including industry, urban, and agricultural areas, as shown in **Fig. 2-1**.

Collection, storage, and transportation of water samples were performed according to standard guidelines (APHA, 2017). Three water samples were randomly collected from each sampling site and then thoroughly mixed into a 1.0–1.5 L sample and transferred to clean 500 and 100 mL polyethylene bottles, respectively. This was undertaken to guarantee representative samples from each sampling point. At the same time, survey work was conducted at every sampling station to collect background information of the sampling area. The 500 mL samples were preserved with 5 mL of 55% HNO₃ and maintained at 4°C in the refrigerator for physical and chemical parameter analysis. The 100 mL samples were preserved with 2 mL of 6 N nitric acid for metal analysis. Before sample collection, all bottles were washed with 10% nitric acid and de-ionized water.

The 100 mL samples were put in a beaker, and 5 mL concentrated HNO₃ was added and boiled at 130 °C on a hot plate until the volume was reduced to about 25 to 30 mL. HNO₃ addition was continued and repeated until the solution became clear. Then, the solution was cooled and filtered with deionized water passing through a Whatman no. 41 filter (Ali et al., 2016; Bhuyan et al., 2019). Ultra-pure HNO₃ was used for sample digestion. Temperature, pH, and total dissolved solids (TDS) were measured on site by a calibrated apparatus. The pH was determined by a portable calibrated pH Meter (HI 2211, HANNA Romania, Romania) and TDS was determined by calibrated multimeter (CT-676, BOECO Germany, Hamburg, Germany). Chloride, total alkalinity, total suspended solids (TSS), total hardness, iron, and manganese were measured by Mohr's titration, acid-base titration, filtration, EDTA complexometric titration, and flame-AAS method, respectively.

All chemicals and reagents used were of analytical grade. Deionized water with electrical conductivity less than 0.5 μS cm⁻¹ and resistivity ~18 MΩ cm at 25 °C was used for the preparation of all solutions. A blank sample was prepared and analyzed for water samples to ensure that the chemicals used in the preparation did not contaminate the samples. By employing approved standard solutions (HACK, Love Land, Colorado, USA), calibration curves (linearity ≥ 0.995) were created to check the quality of measurements. The standard calibration curves were prepared using 2, 5, 10, and 15 mg/L of metals standard solution. The spiked standard was added after every ten samples. Recovery rates of metals spiked in water fluctuated from 93 to 100%. The detection limits were 0.006 and 0.004 mg/L for Fe and Mn, respectively. Replicate analysis (RSD less than 5%) of the traceable Certified Reference Materials (CRM) and randomly selected samples were measured to check the analyses'

precision and accuracy. All samples were measured in triplicate (RSD less than 5%), and the mean was used. Maps of the study area, spatial distribution of water quality indices, and cluster groups were produced using GIS software (QGIS, version 2.18.2).

2.2.3 Water Quality Index (WQI)

The Water Quality Index (*WQI*) is used for the assessment of both groundwater and surface water pollution levels (Molekoa et al., 2021; Noori et al., 2019). The *WQI* is calculated using the weighted arithmetic method, initially proposed by (Horton, 1965) and developed by Brown et al., 1972 (Howladar et al., 2021):

$$WQI = \frac{\sum Q_n W_n}{\sum W_n}, \quad (2-1)$$

where Q_n = quality rating of n -th water quality parameter; W_n = unit weight of n -th water quality parameter. Q_n is calculated by:

$$Q_n = \left[\frac{V_n}{V_s} \right] \times 100, \quad (2-2)$$

For the pH, this becomes:

$$Q_{pH} = \left[\frac{V_n - V_i}{V_s - V_i} \right] \times 100, \quad (2-3)$$

where V_n = actual amount of n -th parameter present; V_i = ideal value of the parameter ($V_i = 0$, except for pH ($V_i = 7$)); V_s = standard permissible value for the n -th water quality parameter.

The unit weight (W_n) of the various water quality parameters is inversely proportional to the standard permissible value for the n th water quality parameter. I used world health organization (WHO) and the Department of Environment (DoE), Bangladesh, standard for maximum permissible concentrations.

$$W_n = \frac{k}{V_s}, \quad (2-4)$$

where k = constant of proportionality calculated by:

$$k = \frac{1}{\sum V_s}, \quad (2-5)$$

I calculated the *WQI* by using measured water quality parameters such as pH, TDS, chloride, total hardness, total suspended solids, iron, and manganese. The *WQI* value falls into five categories

such as WQI : $< 50 \rightarrow$ Excellent, grade 1; $51-100 \rightarrow$ Good, grade 2; $101-200 \rightarrow$ Poor, grade 3; $201-300 \rightarrow$ Very poor, grade 4; and $> 300 \rightarrow$ Likely not suitable for drinking, grade 5 (Wu et al., 2021).

2.2.4 Comprehensive Pollution Index (CPI)

The Comprehensive Pollution Index (CPI) assesses the overall water quality status (Bi et al., 2021; Kumar et al., 2020):

$$PI = \frac{C_i}{S_i}, \quad (2-6)$$

$$CPI = \frac{1}{n} \sum_{i=1}^n PI, \quad (2-7)$$

where PI is the pollution index of the i -th parameter; C_i is the measured concentration of the i -th parameter; S_i is the standard permissible concentration of the i -th parameter in the water, and n is the total number of parameters. The CPI was calculated using measured values of pH, TDS, chloride, total hardness, total suspended solids, iron, and manganese. I used health-based guidelines from the WHO and the Department of Environment (DoE), Bangladesh, standard for maximum permissible concentrations. According to Mekuria et al., (2021), the PI is a Single Factor Evaluation Index ($SFEI$) for each water quality parameter. The water quality can be classified into five categories based on the calculated value of CPI such as CPI : $0-0.20$, Category 1, Clean; $0.21-0.40$, Category 2, Sub clean; $0.41-1.00$, Category 3, Slightly polluted; $1.01-2.00$, Category 4, Medium polluted, and ≥ 2.01 , Category 5, Heavily polluted (Son et al., 2020).

2.2.5 Metal Index (MI)

The MI assesses the overall quality of surface and drinking water by (Ojekunle et al., 2016; Piroozfar et al., 2021):

$$MI = \sum \frac{C_i}{(MAC)_i}, \quad (2-8)$$

where C_i is the mean concentration of i -th metal and MAC is the maximum allowable concentration of each metal. The MI was calculated by using measured metals concentration. The classification of water quality based on MI is < 0.3 , class-I very pure; $0.3-1.0$, class-II pure; $1.0-2.0$, class-III, slightly affected; $2.0-4.0$, class-IV, moderately affected; $4.0-6.0$, class-V, strongly affected; and > 6.0 , class-VI, seriously affected (Withanachchi et al., 2018).

2.2.6 Statistical Analysis

Pearson correlation, principal component analysis (PCA), and hierarchical cluster analysis (HCA) were performed to identify relationships among the examined water quality parameters in the studied area to infer sources (geogenic or anthropogenic). Pearson correlation analysis represents the strength of the relationship between different parameters. PCA and HCA are the most common multivariate statistical methods for classifying and interpreting large datasets from environmental monitoring programs that reduce the dimensionality of the data. Data was processed using SPSS 17.0 for Windows; IBM, USA, and JMP Pro 15.

2.3 Results and Discussion

2.3.1 Water Quality Guidelines

A summary of the analyses results is shown in **Table 2-1**. Concentrations were compared to standard health-based guidelines by the WHO (WHO, 1984; WHO, 2011), and the Department of Environment (DoE), Bangladesh (Department of Environment, 1997). Temperature is an essential physical water quality parameter. The photosynthesis activity of green plants, physicochemical processes, and microbial biodegradation rate are greatly influenced by temperature. According to DoE guidelines for water in Bangladesh, the temperature should be maintained between 20–30 °C. The average and median temperature in the river water of the study area were 28.7 and 29.2 °C, respectively. The maximum and minimum temperature were 31.2 and 18.3 °C at the sampling location PS-16 and PS-9, respectively. The minimum temperature is caused by tidal flows of the river, excessive rainfall (128.7–321.9 mm), or sometimes discharging cooling water from industrial sites. Samples at PS-12, PS-13, PS-14, PS-15, PS-16, PS-17, PS-18, S-19, and PS-20 occasionally exceeded the standard limit (**Table 2-1**). In previous studies, the temperature range of the Buriganga River in Bangladesh varied from 22.8 to 31.4 °C (Fatema et al., 2018).

pH is a chemical water quality parameter that is crucial for aquatic life. The toxicity of metals to aquatic life, different chemical and biochemical reactions, and the suitability of water for different uses are associated with water pH (Mekuria et al., 2021). The recommended pH by WHO and DoE health-based guidelines varies from 6.50 to 8.50. In the study area, the median pH was 8.72 (**Fig. 2-2a**), slightly higher than the recommendations. Maximum and minimum pH was 8.97 and 8.43 at PS-11, PS-13, and PS-18, respectively (**Table 2-1**). All sampling sites showed pH higher than the WHO and Bangladesh standards except PS-18 and PS-19. The low pH value may be attributed to relatively low anthropogenic influence. The higher pH may have been influenced by dissolving alkaline waste materials containing carbonate, and bicarbonate components used as detergents and other activities from Mongla municipal domestic area and poor or untreated industrial effluents from industry near

the study area. Sodium hydroxide (caustic soda), calcium hydroxide (lime), and many other basic chemicals have been used in different purposes in industries. However, these compounds can cause high pH levels if discharged directly without proper treatment. Besides these, photosynthetic consumption of carbon dioxide (especially in algal blooms) can also drive pH to high levels.

Total hardness (TH) is influenced by contents of carbonate, bicarbonate, sulfate, and chloride salt of calcium and magnesium that decrease the water softness for cleaning, heating, and boiler systems. The WHO and national guideline for the total hardness of water is 500, and 200-500 mg/L, respectively, and the average observed concentration was 120.6 mg/L (**Table 2-1**). The maximum and minimum concentration of total hardness was 472.6 and 34.8 mg/L at sampling station PS-20 and PS-9, respectively (**Table 2-1**). The laboratory findings indicated that the concentration of total hardness was within the national and international guidelines.

Total dissolved solids (TDS) consist of dissolved inorganic ions such as any minerals, salts, metals, cations, or anions and some small amounts of organic matter that are dissolved in water. According to WHO and Bangladesh standards the recommended concentration of TDS is 1000 mg/L. The average concentration of TDS in the study area was 241.8 mg/L (**Table 2-1**) and the median was 147.2 mg/L (**Fig. 2-2a**). The maximum and minimum concentration of TDS were 893.3 and 127.7 mg/L at sampling sites PS-20 and PS-4, respectively. TDS in the study area comes from domestic and industrial waste such as detergents, chloride, bicarbonate, fluorides, sulfate, and other ions.

The chloride concentration range in samples was 108.2 to 708.9 mg/L with an average of 243.9 mg/L. The average is within the WHO and national standards (**Table 2-1**). The median value of chloride (214.6 mg/L) was also within the WHO standard limit (**Fig. 2-2a**). The concentration of chloride in sampling locations PS-3, PS-12, PS-16, and PS-20 exceeded the WHO standard limit, whereas the chloride concentration of PS-11 exceeded the WHO and national guidelines of Bangladesh. Thus, the concentration of TDS and chloride at some locations did not exceed the permissible limits. A possible reason for this is the significant runoff of stormwater during the rainy season in the study area (129–322 mm) that can dilute the polluted water.

Total suspended solids (TSS) were calculated from suspended and colloidal materials that increase surface water's turbidity. TSS can affect surface water quality. Excess concentration of TSS affects light transmission and aquatic life. The standard limit of TSS should be maintained below 10.0 mg/L, which is recommended by the Bangladeshi standard (DoE). However, the average TSS concentration was 736.8 mg/L (**Table 2-1**). The median concentration of TSS was 671 mg/L and much higher than the national standard value (**Fig. 2-2a**). The maximum and minimum concentration of TSS in the river water was 1482.7 and 363.2 mg/L at the Omera Petroleum Industrial area (PS-3) and Laudobe ghat area (PS-14), respectively. All sampling sites displayed a higher TSS than permissible levels (**Table 2-1**). This is probably due to the discharge of large volumes of industrial waste and wastewater from nearby industry and local urban bazaars to the river without any treatment.

Table 2-1 Comparative study of physicochemical parameters of Pasur River water with WHO and DoE Standards

Sample ID	Temp. (°C)	pH	TH (mg/L)	TDS (mg/L)	TSS (mg/L)	Chloride (mg/L)	Alkalinity (mg/L)	Fe (mg/L)	Mn (mg/L)
PS-1	27.0	8.57	75.2	144.4	644.0	215.1	100.6	1.48	0.40
PS-2	27.3	8.57	153.8	278.1	791.6	213.1	92.9	2.25	0.68
PS-3	27.3	8.60	71.9	136.7	1482.7	250.9	88.3	1.84	0.51
PS-4	27.7	8.67	64.7	127.7	426.6	224.6	91.7	1.13	0.46
PS-5	28.0	8.80	72.9	147.8	728.3	206.5	94.7	2.10	0.70
PS-6	27.0	8.53	85.1	142.3	567.1	221.1	92.7	1.41	0.38
PS-7	27.6	8.53	78.9	146.5	988.6	241.1	94.0	2.06	0.79
PS-8	28.7	8.73	163.7	354.6	852.6	108.2	106.0	1.97	0.71
PS-9	18.3	8.93	34.8	135.2	582.3	148.6	91.0	1.15	0.34
PS-10	28.3	8.70	56.7	134.8	1004.9	170.5	91.3	2.23	0.19
PS-11	29.7	8.97	173.5	326.2	926.8	708.9	67.7	2.75	1.41
PS-12	30.6	8.87	67.3	163.8	657.5	271.5	92.0	2.32	0.86
PS-13	30.3	8.97	207.5	455.2	764.0	212.3	93.3	2.49	1.01
PS-14	31.0	8.87	79.7	153.1	363.2	233.1	87.3	1.14	0.44
PS-15	30.5	8.93	276.6	524.6	666.3	214.1	98.7	1.86	0.68
PS-16	31.2	8.93	57.7	151.7	807.9	261.3	88.7	2.32	0.97
PS-17	30.3	8.70	77.5	142.5	582.3	205.0	98.0	2.19	0.79
PS-18	31.0	8.43	76.9	144.6	674.9	191.7	93.0	2.22	0.78
PS-19	30.3	8.47	65.2	133.6	572.2	211.1	97.7	1.62	0.55
PS-20	31.0	8.80	472.6	893.3	652.5	368.9	165.3	1.72	0.61
Maximum	31.2	8.97	472.6	893.3	1482.7	708.9	165.3	2.75	1.41
Minimum	18.3	8.43	34.8	127.7	363.2	108.2	67.7	1.13	0.19
Average	28.7	8.73	120.6	241.8	736.8	243.9	96.2	1.91	0.66
STD. Dev.	±2.9	±0.18	±102.9	±193.1	±242.8	±120.8	±17.9	±0.47	±0.28
WHO ^{a,b}		6.5–8.5	500	1000	-	250	-	0.3	0.1
DoE STD. ^c	20–30	6.5–8.5	200–500	1000	10	150–600	-	0.3–1.0	0.1

^{a, b} World Health Organization (WHO) (WHO, 1984; WHO, 2011). ^c Department of Environment (DoE), Bangladesh (Department of Environment, 1997).

Total alkalinity is related to the contents of carbonate, bicarbonate, and hydroxyl ions in the water. The average concentration of total alkalinity in the samples was 96.2 mg/L. Maximum and

minimum concentrations were 165.3 and 67.7 mg/L at sampling points PS-20 and PS-11 (**Table 2-1**), respectively. At PS-20, the total alkalinity concentration was higher than other sampling points due to alkaline household and industrial waste discharged into the river without treatment.

Iron is a common metal in surface water that may dissolve from surface sediments and suspended matter. Dissolved iron in the surface water is usually not a health hazard, but it may create a bitter taste, stain, and discolor laundry. In addition, high iron contents are not suitable for heating systems and boilers. According to the WHO standard, iron concentrations should be below 0.30 mg/L. However, the average concentration of iron in the samples was 1.91 mg/L (**Table 2-1**). The median value of Fe was 2.0 mg/L, and much higher than the standard limit (**Fig. 2-2a**). The maximum and minimum concentration of iron in river water was 2.75 and 1.13 mg/L at sampling sites PS-11 and PS-4, respectively. High iron concentrations probably stem from suspended matter and industrial waste (**Table 2-1**). Thus, it can be concluded that the river water is not fit for use in household activities and industrial purposes without treatment. Iron forms several sulfides in nature, such as pyrite (FeS_2), marcasite (FeS_2), pyrrhotite ($\text{Fe}_{11}\text{S}_{12}$), troilite (FeS), and numerous other more complex compounds. Iron exists naturally in rivers; it may also be released to water from natural geologic deposits. Iron at average temperature is usually deposited from solutions such as hydrous sesquioxide, carbonates, sulfides or hydrous silicates of iron and potash known as glauconite. Anthropogenic sources such as untreated industrial effluents, improper disposal of domestic waste, and agricultural runoff are the main contributors to iron pollution in the Pasur River.

Manganese is an essential natural element in surface water but may adversely affect aquatic ecosystems (U.S. Department of Health and Human Services, 2012). The manganese concentration should be below about 0.1 mg/L according to the WHO and Bangladeshi standards for water. The average manganese concentration in the study area was 0.66 mg/L. The median value was 0.68 mg/L, and consequently much higher than recommended standards (**Fig. 2-2a**). The maximum and minimum manganese concentration in the study area was 1.41 and 0.19 mg/L at sampling points PS-11 and PS-10, respectively (**Table 2-1**). The concentration of metals in the water of the Pasur River is compatible with that of surface water of other aquatic systems in Bangladesh and worldwide (Aradpour et al., 2020; Bhuyan et al., 2019; Islam et al., 2022; Peluso et al., 2021). The manganese concentration in the Pasur River is alarming for aquatic environments, most likely caused by dissolved, suspended solids and industrial waste. Manganese sources can be geogenic or anthropogenic. Manganese forms two sulfides, alabandite (MnS) and hauerite (MnS_2). Both minerals are scarce and so unstable that they rapidly oxidize on exposure. Alabandite is the less rare form and usually occurs as a subordinate constituent of metalliferous veins or allied deposits. The anthropogenic sources of Mn are industrial effluents, runoff from agricultural activities, and uncontrolled release or leakage from landfill sites. The Sela River at Sundarbans area, an ecologically important river like the Pasur River, has drawn global attention after an oil spill accident in December 2014, when about 94,000 gallons of heavy fuel

were released into the river, causing instant damage to the mangrove habitat and wildlife. Thus, chemical accidents or disasters in adjacent rivers are also sources of physicochemical and toxicological pollution.

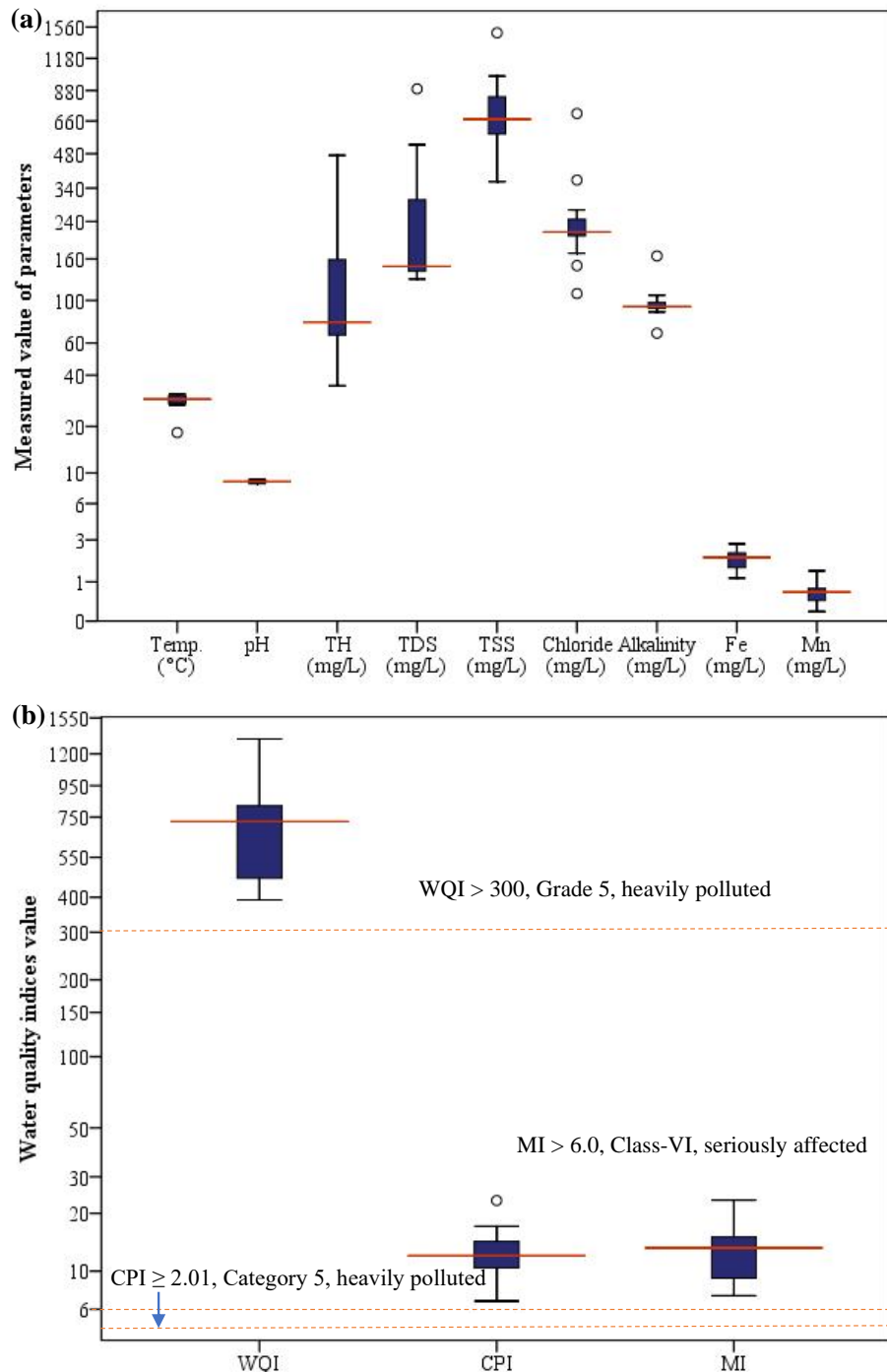


Fig. 2-2 Boxplots for (a) descriptive statistics and (b) water quality indices (In the boxplot, the box (interquartile range) indicates the range in which the middle 50% of all data lies, and the solid red line bars indicate the median. The circles that are further away are considered as outliers).

2.3.2 Water Quality Indices

The water quality indices in the analyzed water were expressed by box plots. The three water quality indices are shown in (Fig. 2-2b). The *WQI* was within the range of 391–1336. The median was 725 and greatly exceeded the maximum limit of 300, which indicates the pollution status of grade 5. Thus, water in all locations falls under the “very poor water” and “likely not suitable for drinking purposes” categories. The highest *WQI* was found at PS-11 (Table 2-2). The metal contamination in this location is very high, which is a major concern. The high *WQI* in the study area is due to both geogenic sources of pollutants and discharge of municipal wastewater and industrial effluents, fishing boats, agricultural runoff, loading–unloading, and construction activities in the Mongla seaport area.

The *CPI* was applied to understand the overall status of Pasur River water pollution. This varied between 6.7–23.1, with an average of 12.8 (Table 2-2), and a median of 12.1 (Fig. 2-2b). The median *CPI* (12.1) indicates high pollution levels. All sampling locations exceeded the maximum limit of ≥ 2.0 , indicating Category 5 and heavy pollution. The highest *CPI* was recorded at PS-3. The reason is discharge of domestic waste, sewerage, and septic waste. At the same time, metals are generated from garages, vehicle battery maintenance shops, and other adjacent industries.

To assess and evaluate the combined effects of metals, *MI* was used. The *MI* ranged from 7.2–23.0 with a median of 13.0 (Fig. 2-2b). The median exceeded the maximum limit of 1 ($MI > 1$ is a threshold of warning). All sampling locations were clearly above the maximum limit of > 6.0 (class-VI, seriously affected). Highest *MI* was found at PS-11 (Table 2-2). The source of metals may be anthropogenic or geogenic. Anthropogenic sources of metal contamination are probably due to industrial wastewater from workshops and garages, vehicle batteries, paints and pigment, fishing boats, fuel stations, and agrochemicals.

2.3.3 Spatial Distribution of Water Quality Indices

GIS analysis was applied to improve the understanding of the spatial distribution of the different water quality indices (*WQI*, *CPI*, and *MI*) (Table 2-2). The QGIS (version 2.18.2) was used for this purpose (Nakagawa et al., 2019). The distribution maps, thus, show the concentration variation of water quality parameters within the region. Lower values of quality indices are represented by light red color while deep red indicates a polluted area (Fig. 2-(3–5)).

The spatial variation of *WQI* is shown in Fig. 2-3. The *WQI* ranged from 391 to 1336, calculated using pH, TDS, chloride, total hardness, TSS, Fe, and Mn. It can be concluded that the southeast part of the study area had the highest values. The sampling points were close to the Mongla Seaport associated with intense urban activities, including trunk roads with many landfills, garbage dumps, and municipal waste. Urban waters take on large amounts of pollution from a variety of sources, including industrial discharges, mobile sources (e.g., cars/trucks), residential and commercial

Table 2-2 Water quality index (*WQI*), Comprehensive Pollution Index (*CPI*), Metal Index (*MI*), and pollution status

Sample ID	<i>WQI</i>	<i>CPI</i>	<i>MI</i>	Pollution Level
PS-1	466.4	10.80	8.93	High
PS-2	746.6	13.72	14.30	High
PS-3	638.8	23.13	11.23	High
PS-4	466.1	7.62	8.37	High
PS-5	744.8	12.73	14.00	High
PS-6	440.2	9.65	8.50	High
PS-7	826.5	16.58	14.77	High
PS-8	750.6	14.46	13.67	High
PS-9	391.3	9.64	7.23	High
PS-10	399.9	15.99	9.33	High
PS-11	1336.1	17.24	23.27	High
PS-12	875.6	12.09	16.33	High
PS-13	1008.1	13.96	18.40	High
PS-14	447.9	6.71	8.20	High
PS-15	706.1	11.82	13.00	High
PS-16	967.9	14.39	17.43	High
PS-17	807.5	10.82	15.20	High
PS-18	808.9	12.13	15.20	High
PS-19	582.9	10.05	10.90	High
PS-20	641.9	11.65	11.83	High
Average	702.7	12.76	13.0	High

wastewater, trash, and polluted stormwater runoff from urban landscapes that discharge to river environment and pollute river water. During precipitation the leachate is created due to surface runoff, or a high groundwater table infiltrates into a landfill or dump. Water percolation through the waste causes chemical compounds to be dissolved or suspended in the leachate. This can become toxic and thus contaminate nearby river water that impacts on the lives of marine species and damages the habitat of many organisms. Probably these are the primary pollution sources responsible for increasing pollution and hence *WQI*. The lowest *WQI* was at the center of the area and decreasing when moving from south to north. High *WQI* is probably related to domestic waste, untreated or poorly treated effluents from industry and nearby local markets, and agricultural runoff. Tidal processes and rainy period stormwater runoff are likely important for the transport characteristics of *WQI* pollutants. Runoff can also wash away topsoil particles and contribute to riverbank erosion.

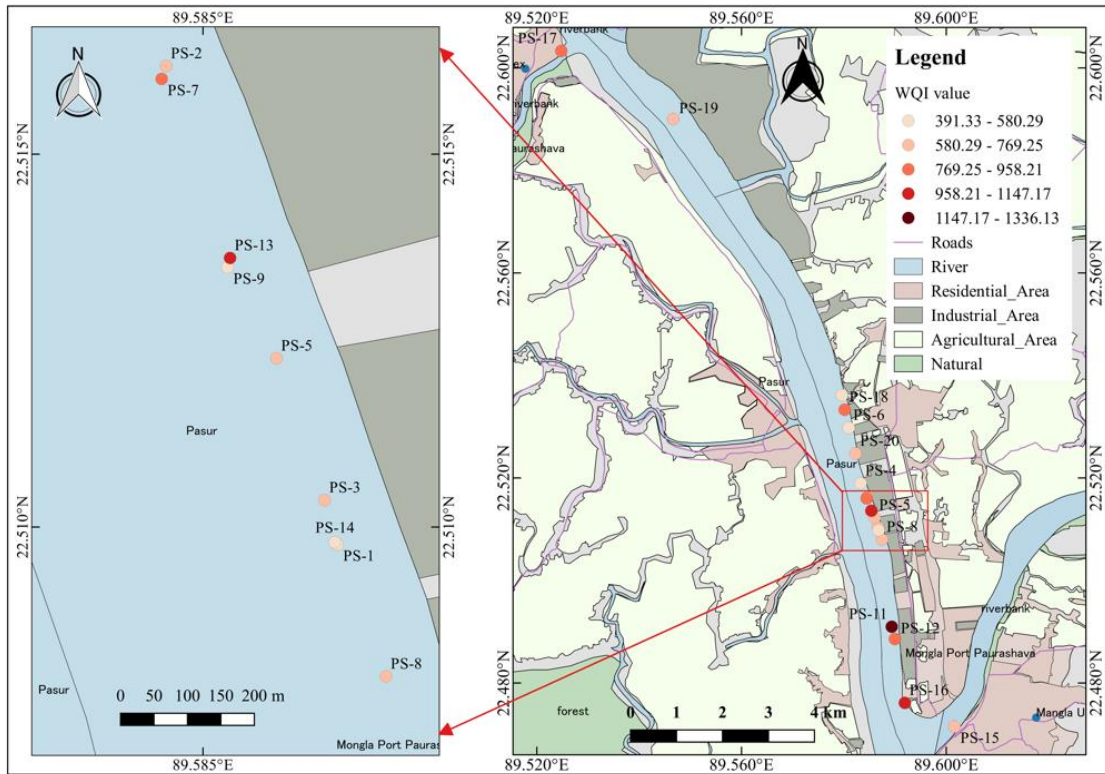


Fig. 2-3 Spatial distribution of Water Quality Index (*WQI*).

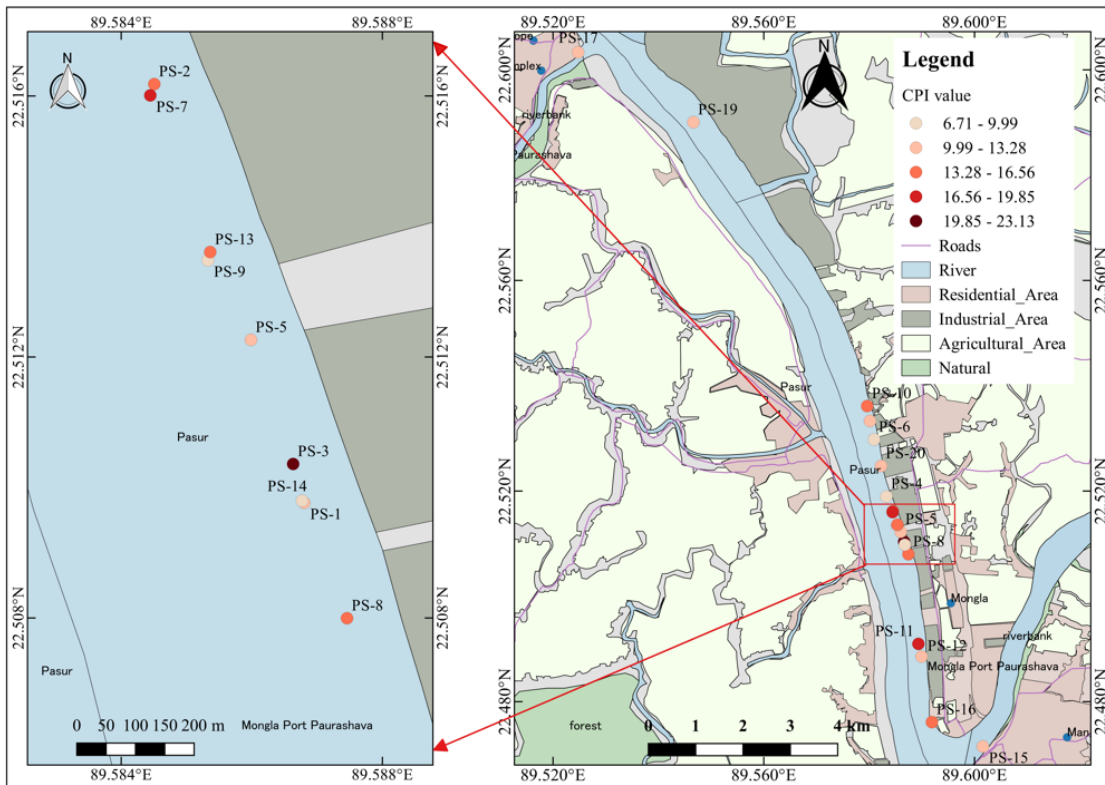


Fig. 2-4 Spatial distribution of Comprehensive Pollution Index (*CPI*).

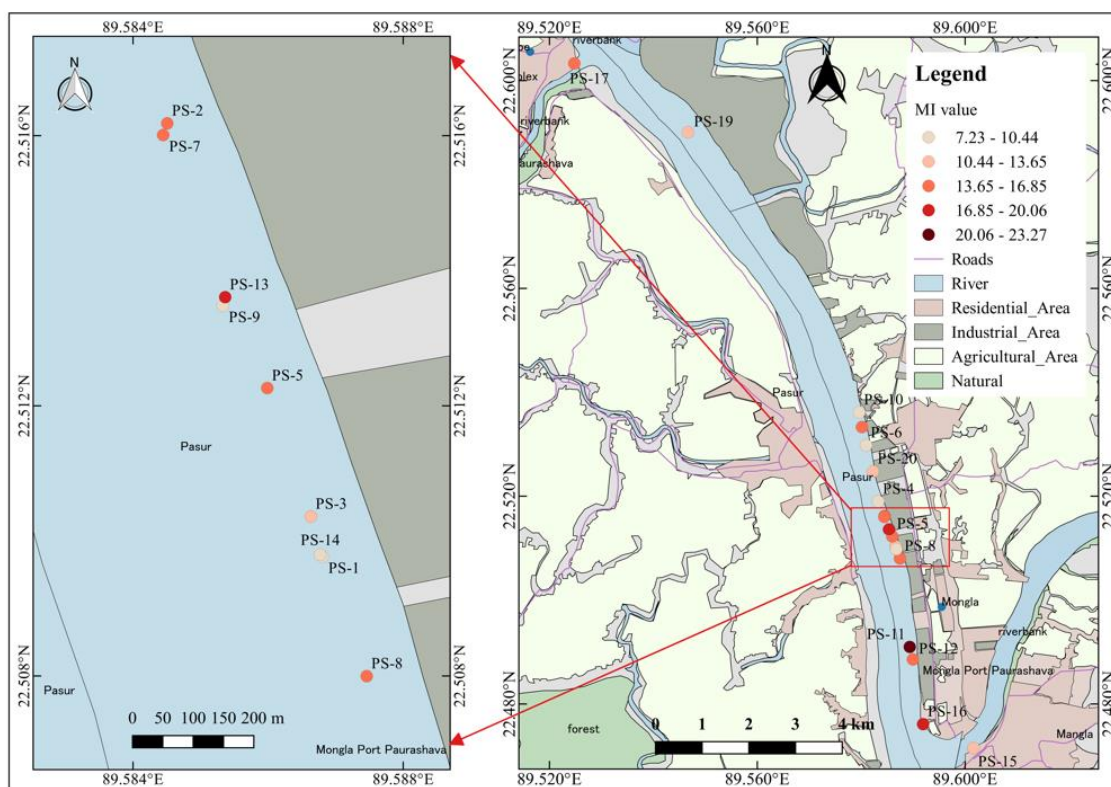


Fig. 2-5 Spatial distribution of Metal Index (*MI*).

As the flow rate increases, resuspension can mobilize bottom sediments, further raising TSS concentrations.

The spatial distribution of *CPI* is shown in **Fig. 2-4**. The trend of *CPI* distribution is somewhat similar to the distribution for *WQI*. The *CPI* gradually decreases from south to north in the study area. Highest *CPI* was found in the south and south-eastern parts, whereas the north region is associated with low *CPI* (**Fig. 2-4**). The sites with high pollution load are densely populated urban areas including a trunk road, bazaars, shops, car washing garages, and many small and heavy industries situated beside the bank of Pasur River. The pollution from industrial effluents, urban and agricultural waste, municipal and household waste in some rivers in Bangladesh has reached alarming levels. When temperature levels increase, the pH level drops that helps to increase the metal toxicity due to more solubility and bioavailability.

The spatial variation of *MI* is shown in **Fig. 2-5**. The spatial distribution indicates a trend with increasing concentrations from north to south. The southern study area thus indicates higher pollution pressure (**Fig. 2-5**). The southern region is close to Mongla Seaport and urban areas with heavy industries. The highest value of *MI* was found in sampling location PS-11, which is closely associated with the Mongla seaport area. Many ships gather here for extensive loading and unloading activities.

This may be the probable reason for higher metal pollution at this site. The *MI* index exceeded the standard limit ($MI > 1$) for all sampling points. Thus, it can be concluded that the entire study area is seriously threatened by metal pollution by domestic sewage, industrial wastewater, and runoff from agricultural fields. Moreover, the high *MI* is probably due to industrial, seaport, and construction activities, shipping and fishing boats.

2.3.4 Multivariate Analysis

2.3.4.1 Pearson's Correlation Matrix

Pearson correlation was used to study relationships between surface water contaminants with significance levels at $p < 0.01$ and $p < 0.05$ (El-Sorogy and Youssef, 2021; Huang et al., 2021; Jahan and Strezov, 2017). **Table 2-3** presents the Pearson correlation for physicochemical parameters. Parameters that correlated positively with one another included Mn with Fe ($r = 0.757$), $p < 0.01$); total hardness (TH) with alkalinity ($r = 0.739$, $p < 0.01$) and TDS ($r = 0.992$, $p < 0.01$), and TDS with alkalinity ($r = 0.735$, $p < 0.01$). TSS was moderately correlated with Fe ($r = 0.483$) and chloride was moderately related to Fe ($r = 0.641$, $p < 0.05$). Higher correlation between variables may indicate common sources, mutual dependence, and similar or nearly identical metal accumulation properties in surface water. The strong correlation between total hardness with alkalinity indicates a common source of contamination. Hardness is mainly caused by calcium and magnesium salts. These salts are dissolved from geologic deposits through which water travels. Most alkalinity in surface water comes from calcium carbonate, CaCO_3 , leached from rocks and soil. The anthropogenic sources for both are

Table 2-3 Pearson's correlation matrix

Parameter	Temp.	pH	TH	TDS	TSS	Chloride	Alkalinity	Fe	Mn
Temp.	1								
pH	0.344	1							
TH	0.104	0.292	1						
TDS	0.137	0.365	0.992**	1					
TSS	-0.259	-0.097	-0.022	-0.021	1				
Chloride	0.068	0.328	0.32	0.287	0.165	1			
Alkalinity	0.015	-0.062	0.739**	0.735**	-0.159	-0.123	1		
Fe	0.127	0.2	0.133	0.146	0.483*	0.391	-0.205	1	
Mn	0.239	0.391	0.226	0.236	0.17	0.641**	-0.227	0.757**	1

** Correlation is significant at the 0.01 level (2-tailed), * Correlation is significant at the 0.05 level (2-tailed).

industrial effluents, municipal wastewater discharge, or excessive application of lime to the soil in agricultural areas.

The strong correlation between TDS and alkalinity indicates a similar source. TDS in surface water may come from agricultural and residential (urban) runoff, leaching of soil contamination, and point source water pollution discharge from industrial or sewage treatment plants. Fe and Mn were strongly correlated. Both have a similar geogenic source. Carbonates of Fe and Mn are isomorphous with each other, hence a possible cause of their association, such as is seen in almost all manganiferous spathic iron ores, whether these ores are formed by direct precipitation or by replacement of carbonate of lime. The oxidation of such a mixture would give a combined iron and manganese ore of the common form. Common anthropogenic sources of Fe and Mn are industrial effluents and local urban wastewater discharge. TSS did not show a strong correlation with any variable. Thus, the source is probably different as compared to other pollutants.

2.3.4.2 Principal Component Analyses

The sources of pollutants were further investigated using PCA and HCA. The results of the PCA are shown in **Table 2-4**. The total number of components (common factors) in the PCA was determined based on the Kaiser criterion (Nakagawa et al., 2016). Under this criterion, the only component with eigenvalues ≥ 1 should be accepted as a possible source of variance in the data, with the highest priority ascribed to components with the highest eigenvector sum. Scree plots were used to identify the number of PCs to be retained to comprehend the underlying data structure (Hossain et

Table 2-4 Results of principal component analysis

	PC 1	PC 2	PC 3
Temperature	0.57	0.10	0.24
pH	0.48	0.10	-0.70
TH	0.81	-0.54	0.06
TDS	0.81	-0.54	0.02
TSS	0.14	0.43	0.63
Chloride	0.63	0.38	-0.22
Alkalinity	0.38	-0.83	0.25
Fe	0.59	0.63	0.30
Mn	0.70	0.59	-0.12
Eigen values	3.29	2.40	1.16
% Of variance	36.6	26.6	12.8
Cumulative %	36.59	63.23	76.07

al., 2019). This indicated that the first three components capture the most significant variation in the data. Thus, three PCs were extracted. The eigenvalues for these PCs ranged from 1.16 to 3.29, explaining 76.1% of the total variance. PC 1, PC 2, and PC 3 explained 36.6, 26.6, and 12.8% of the total variance, respectively (**Table 2-4**).

PC 1, accounting for 36.6% of the total variance, had positive loadings for all parameters but especially high loading for total hardness, TDS, Mn, and chloride ($r = 0.63\text{--}0.81$), and moderately associated with pH, alkalinity, temperature, and Fe. The Pearson correlation matrix showed that total hardness was strongly correlated with TDS. These pollutants have similar geogenic and anthropogenic sources such as untreated industrial effluents, agricultural runoff, municipal waste, and landfills from nearby urban areas. PC 2 was strongly associated with Fe, Mn, and TSS also confirmed from the correlation matrix. The strong association between Fe and Mn indicates that similar sources are at hand. PC 3 had a high association with TSS (**Table 2-4**).

2.3.4.3 Hierarchical Cluster Analysis (HCA)

The HCA was based on Ward's method with squared Euclidean distance (Hossain et al., 2019; Khan et al., 2020; Sharma et al., 2021) and performed on standardized data based on the three PC scores outlined above. The 20 samples were classified into four distinct groups, clusters A, B, C, and D. The average concentration of each cluster group is shown in **Table 2-5**. The table shows that cluster A was not strongly related with any parameters. Cluster B was related to high TSS, Fe, and Mn. Cluster B contained higher indices values (*WQI*, *CPI*, and *MI*) than cluster A and D. Cluster C and D, in which only one sample was classified of each. High TSS, pH, chloride, Fe, and Mn were classified in cluster C. Cluster C was ranked as the most polluted area among the four clusters with respect to *WQI*, *CPI*, and *MI*. Cluster D was related to pH, TDS, and chloride. This cluster's *WQI*, *CPI*, and *MI* values were lower than cluster B and C but higher than cluster A. The decreasing order of indices was cluster C > cluster B > cluster D > cluster A (**Table 2-5**). Thus, cluster C was most polluted, and cluster A the least.

The scatter plot of the 20 samples described by principal components (a): PCs 1 and 2; (b): PCs 1 and 3; (c): PCs 2 and 3 and classified into four clusters is shown in **Fig. 2-6**. If a PC score is greater than 0, the water quality parameter characteristics influence the component at the site. Conversely, if a PC score is less than 0, it means that the component was not significantly affected by the water chemistry at the site (Amano et al. 2018; Yu et al., 2018). In PC 1, cluster C and D are separated from cluster A, and B. PC 1 has smaller scores for cluster A indicating that it had less concentration of the quality parameters than cluster B, C, and D. Thus, it can be confirmed that samples of cluster A were less polluted than others. Cluster B contained higher PC 1 scores than cluster A. In addition, due to positive PC 2 scores of cluster B compared to cluster A, samples of this cluster had a

Table 2-5 Average concentration of water quality parameters in each cluster group

	Cluster A	Cluster B	Cluster C	Cluster D
No. of samples	5	13	1	1
Temperature (°C)	26.2	29.34	29.67	31.0
pH	8.71	8.71	8.97	8.8
TH (mg/L)	67.92	109.74	173.47	472.64
TDS (mg/L)	140.56	224.19	326.18	892.27
TSS (mg/L)	516.65	813.36	926.84	652.45
Chloride (mg/L)	208.49	212.10	708.93	368.87
Alkalinity (mg/L)	92.66	94.5	67.67	165.33
Fe (mg/L)	1.26	2.11	2.75	1.72
Mn (mg/L)	0.40	0.71	1.41	0.61
<i>WQI</i>	442.4	758.8	1336.1	641.9
<i>CPI</i>	8.88	14.0	17.2	11.7
<i>MI</i>	8.25	14.14	23.3	11.8

higher concentration of water quality parameters than cluster A. The higher concentrations are due to geogenic and anthropogenic sources such as untreated industrial wastewater, domestic and municipal wastewater discharge from the urban areas, and agricultural runoff. Both cluster C and the majority sample of cluster B showed a positive score for PC 1 and 2, indicating that both clusters contained high concentration pollutants from industrial, agricultural, and urban areas. This is also confirmed from the average *WQI*, *CPI*, and *MI* value of **Table 2-5**. Both cluster C and cluster B showed positive scores for PCs 1 and 2, but cluster C was more affected than cluster B (**Fig. 2-6**). PC 3 revealed that cluster B is significantly more influenced than cluster D. Thus, the sample of cluster B was more affected and polluted than cluster D.

The spatial distribution of each cluster can be observed in **Fig. 2-7**. Cluster C is generally located nearer the Sundarban mangrove forest in the west part of the study area and the southeast region in the urban area. Cluster C is the study area's most contaminated sampling point containing the highest metal contamination and water quality indices (*WQI*, *CPI*, *MI*). The location of cluster C is associated with Mongla Seaport. Many ships and vessels are taking part in loading and unloading activities for different types of goods. Sometimes they discharge waste, including used oil and oily substances, coal, asbestos, and chemicals directly into the river. The high TSS may come from local bazaars in urban areas and municipal wastewater and landfills. Cluster B is located south to north at different study area sites (**Fig. 2-7**). The samples of this cluster contained high metal concentrations and high-water quality indices (*WQI*, *CPI*, *MI*), indicating a metal contamination area. The contamination of this area is higher than for cluster D and cluster A. Sample of cluster D is in the

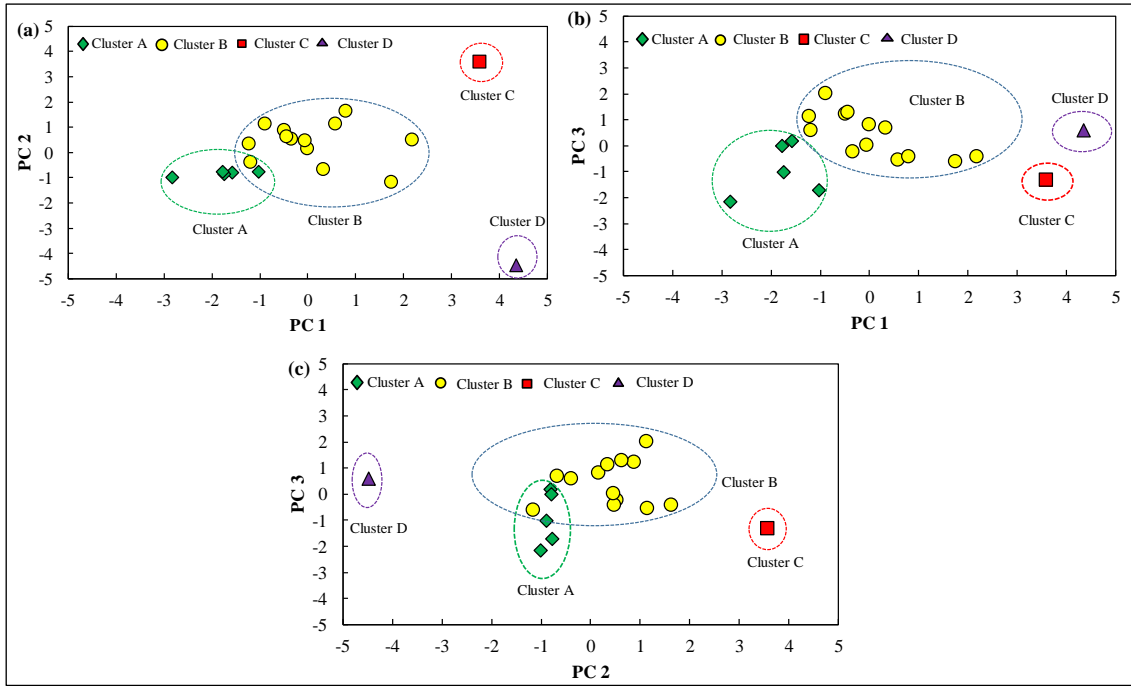


Fig. 2-6 Scatter plots for two principal components with respect to clusters; (a) PCs 1 and 2, (b) PCs1 and 3, and (c) PCs 2 and 3.

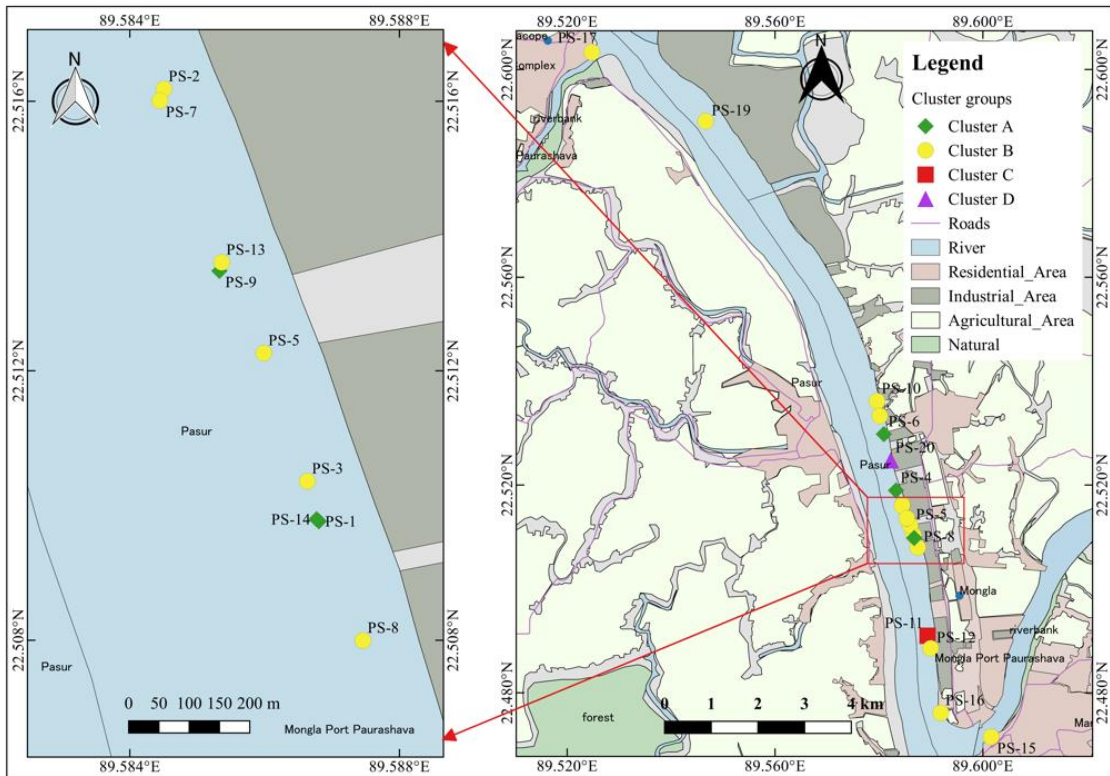


Fig. 2-7 Distribution of each cluster in the study area.

southeast region and near the residential area. The sample of these points contained high calcium and magnesium carbonates, bicarbonates and sulfates, and combined content of all inorganic and organic substances present in a liquid in molecular, ionized, or micro-granular (colloidal sol) suspended form. For this reason, it contains the highest value of total hardness and TDS. The source of these pollutants is agricultural runoff and residential (urban) runoff. This area had high metal contents and TSS. All samples of cluster A are in the southeast area but far from cluster C. Samples of cluster A contain the lowest value of metals and other physicochemical parameters. Thus, these samples were less polluted than other clusters. To conclude, this study shows that the pollution level of the study area is divided into four main groups.

2.4 Conclusions

Rivers are essential sources of water supply for humans and the environment with critical conditions for water quality. This study concluded that iron, manganese, total suspended solids, chloride at some locations, and pH had much higher concentrations in the river water than recommended by WHO and Bangladesh Environmental standards (DoE) and thus are not safe for household use or aquatic ecosystems. I used water quality indices, spatial distribution, and multivariate statistical analyses to evaluate the pollution level and source determination. Multivariate analysis was used to improve the knowledge regarding the source of pollution. Based on the PCA results, four distinct groups were obtained by HCA. The concentration of different water quality parameters was different regarding land use and the importance of the three PC scores. The cluster groups revealed that the sample of cluster C was most polluted, and the samples of cluster A were the least polluted in the study area. The severe enrichment of pollutants in this area is primarily due to anthropogenic sources related to industrial, agricultural, urbanization, and fishing activities.

Mongla Seaport Authority, Mongla Export Processing Authority, Mongla Municipal Corporation, District Administration, and the Department of Environment can take the initiative to protect the river water from pollution and untreated industrial and municipal waste. Monitoring of coastal activities is essential to save the coastal ecosystems. This monitoring system can give policymakers and stakeholders an interest in the coastal environment and resources. A systematic and periodic inspection of each industry located beside the river should be performed before certificates of compliances are issued by the Department of Environment (DoE), Bangladesh. Short- and long-term scientific studies should be immediately started to assess the impacts of industrial activities on coastal water, soil, and fishery resources, as well as human health. Thus, this study recommends that continuous monitoring and modern remediation technologies for reducing the pollution level of the Pasur River as well as adjoining agricultural areas should be assessed regarding the risk for human health and ecosystems in the vicinity of the river. To avoid and alleviate environmental contamination, effective approaches for extracting harmful heavy metals from sewage and industrial effluents are

urgently needed before the effluent is released into the environment. As well, traditional treatment techniques are necessary for water used for domestic purposes. Finally, public awareness of the impacts and remedies of pollution should be raised so that they can play a key role in pollution reduction.

Chapter 3

Toxicity and source identification of pollutants in an urban river in Bangladesh

3.1 Introduction

Increasing pollution levels in urban rivers are causing severe toxicity problems for aquatic ecosystems and human health (Karunanidhi et al., 2022). It is foremost the ongoing rapid urbanization together with industrialization without progress of treatment facilities for domestic and industrial effluents in many developing countries in Asia. Among the potential pollutants, heavy metals have dangerous health effects on the aquatic environment due to their high toxicity, persistence, and bioaccumulation properties (Lipy et al., 2021). Heavy metal contamination is currently of severe concern in Bangladesh. Increasing industrialization, urbanization, and agricultural activities release untreated effluents to rivers, creating an alarming situation (e.g., Proshad et al., 2021).

The fluvial environment consists of two fundamental constituents: water and sediment. These form potential sinks and sources of pollutants, including heavy metals (Kumar et al., 2021). Both geogenic and anthropogenic sources are responsible for heavy metals in river water and sediments. The geogenic sources include rock-water weathering, sediment erosion, and riverine system flow regime changes. In contrast, anthropogenic sources of heavy metals in river water and sediments consist of human activities such as urban effluents, sewage discharge, agricultural runoff, combustion, corroded underground pipes, wastewater discharge from industrial plants, smelting, and vehicles (Astatkie et al., 2021; Fang et al., 2019; Guo and He, 2013; Rajesh et al., 2018). Severe health effects such as cancer, developmental and behavioral problems, impaired intelligence, kidney damage have been shown to be caused by the exposure of heavy metals through water and sediment pollution (e.g., Alomary and Belhadj, 2007).

Metals are introduced into the river environment by anthropogenic activities and absorbed or incorporated into the sediments. The solubility of heavy metals is usually poor in water, thus, heavy metal concentration in water is normally lower than sediments. Suspended particles in water, however, may adsorb heavy metal ions and settle as sediment (Algul and Beyhan, 2020). High concentration of heavy metals in sediments indicates that anthropogenic sources are involved. Thus, heavy metals that are entered into the food chain in the aquatic environment cause severe threats to living organisms (Alrabie et al., 2019; Tylmann et al., 2011; Salati and Moore, 2021; Wang et al., 2021).

The Shitalakshaya River is an important source of drinking water in Bangladesh. It supplies freshwater to the Dhaka and Narayanganj Cities. Due to its geographical position the river plays a vital role in the economy of the two cities. In recent decades, this area has faced rapid urbanization due to unplanned industrial development. This has led to substantial outputs of industrial and domestic waste

and wastewater that are not managed and treated properly. Thus, the river serves as the recipient for untreated effluents with heavy metals from industries, wastewater discharge from the municipal areas, and agricultural runoff from fields along the riverbank. The farmland surrounding the river is gradually degrading the quality of water and sediment due to overuse of fertilizers and pesticides, washed out through stormwater, or leaching ultimately affecting the aquatic biota.

The river is, however, also an intensive fishing area and has a high potential for fish production. The local population consumes fish caught in the river. Fish is an important protein source for the local population. Thus, there is a clear risk of health effects from, e.g., heavy metals (Ahsan et al., 2018). The local population also use the river water for bathing, washing, cooking, and other household activities. Therefore, especially women and children are exposed to the threats from the pollution. Common apparent diseases in the area are different types of water-borne illnesses such as nausea, irritation in the respiratory tract, typhoid, dysentery, cholera, and viral hepatitis (Sultana et al., 2009). Moreover, there is a close relation between heavy metals accumulated in sediment and the content of them in the river water. River sediments mostly act as a sink for heavy metals but as well can act as a source to the overlying water, causing secondary pollution that can cause significant damage to the ecological status of the aquatic system.

Baseline data on heavy metal contents and the connection between heavy metals deposition and their source apportionment in surface water and sediment are very limited in Bangladesh. Therefore, it is very important to establish heavy metal profiles for different polluted rivers. Few studies have concentrated on the Shitalakshaya River (Alam et al., 2020; Pia et al., 2018) despite its serious pollution. To our knowledge no attention has been given to both surface water and sediments of industrial areas at the study sites together with proper mapping of source identification. As sources of pollutants often are complex the mapping of contaminated areas is difficult. Our present research is imperative for ecological and human health perspective, and the mapping of water quality and ecological risk areas of pollutants are aiming to improve the understanding of polluted urban water environments.

In view of the above, I investigated physicochemical and toxicological parameters of water and sediment from the Shitalakshaya River by using environmental quality evaluation indices. To assess the contamination levels of pollutants and identification of sources we used water quality index (*WQI*), heavy metal evaluation index (*HEI*), and contamination index (*C_d*) (Gad et al., 2021; Ghaderpoori et al., 2018; Ram et al., 2021; Son et al., 2020). The risks posed by heavy metals in sediment were investigated by using sediment quality guidelines (*SQGs*), potential ecological risk index (*PERI*), geo-accumulation indices (*I_{geo}*), enrichment factors (*EFs*), contamination factors (*CFs*), and pollution load indices (*PLIs*) (Debnath et al., 2021; Kaushik et al., 2021; Xie et al., 2020) to obtain more robust outcomes. Multivariate analyses such as Pearson correlation matrix, principal component analysis (PCA), and hierarchical cluster analysis (HCA) were used to determining sources of water

and sediment pollutants (Amankwaa et al., 2021; Amano et al., 2018; Xiong et al., 2021). Thus, the specific aims of the study were to (i) determine the physicochemical parameters (temperature, pH, EC, TDS, TSS, chloride, alkalinity, total hardness, and COD) of water and toxicological parameters (Fe, Mn, Cd, Co, Cr, Cu, Pb, Ni, and Zn) of water and sediment including spatial distribution of the pollutants in the Shitalakshaya River, (ii) use water and sediment quality indices such as *WQI*, *HEI*, and *Cd* for water and *PERI*, *I_{geo}*, *EF*, and *PLI* for sediment, to assess the physicochemical quality of water and heavy metal contents in water and sediment and identify the risks they pose, and (iii) to identify the source of pollutants including heavy metals in water and sediments using multivariate analysis methods.

3.2 Materials and Methods

3.2.1 Study area

Shitalakshaya River is a tributary of the Brahmaputra River with experimental study area location 23°67' N and 23°74' north latitude, 90°53' and 90°51' E east longitude. The length of the river is about 110 km, and it has a width of about 300 m at Narayanganj City. The maximum depth of the river is about 21 m, with an average depth of about 10 m. The river flow at Demra municipal area is about 74 m³/s (Pia et al., 2018). The river flows southward through the eastern part of Dhaka City, through Narayanganj City, and joins Meghna River at Kolagachia of Munshiganj district. Narayanganj is the 6th largest city in Bangladesh with a population of about 1.5 million and located 20 km southeast of Dhaka on the flat Ganges-Brahmaputra-Meghna alluvial plain. The Shitalakshaya River divides the town into the Narayanganj municipal and Kadam Rasul municipal areas.

In Narayanganj City many industries and factories for jute, hardboard, paper, and sugar mills are located on the Shitalakshaya riverbank. Other industries are fertilizer and pharmaceutical products, cement, textile, dairy plants and food processing industries, and thermal power plants. The riverbank industries have a common denominator of not having efficient treatment of wastewater. More than 80% of the industries directly or indirectly dump their waste into the Shitalakshaya River (Islam et al., 2015). Thus, a large amount of industrial and municipal wastewater is discharged directly without treatment to the river. A river port is situated in Narayanganj, where many boats, barges, and ships visit and transport industrial material throughout the year. Unfortunately, the local population utilizes the river water for different purposes such as bathing, household washing, fishing, cooking, and other necessary daily duties. Therefore, there are obvious human health risks as well as a general ecosystem pollution. Wastewater discharge is partly diluted with stormwater runoff during rainfall events. Mass transport of pollutants to canals and the river increases due to overland flow and wash-off of accumulated contaminants on impermeable or semi-impermeable surfaces.

3.2.2 Sample collection, preparation, and analysis

A total of 10 water and 10 sediment samples were collected from 10 different locations of the Shitalakshaya River on 28 May (normal weather conditions: mostly cloudy, humidity: 60%, wind: 19 km/h), 10 June (normal weather conditions: mostly cloudy, humidity: 79%, wind: 3 km/h), and 18 June (normal weather conditions: mostly cloudy, humidity: 89%, wind: 7 km/h), 2021. The sampling periods were selected during the summer monsoon period. Generally, average annual rainfall in the area is about 2550 mm with a wet period between May and July. A reconnaissance survey was conducted for the selection of sampling stations to assess background information of the study area. Sampling sites were selected to be representative of function, including industrial, urban, and agricultural areas, as shown in **Fig. 3-1**. The sampling points are surrounded by heavy manufacturing industry mixed with urban areas, upland fields, residential buildings including business infrastructure such as markets, office, local bazars, car workshops, bazar ghats, and trunk roads. Along the roads, many car workshops and garage were situated that discharge petrol and oil spills, car washing wastewater together with stormwater runoff from the road surfaces during the rainy season. The sampling points also overlap with adjacent bazar landfills, small and large artificial canals, and sewage outlet fed by monsoon rain, industrial and municipal wastewater.

During the rainy season, due to increased rain, the concentration of pollutants in surface water can either be decreased by dilution or increase due to first-flush in surface runoff from anthropogenic activities. The sampling procedure, pretreatment, storage, and transportation of water and sediment samples followed standard guidelines (APHA, 2017; EPA, 2001). For each sampling station, three water samples were collected randomly from the middle-reach of the river by boat. Then the samples were thoroughly mixed into a 1.0-1.5 L sample and transferred to clean 500 mL and 100 mL polyethylene bottles to guarantee representative samples. To prevent metal adsorption on the inner surface of the bottles, the samples were preserved by 5 mL of 55% HNO₃ per liter of water. A well-mixed volume of 100 mL of the acidified sample was taken and digested with 5 mL of concentrated HNO₃ in a beaker at 130°C. The digested solution was then filtered by Whatman no. 42 filter paper. The filtrate was diluted to 100 mL volume with distilled water. A plastic container rinsed with 0.01 N HNO₃ was used to store the final sample and kept in a deep freezer before the time of analysis.

The sediment samples were taken simultaneously at the same sites for water samples. For collecting sediment samples, a Petersen grab sampler was used for sediment at 0-10 cm depth. The sediment samples were stored in clean polyethylene bags and transferred to the laboratory. Collected sediment samples were dried, ground, and sieved with a 2 mm sieve to ensure a representative sample. For the metal analyses, 2.0 g of each sample was treated with 15 mL concentrated HNO₃ and digested at 130°C until a transparent solution was obtained with 2-3 mL remaining in the beaker. The digested solution was then filtered with Whitman-41 filter paper by repeated washing with 0.1 M HNO₃.

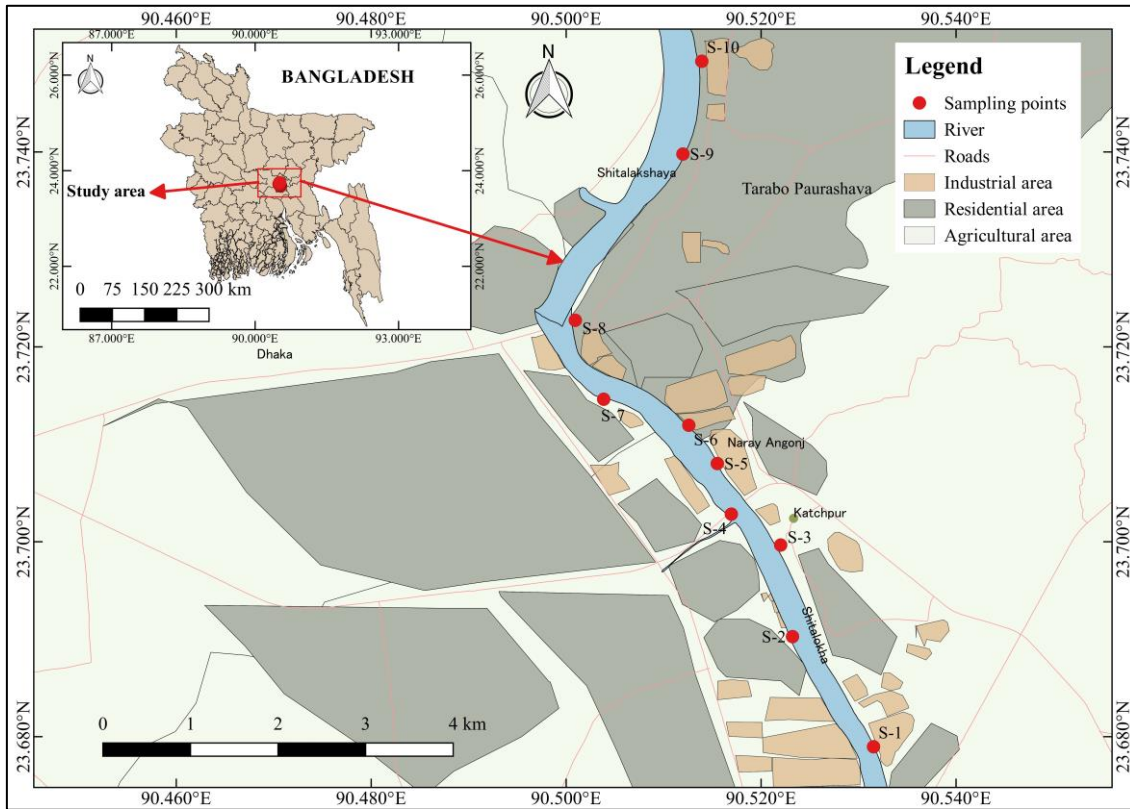


Fig. 3-1 Locations showing the sampling points in the study area.

solution and addition up to 100 mL with distilled water (Ali et al., 2016; Duncan et al., 2018). Temperature, electrical conductivity (EC), and pH were measured in situ. The pH was determined by a calibrated pH Meter (HI 2211, HANNA Instruments) and EC and TDS were determined by calibrated multimeter (CT-676, BOECO Germany). The temperature was measured by a calibrated thermometer, total suspended solids (TSS) were analyzed by filtration apparatus attached with suction flask using filtration method. COD was assayed by reflux apparatus using the open reflux method. Alkalinity and chloride were analyzed by the titrimetric and Mohr’s methods, hardness (EDTA) was determined by EDTA titrimetric method (Islam et al., 2022). The concentration of metals such as Fe, Mn, Cr, Cd, Pb, Co, Ni, Cu, and Zn in both the prepared water and sediment samples was determined by using atomic absorption spectrophotometer (AAS, Model: a. AA240FS, b. GTA 120-AA240Z, Varian, Australia) (Ahsan et al., 2019; Siddique et al., 2020). Analytical grade chemicals were used for all analyses, and the multimeter was calibrated by certified reference material (CRM) solution.

3.2.3 Data reliability

For producing reliable data, employment of ‘good laboratory practices’ was ensured. Deionized water was used for sample preparation with electrical conductivity less than 0.5 $\mu\text{S}/\text{cm}$ and

resistivity ~ 18 MΩ cm at 25°C. All chemicals and reagents were of analytical grade. All containers were immersed in 10% HNO₃ before sample preparation, stored for more than 24 h, and then washed repeatedly with tap water and deionized water. Calibration curves (linearity ≥ 0.99) were prepared for checking quality of measurements by using the NIST (National Institutes of Standards and Technology, USA) traceable Certified Reference Materials (CRM). Replicate analysis (RSD less than 5%) of the CRM and randomly selected samples were measured to check the analyses' precision and accuracy. A blank sample was prepared and analyzed for both water and sediment samples to ensure that the chemicals used in the preparation did not contaminate the samples. Procedural blank and standard samples were analyzed after every ten samples to verify the accuracy of the analyses, and spike recovery in the analysis was 100±10%. The detection limits were 0.0677 mg/L, 0.0031 mg/L, 0.4068 µg/L, 0.2910 µg/L, 1.1970 µg/L, 2.1319 µg/L, 2.1716 µg/L, 0.0062 mg/L, and 0.0075 mg/L for Fe, Mn, Cr, Cd, Pb, Co, Ni, Cu, and Zn, respectively. All samples were measured in triplicate (RSD less than 5%), and the mean was used for further analyses.

3.3 Water quality assessment methods

3.3.1 Water quality index (WQI)

The water quality index (*WQI*) was initially proposed by Horton, (1965) and developed by Brown et al., (1972). The *WQI* was calculated using measured value of pH, TDS, total hardness, TSS, chloride, COD, Fe, Mn, Cr, Cd, Pb, Ni, Cu, and Zn (by considering BDL value as zero). The *WQI* is calculated by:

$$WQI = \frac{\sum Q_n W_n}{\sum W_n}, \quad (3-1)$$

$$Q_n = \left[\frac{V_n}{V_s} \right] \times 100, \quad (3-2)$$

$$W_n = \frac{k}{V_s}, \quad (3-3)$$

For pH by:

$$Q_{pH} = \left[\frac{V_n - V_i}{V_s - V_i} \right] \times 100, \quad (3-4)$$

where Q_n = quality rating of n_{th} water quality parameter; W_n = unit weight of n_{th} water quality parameter, V_n = actual amount of n_{th} parameter present; V_i = ideal value of the parameter [$V_i = 0$, except for *pH* ($V_i = 7$)]; V_s = standard permissible value for the n_{th} water quality parameter. In this study, I used world health organization (WHO) and the Department of Environment (DoE), Bangladesh, standard for maximum permissible concentrations.

The k = constant of proportionality was calculated by:

$$k = \frac{1}{\sum V_s} \quad (3-5)$$

The WQI value falls into five categories as WQI : $< 50 \rightarrow$ Excellent, grade 1; $51-100 \rightarrow$ Good, grade 2; $101-200 \rightarrow$ Poor, grade 3; $201-300 \rightarrow$ Very poor, grade 4; and $> 300 \rightarrow$ Likely not suitable for drinking, grade 5 (Howladar et al., 2021; Molekoa et al., 2021).

3.3.2 Heavy Metal Evaluation Index (HEI)

The heavy metal evaluation index (HEI) provides overall quality of the water concerning toxic metals. The HEI was calculated by (Khadija et al., 2021; Proshad et al., 2021):

$$HEI = \sum_{i=1}^n \frac{H_c}{H_{mac}}, \quad (3-6)$$

where H_c is the observed value and H_{mac} is the maximum allowable concentration of the i -th parameter. In this study, Fe, Mn, Cr, Cd, Pb, Ni, Cu, and Zn were determined and used for calculating the HEI value. There are three categories of calculated HEI values; $HEI > 20$ indicates high contamination; $HEI = 10-20$, medium contamination; and $HEI < 10$, low contamination (Kabir et al., 2020).

3.3.3 Degree of Contamination (C_d)

The degree of contamination (C_d) represents adverse effects on surface water quality (Gad et al., 2021; Ndong et al., 2021). The C_d is computed separately for each water sample as a sum of the contamination factors of individual components exceeding the upper permissible value. The contamination index is calculated as:

$$C_d = \sum_{i=1}^n C_{fi}, \quad (3-7)$$

$$C_{fi} = \frac{C_{Ai}}{C_{Ni}} - 1, \quad (3-8)$$

where C_{fi} , C_{Ai} , C_{Ni} represents the contamination factor, analytical value, and upper permissible concentration of the i -th component, respectively. In this study the, I calculated the C_d value by using the measured value of Fe, Mn, Cr, Cd, Pb, Ni, Cu, and Zn. The $C_d < 1$, indicates low contamination, $C_d = 1-3$, medium, and $C_d > 3$, high contamination (El-Hamid and Hegazy, 2017; Khan et al., 2021).

3.4 Sediment assessment methods

3.4.1 Potential Ecological Risk Index (PERI)

The contamination status of heavy metals in sediment was determined by the potential ecological risk index (PERI). With the combination of ecological and toxicological factors, it expresses the comprehensive potential ecological risk of heavy metals in sediments according to (Hakanson, 1980):

$$E_f^i = T_{fr}^i \times C_f^i, \quad (3-9)$$

$$C_f^i = C_s^i / C_n^i, \quad (3-10)$$

$$RI = \sum_f^i E_f^i, \quad (3-11)$$

where E_f^i represents the potential ecological risk for a single element, C_f^i is the contamination factor for an individual element, and T_{fr}^i represents the toxic response factor, which accounts for the toxic requirement and the sensitivity requirement. The T_{fr}^i is the toxic response factor of heavy metals i and has values of Mn (1), Cr (2), Cu (5), Pb (5), Ni (5), Cd (30), Zn (1), and Co (5) (e.g., Kang et al., 2020; Xie et al., 2020). The C_s^i indicates the concentration of individual elements in the sediment, and C_n^i is the background reference value for each element. Environmental quality standards (EQSs) for heavy metals in sediments do not exist for Bangladesh. As a result, Turekian and Wedepohl's Average Shale Values (ASVs) were used as background reference values in the present study. The RI represents the sum of potential ecological risks for heavy metals at each sampling location. Based on these factors, the pollution level was classified as: when $E_f^i < 40$, $RI < 150$, then low risk; $40 \leq E_f^i < 80$, $150 \leq RI < 300$ represents moderate risk; considerable risk: $80 \leq E_f^i < 160$, $300 \leq RI < 600$; $160 \leq E_f^i < 320$, $RI \geq 600$ indicates high risk; and when $E_f^i > 320$, then very high risk exists (e.g., Bahloul et al., 2018; Kang et al., 2020).

3.4.2 Enrichment Factor (EF)

Enrichment Factor (EF) can determine the anthropogenic contamination of heavy metals. The Fe was chosen as the normalizing element for identifying anomalous heavy metal contribution to calculate this factor. The following equation was used for the calculation of EF (Debnath et al., 2021):

$$EF = \frac{C/Fe(sample)}{C/Fe(background)}, \quad (3-12)$$

where $C/Fe_{(sample)}$ and $C/Fe_{(background)}$ represent Fe ratios in the current study and background. Turekian and Wedepohl's Average Shale Values (ASVs) were used as background reference values. The classification of contamination level based on EF was categorized as: $EF > 40$, representing extremely high contamination, similarly 20-40, very high; 5-20, significant; 2-5, moderate; and $EF < 2$, indicating minimal level of contamination (e.g., Malsiu et al., 2020).

3.4.3 Geo-accumulation Index (I_{geo})

Geo-Accumulation Index (I_{geo}) assesses the pollution level of each heavy metal in surface sediments. It can be used to evaluate the pollution status of sediments based on heavy metal concentration and calculated as (Muller, 1981, Wang et al., 2021):

$$I_{geo} = \log_2 \left[\frac{C_n}{1.5B_n} \right], \quad (3-13)$$

where C_n represents the heavy metal concentration in the sample and B_n is the background value for each evaluated metal. The I_{geo} represents seven categories of pollution levels according to $I_{geo} < 0$ (unpolluted), $0 < I_{geo} < 1$ (unpolluted to moderate pollution), $1 < I_{geo} < 2$ (moderately polluted), $2 < I_{geo} < 3$ (moderate to heavily polluted), $3 < I_{geo} < 4$ (heavily polluted), $(4 < I_{geo} < 5)$ (heavily polluted to extreme pollution), and $5 < I_{geo}$ (extreme pollution) (Calmuc et al., 2021; Luo et al., 2021).

3.4.4 Pollution Load Index (PLI)

The heavy metal pollution status of sediment was also evaluated using the Pollution load index (PLI) (e.g., Nkinda et al., 2021; Rahman et al., 2022, Shirani et al., 2020):

$$CF = \frac{C_s}{C_{ref}}, \quad (3-14)$$

$$PLI = \sqrt[n]{CF_1 \times CF_2 \times CF_3 \times \dots \dots CF_n} \quad (3-15)$$

where CF is the contamination factor, C_s and C_{ref} represent the present concentration of the metals and the background value, respectively; n is number of metals. In this study the, the PLI was calculated by using the measured value of Fe, Mn, Cr, Cd, Pb, Ni, Cu, and Zn. Based on CFs the classification is: $CF < 1$, low contamination; $1 < CF < 3$, moderate; $3 < CF < 6$, considerable; $CF \geq 6$, very high contamination. When $PLI = 1$, it suggests baseline levels of pollutants, and no pollution when $PLI < 1$, but $PLI > 1$ indicates progressive deterioration (Anwar, 2019; Singh et al., 2017).

3.4.5 Statistical analysis

The Pearson correlation was used to evaluate the interrelationship between the quality

parameters in surface water and sediment using SPSS 17.0 (Windows; IBM, USA). Furthermore, multi-variate analyses by principal component analysis (PCA) were used to identify potential sources of pollutants. The PCA was performed using the varimax normalized rotation method. Similarly, hierarchical cluster analysis (HCA) was carried out using Ward's method. HCA was applied to classify sampling sites into sub-clusters. The PCA and HCA were processed using JMP Pro 15.

3.5 Results and Discussion

3.5.1 Water pollutants

The physicochemical parameters in surface water are summarized in **Table 3-1** and compared with standards from World Health Organization (WHO, 2011; WHO, 1984), Department of Environment, Bangladesh (DoE) (Department of Environment, Peoples' Republic of Bangladesh, 1997), United States Environmental Protection Agency (USEPA, 2009) for health-based guidelines, and Canadian Council of Ministers of the Environment (CCME) for aquatic life (Canadian Council of Ministers of the Environment, 2007). The water temperature was between 27.3 and 28.5 °C with mean 27.7 ± 0.42 °C. The highest and lowest temperature was found at sampling location S-3 and S-7, respectively. As the sampling was performed at different times of the day, the temperature might have varied slightly with sampling time during the day. The low temperature may be due to contribution of heavy stormwater runoff and industrial cooling water.

The toxicity of metals is greatly influenced by the pH. The pH ranged from 7.1 to 7.6 (mean of 7.4 ± 0.20) and indicated slightly alkaline river water. Untreated industrial and municipal wastewater is likely resulting in alkaline conditions (Sultana et al., 2016). Upstream water and heavy rainfall tend to keep the pH neutral during the rainy season.

The EC ranged from 336.0 to 467.0 $\mu\text{S}/\text{cm}$ (mean 418.6 ± 33.6 $\mu\text{S}/\text{cm}$). TDS ranged from 156.0 to 178.0 mg/L (mean 163.3 ± 6.5 mg/L). TDS was within national and international recommended standards. The TDS value of Shitalakshaya River is comparable with the reported value of Ganges River, Bangladesh (Haque et al., 2020).

TSS mean was 1023.8 ± 863.5 mg/L with a range from 70.0 to 2540.0 mg/L. All TSS concentrations exceeded the DoE standard limits. High TSS at most locations can be attributed to anthropogenic sources. The S-8 and S-9 showed the highest TSS. These stations are close to the Tarabo Bazar and edible oil industry. Human activities include Narangonj City municipal waste discharge, landfills close to the bazar, domestic wastewater, surface drainage for irrigated vegetables, canals carrying soil and agrochemicals, and car workshops situated on the riverbank. The light transmission in the riverine system and aquatic life are affected by the high TSS contents (Islam et al., 2022).

Total alkalinity was 78.7 ± 7.5 mg/L on average, with a range of 68.3 to 91.0 mg/L. The chloride concentration ranged from 2.2 to 4.2 mg/L with an average of 2.6 ± 0.60 mg/L. The average

Table 3-1 Descriptive statistics of physicochemical parameters in water and comparative study with standards

Sample ID	Temp. °C	pH	EC $\mu\text{S/cm}$	TDS mg/L	TSS mg/L	Cl ⁻ mg/L	Alkalinity mg/L	Total Hardness mg/L	COD mg/L
S-1	27.5	7.4	406.0	156.0	684.0	2.2	84.5	163.3	53.2
S-2	28.2	7.1	442.0	169.0	610.0	2.8	78.0	166.7	69.7
S-3	28.5	7.1	467.0	178.0	1586.0	4.2	68.3	160.0	83.9
S-4	27.4	7.6	430.0	164.0	708.0	2.5	91.0	173.3	53.2
S-5	27.5	7.6	427.0	165.0	562.0	2.5	87.8	160.0	46.1
S-6	27.4	7.5	418.0	161.0	578.0	2.3	71.5	156.7	43.7
S-7	27.3	7.6	416.0	160.0	444.0	2.2	74.8	193.3	108.8
S-8	27.5	7.6	428.0	164.0	2456.0	2.8	71.5	180.0	42.6
S-9	27.4	7.5	416.0	159.0	2540.0	2.2	78.0	173.3	61.5
S-10	28.1	7.4	336.0	157.0	70.0	2.3	81.3	146.7	43.7
Max.	28.5	7.6	467.0	178.0	2540.0	4.2	91.0	193.3	108.8
Min	27.3	7.1	336.0	156.0	70.0	2.2	68.3	146.7	42.6
Mean \pm	27.7 \pm	7.4 \pm	418.6 \pm	163.3 \pm	1023.8 \pm	2.6 \pm	78.7 \pm	167.3 \pm	60.6 \pm
SD	0.42	0.20	33.6	6.5	863.5	0.60	7.5	13.2	21.5
WHO	-	6.5-8.5	-	1000	-	250	-	500	-
DoE	20-30	6.5-8.5	-	1000	10	600	-	200-500	4
USEPA	-	6.5-8.5	-	500	-	250	-	-	-
CCME (Fish and aquatic live)		7.0-8.7	-	-	-	120	-	200-250	-

WHO=World Health Organization (WHO, 1984; 2011), DoE=Department of Environment (Department of Environment, Peoples' Republic of Bangladesh, 1997), USEPA=United State Environmental Protection Agency (USEPA, 2009), CCME=Canadian Council of Ministers of the Environment (Canadian Council of Ministers of the Environment, 2007).

concentration of total hardness was 167.3 ± 13.2 mg/L. The chloride concentration and total hardness were within the health-based guidelines of WHO, DoE, and CCME for fish and aquatic life.

The COD ranged from 42.6 to 108.8 mg/L with an average of 60.6 ± 21.5 mg/L (**Table 3-1**).

COD exceeded the DoE maximum concentration at all locations. The COD levels indicate a high organic load to the river. Municipal domestic waste, sewage outfalls, cattle and sheep manure, septic tank discharge, and urea-like fertilizers in agricultural areas are the river's primary sources of organic pollutants (e.g., Mekuria et al., 2021). Thus, Shitalakshaya River is highly contaminated with organic pollutants. High COD and hence organic pollutants affect the river water quality due to foul odor and reduced aesthetic value of the river. The high COD and organic contamination make the river watercolor look black.

The concentrations of Fe, Mn, Cr, Cd, Pb, Co, Ni, Cu, and Zn in surface water and comparison with health-based guidelines of WHO, DoE, USEPA, and CCME are shown in **Table 3-2**. The concentration of Fe, Mn, Cr, Pb, Co, Ni, Cu, and Zn ranged from 267.0–53156.0, 5.0–60.0, (< 0.41)–329.0, 150.0–200.0, (< 2.1)–35.0, (< 2.2)–25.0, 21.0–123.0, and 120.3–412.6 $\mu\text{g/L}$, respectively.

The concentration of Cd for all sampling points was below the detection limit (BDL) (< 0.29 $\mu\text{g/L}$). Thus, the metal concentrations of the Shitalakshaya River are high but compatible with other Bangladesh rivers (**Table 3-3**). The average concentration of heavy metals in water samples was in the decreasing order Fe (14043.1 ± 18488.2) > Zn (229.9 ± 97.3) > Pb (172.0 ± 18.1) > Cu (49.3 ± 34.6) > Cr (32.9 ± 0.0) > Mn (27.4 ± 16.8) > Co (10.3 ± 9.5) > Ni (6.3 ± 6.7) > Cd (BDL) (< 0.2910) $\mu\text{g/L}$. According to DoE, health standard guidelines for water is Fe (300-1000) $\mu\text{g/L}$, Mn (100 $\mu\text{g/L}$), Cr (50 $\mu\text{g/L}$), Cd (5 $\mu\text{g/L}$), Pb (50 $\mu\text{g/L}$), Ni (100 $\mu\text{g/L}$), Cu (1000 $\mu\text{g/L}$), and Zn (5000 $\mu\text{g/L}$) (**Table 3-2**).

The concentration of Fe and Pb for all sampling sites was higher than the WHO, DoE, and USEPA maximum permissible limits for drinking water. The maximum and minimum Fe concentration was found at S-2 (53.2 mg/L) and S-9 (267.0 $\mu\text{g/L}$), respectively. Iron exists naturally in river water due to natural geologic deposits. Iron at average temperature is usually deposited from solutions such as hydrous sesquioxide, carbonates, sulfides, or hydrous silicates of iron and potash known as glauconite. The primary anthropogenic sources of Fe contents in the Shitalakshaya River are untreated industrial effluents, improper disposal of domestic waste, and agricultural runoff.

The mean, maximum, and minimum concentration of Pb in the study area was 172.0 ± 18.1 $\mu\text{g/L}$, 200.0 $\mu\text{g/L}$ (S-9, S-10), and 150.0 $\mu\text{g/L}$ (S-5, S-7), respectively. The data indicate that Pb is associated with anthropogenic sources. The sampling locations S-9 and S-10 are close to the heavily residential area of Taraba Paourashava and a trunk road with heavy traffic. Many car garages, shipping boats, transport, and fishing boats are situated close to these locations. In Dhaka (Bangladesh), the value of $\text{PM}_{2.5}$ in the motorized area is 4-times and 2-times higher than the WHO standard and Bangladesh standards, respectively, as compared to vehicle-free areas (Kumar et al., 2021). In coastal areas of Bangladesh, the anthropogenic sources of Pb are related to fishery, painting, shipping, industrial effluents, and sewage discharge (Sarker et al., 2020). High Pb concentration may be related to gasoline additives, wear from axle bearing of vehicles, rust preventive agents for wheels, lubricating

Table 3-2 Descriptive statistics of heavy metals in water and comparative study with standards

Sample	Fe	Mn	Cr	Cd	Pb	Co	Ni	Cu	Zn
ID	µg/L	µg/L	µg/L	µg/L	µg/L	µg/L	µg/L	µg/L	µg/L
S-1	6788.0	37.0	BDL	BDL	170.0	9.0	16.0	92.0	412.6
S-2	53156.0	60.0	BDL	BDL	180.0	14.0	12.0	66.0	287.1
S-3	6764.0	21.9	BDL	BDL	170.0	16.0	BDL	34.0	339.8
S-4	850.0	13.7	329.0	BDL	160.0	BDL	BDL	21.0	242.7
S-5	951.0	19.9	BDL	BDL	150.0	BDL	BDL	29.0	132.1
S-6	1617.0	14.5	BDL	BDL	160.0	BDL	BDL	25.0	120.3
S-7	5380.0	19.2	BDL	BDL	150.0	9.0	BDL	30.0	124.8
S-8	30400.0	41.9	BDL	BDL	180.0	13.0	25.0	52.0	195.9
S-9	267.0	5.0	BDL	BDL	200.0	7.0	BDL	21.0	186.8
S-10	34258.0	40.7	BDL	BDL	200.0	35.0	10.0	123.0	256.8
Max.	53156.0	60.0	329	-	200.0	35.0	25.0	123.0	412.6
Min.	267.0	5.0	BDL	-	150.0	BDL	BDL	21.0	120.3
Mean ±	14043.1 ±	27.4 ±	32.9±	-	172.0 ±	10.3 ±	6.3 ±	49.3 ±	229.9±
SD	18488.2	16.8	0.00	-	18.1	9.5	6.7	34.6	97.3
WHO	300	100	50	3	10	-	70	2000	5000
DoE	300-1000	100	50	5	50	-	100	1000	5000
USEPA	300	50	100	5	15	-	-	1300	5000
CCME			1.0						
(Fish and aquatic live)	-	430	(VI), 8.9 (III)	0.09	-	-	-	-	7

BDL=Bellow Detection Limit (Cr=0.4068 µg/L, Cd=0.2910 µg/L, Co=2.1319 µg/L, Ni=2.1716 µg/L); WHO=World Health Organization (WHO, 1984; 2011), DoE=Department of Environment (Department of Environment, Peoples' Republic of Bangladesh 1997), USEPA=United State Environmental Protection Agency (USEPA, 2009), CCME=Canadian Council of Ministers of the Environment (Canadian Council of Ministers of the Environment, 2007).

oil from ships, boats, and local car workshops wastes. Thus, automobile emission, shipping and fishing boats, and stormwater runoff from highways are possible sources of Pb contamination in this area.

The maximum and minimum Zn contents were found at S-1 (412.6 µg/L) and S-6 (120.3 µg/L), respectively. All samples exceeded the maximum allowable concentration of CCME for aquatic life. Probable anthropogenic sources of Zn are agricultural runoff, excessive use of fertilizers and pesticides,

and industrial wastewater (Kibria et al., 2016). As the sampling points are associated with dense urban areas, urban stormwater may also be an important source of Zn pollution. Mn concentration ranged between 5.0-60.0 µg/L.

Mn concentration at S-2 was higher than USEPA standard limits. The sources of Mn can be both natural and anthropogenic. Mn is often found in chemical fertilizers as it is an essential element for crop production. Thus, it is likely that Mn origins from uplands agricultural fields. Besides, Mn can also stem from industrial effluents, and uncontrolled release or leakage from landfill sites of the study area. The concentration of Cr at all sampling stations was below the detection limit (< 0.41 µg/L) except at S-4. The concentration of Cr at S-4 was higher than standard limits of WHO, DoE, USEPA, and CCME. The Cr is introduced in aquatic habitats by different types of industrial activities, metal ceramics, textile, tanneries dyes, jewelry, and foundry products (Sarker et al., 2020). A large sewage outlet and stormwater canals are associated with this sampling station containing industrial leather and dyeing wastewater, cooling tower additives with high Cr content, and domestic wastewater from urban areas.

3.5.2 Metal distribution in sediment

Ecotoxicological analyses and studies to identify baseline values, especially in river sediments, are limited in developing nations, particularly Bangladesh. As a result, instead of ecotoxicological data, consensus-based sediment quality guidelines (SQGs) were used in the present study. Environmental quality standards (EQSs) for heavy metals in sediments do not exist for Bangladesh. As a result, the heavy metal contamination in shallow sediments of the Shitalakshaya River was assessed using consensus based SQGs. Turekian and Wedepohl's Average Shale Values (ASVs) are often employed as background values in evaluating sediment pollution (Algul and Beyhan, 2020; Ali et al. 2016; Gaonkar et al., 2021). Thus, we used ASVs instead of background values in the present study. SQGs provide standards for evaluating sediment quality and the environmental danger of heavy metals. For the sediment chemistry and biological effects, empirical SQGs are the most used guideline. The geometric means of different SQGs, including those generated using USEPA and similar guidelines, were used to calculate consensus based SQGs. The threshold effect concentration (TEC) and probable effect concentration (PEC) are effect estimates that can be used as SQGs. Heavy metals are unlikely to harm organisms if the sediment contents are below the TEC. Toxic effects are likely to emerge if heavy metal concentrations in the sediment exceed PEC. The mean concentrations of the selected heavy metals such as Fe, Mn, Cr, Cd, Pb, Co, Ni, Cu, and Zn in sediment samples were compared with the maximum permissible levels (MPL) of heavy metals set by the ASV (Algul and Beyhan, 2020; Ali et al., 2016), TEC, PEC (Algul and Beyhan, 2020), China National Environment Monitoring Center (CNEMC) (Xie et al., 2020), and CCME standard limit for aquatic life (Canadian Council of Ministers of the Environment, 2007) (**Table 3-4**).

Table 3-3 Comparison of mean concentration of heavy metals in water ($\mu\text{g/L}$) and sediment (mg/kg) of Shitalakshaya River along with relevant literature data

River	City	Country	Conc. of metal in surface water($\mu\text{g/L}$)									Reference
			Fe	Mn	Cr	Cd	Pb	Co	Ni	Cu	Zn	
Shitalakshaya	Dhaka	Bangladesh	14043.1	27.4	32.9	BDL	172.0	10.3	6.3	49.3	229.9	Present Study
Halda	Chittagong	Bangladesh	3320.0	100.0	-	0.92	24.5	6.6	9.4	23.8	24.0	(Islam et al., 2020)
Dhaleshwari	Dhaka	Bangladesh	-	-	2970.0	1705.0	1170.0	-	-	1050.0	-	(Lipy et al., 2021)
Pashur river	Mongla	Bangladesh	-	-	48.9	1.6	23.4	-	-	-	-	(Ali et al., 2018)
Brahmaputra	Narsingdi	Bangladesh	-	1440.0	10.0	1.0	110.0	200.0	440.0	120.0	10.0	(Bhuyan et al., 2019)
Dhalai Beel and Bangshi	Dhaka	Bangladesh	-	88.0	93.0	7.0	108.0	-	35.0	1050.0	3320.0	(Rahman et al., 2014)
Turag and Burigonga	Dhaka	Bangladesh	7000.0, 12310.0	-	610.0, 1990.0	-	320.0, 280.0	-	960.0, 1050.0	750.0, 690.0	1600.0, 1065.0	(Hossain et al., 2021)
Korotoa	Bogura	Bangladesh	-	-	78.0	9.5	31.0	-	35.5	67.0	-	(Islam et al., 2015)
Bhairab	Khulna	Bangladesh	-	-	31.7	1.4	23.8	-	-	-	-	(Ali et al., 2022)
Nakuvadra-Rakiraki	Rakiraki	Fiji	198.0	358.0	133.0	3.1	12.4	67.2	50.2	22.4	46.1	(Kumar et al., 2021)
River	City	Country	Conc. of metal in sediments (mg/kg)									Reference
			Fe	Mn	Cr	Cd	Pb	Co	Ni	Cu	Zn	
Shitalakshaya	Dhaka	Bangladesh	611.9	234.5	20.7	BDL	71.8	8.3	24.3	55.3	113.0	Present Study
Halda	Chittagong	Bangladesh	-	628.0	90.7	0.42	18.2	13.8	37.0	17.8	54.5	(Islam et al., 2020)
Dhaleshwari	Dhaka	Bangladesh	-	-	107.2	1.7	24.9	-	-	22.7	-	(Lipy et al., 2021)
Pashur river	Mongla	Bangladesh	-	-	51.3	1.7	27.8	-	-	-	-	(Ali et al., 2018)
Brahmaputra	Narsingdi	Bangladesh	-	126.2	6.6	0.48	7.6	4.1	12.8	6.2	52.7	(Bhuyan et al., 2019)
Dhalai Beel and Bangshi	Dhaka	Bangladesh	-	483.4	98.1	0.61	59.9	-	25.7	31.0	117.2	(Rahman et al., 2014)
Turag and Burigonga	Dhaka	Bangladesh	4233.0, 4655.0	-	70, 106.0	-	31, 17.0	-	56, 33.0	48.0, 31.0	163.0, 29.0	(Hossain et al., 2021)
Korotoa	Bogura	Bangladesh	-	-	109.0	1.2	58.0	-	95.0	76.0	-	(Islam et al., 2015)
Bhairab	Khulna	Bangladesh	-	-	34.2	1.7	25.5	-	-	-	-	(Ali et al., 2022)
Nakuvadra-Rakiraki	Rakiraki	Fiji	28,651.0	590.0	108.0	0.99	32.0	14.5	71.5	42.1	53.7	(Kumar et al., 2021)

Table 3-4 Descriptive statistics of heavy metals in sediment and comparative study with standards

Sample ID	Fe mg/kg	Mn mg/kg	Cr mg/kg	Cd mg/kg	Pb mg/kg	Co mg/kg	Ni mg/kg	Cu mg/kg	Zn mg/kg
S-1	607.2	210.2	16.8	BDL	389.3	5.0	13.9	282.7	184.9
S-2	612.7	206.7	20.5	BDL	44.4	7.1	21.1	24.2	97.2
S-3	615.3	238.2	26.3	BDL	28.5	10.6	30.3	52.2	199.4
S-4	613.1	235.4	18.0	BDL	15.5	10.4	28.3	23.7	67.9
S-5	610.5	161.5	18.5	BDL	69.3	5.5	20.8	34.3	149.4
S-6	613.0	285.8	26.4	BDL	16.5	11.6	34.1	34.1	98.9
S-7	611.2	267.3	18.9	BDL	52.5	7.0	15.4	26.6	94.4
S-8	610.3	208.0	14.5	BDL	27.4	5.9	19.6	20.9	82.8
S-9	610.2	261.3	20.5	BDL	51.2	9.1	26.9	27.2	98.2
S-10	615.5	270.4	26.6	BDL	22.9	10.7	32.4	27.5	56.9
Max.	615.5	285.8	26.6	-	389.3	11.6	34.1	282.7	199.4
Min.	607.2	161.5	14.5	-	15.5	5.0	13.9	20.9	56.9
Mean ± SD	611.9± 2.5	234.5± 38.2	20.7± 4.3	-	71.8± 112.9	8.3± 2.5	24.3± 7.1	55.3± 80.4	113.0± 48.4
ASV	47200	850	90	0.3	20	19	68	45	95
TEC	-	-	43.4	0.99	35.8	-	22.7	31.6	121
PEC	-	-	111	4.99	128	-	48.6	149	459
CNEMC	14355	462	31.9	0.119	10.9	-	18.8	17	61.1
CCME for aquatic live	-	-	37.3	0.6	35	-	-	35.7	123

BDL=Bellow Detection Limit (Cd=0.2910 µg/L); ASV=Average Shale Value (Algul and Beyhan, 2020; Ali et al., 2016), TEC=Threshold Effect Concentration (Algul and Beyhan, 2020), PEC=Probable Effect Concentration (Algul and Beyhan, 2020), CNEMC=China National Environment Monitoring Center (Xie et al., 2020), CCME=Canadian Council of Ministers of the Environment (Canadian Council of Ministers of the Environment, 2007).

The concentration range of metals Fe, Mn, Cr, Cd, Pb, Co, Ni, Cu, and Zn was 607.2–615.5 mg/kg, 161.5–285.8 mg/kg, 14.5–26.6 mg/kg, BDL (< 0.291 µg/kg), 15.5–389.3 mg/kg, 5.0–11.6 mg/kg, 13.9–34.1 mg/kg, 20.9–282.7 mg/kg, and 56.9–199.4 mg/kg, respectively. The mean concentration of Fe, Mn, Cr, Cd, Pb, Co, Ni, Cu, and Zn in sediments for all the sampling points was 611.9 ± 2.5 mg/kg, 234.5 ± 38.2 mg/kg, 20.7 ± 4.3 mg/kg, BDL (< 0.2910), 71.8 ± 112.9 mg/kg, 8.3 ± 2.5 mg/kg, 24.3 ± 7.1 mg/kg, 55.3 ± 80.4 mg/kg, and 113.0 ± 48.4 mg/kg, respectively. The mean

metal concentrations were in descending order Fe > Mn > Zn > Pb > Cu > Ni > Cr > Co > Cd. The concentration of heavy metals in the sediment of the Shitalakshaya River is compatible with that of other river sediment in Bangladesh (**Table 3-3**).

The mean concentration of Fe, Mn, Cr, Cd, Co, and Ni in sediment for all sampling points was lower than the ASV permissible limits. The mean concentration of Pb (71.8 ± 112.9 mg/kg) in sediment for all locations was much higher than ASV, TEC, CNEMC, and CCME standards for aquatic life. High Pb contents most probably stem from anthropogenic sources such as shipping and fishing boat exhaust, paint products, and car traffic from impermeable surfaces. The mean concentration of Ni (24.3 ± 7.1 mg/kg) was higher than the TEC and CNEMC standards. A possible source of Ni may be paper mills and dockyards on the bank of the Shitalakshaya River. Also, car exhausts and wear, fossil fuel burning, municipal and industrial waste may contribute to the high Ni contents in the study area.

The average concentration of Cu (55.3 ± 80.4 mg/kg) was higher than the standards of ASV, TEC, CNEMC, and CCME for aquatic life. The S-1 concentration of Cu exceeded the maximum limit of PEC. The primary anthropogenic source of Cu in sediment is related to Cu-containing pesticides (copper oxychloride) and fertilizers (copper sulfate, cuprous, and cupric oxide) from agricultural field. Antifouling paint used for boats is another important source of Cu in river sediment (e.g., Nazneen et al., 2018).

The mean concentration of Zn (113.0 ± 48.4 mg/kg) was much higher than the ASV and CNEMC standard. Zn at S-1, S-3, and S-5 exceeded the maximum limit of TEC and CCME standards for aquatic life. Smelting, soil erosion due to rainfall, fossil fuel, and land construction activities are potential anthropogenic sources of Zn (Singh et al., 2017). In view of the above, SQGs indicate that Pb, Co, Ni, Cu, Zn, and mostly Pb, Cu, Zn in sediment pose a severe threat to the ecosystem in the Shitalakshaya River.

3.5.3 Water and sediment pollution indices

3.5.3.1 Water pollution indices

WQI classifies the quality of water and pollution level. The *WQI* was calculated using water pH, TDS, total hardness, TSS, chloride, COD, Fe, Mn, Cr, Cd, Pb, Ni, Cu, and Zn (by considering BDL value as zero). The *WQI range* was 315.5–499.8, with a mean value of 395.6. The higher and lower values of *WQI* were found at S-2 and S-5, respectively. The average *WQI* exceeded the limit of > 300, which indicates the pollution status is in grade 5 that the water in all these locations falls under the “very poor water” category. The calculated *WQI* were in decreasing order S-2 > S-10 > S-8 > S-9 > S-3 > S-1 > S-4 > S-6 > S-7 > S-5 (**Table 3-5**). The spatial distribution of different water quality

indices (*WQI*, *HEI*, and C_d) was evaluated by the QGIS (version 2.18.2). Lower values of quality indices are represented by light red color while deep red indicates a highly polluted area (**Fig. 3-2**). The spatial variation of *WQI* is shown in **Fig. 3-2a**. The figure shows that the northern region of the study area has the highest pollution pressure. The lowest *WQI* is at the center of the area, and there is an individual extreme high pollution in a southern area.

The *HEI* and C_d were calculated (by considering BDL as zero) from the concentrations of Fe, Mn, Cr, Cd, Pb, Ni, Cu, and Zn. The *HEI* was used to determine the overall quality of water in terms of heavy metal content, which is an essential tool for quantifying water pollution. The river water *HEI* range and average values were 18.4-196.0 and 65.1, respectively. The maximum and minimum values were for S-2 and S-5, respectively. All sampling locations (except S-5, which contained a medium pollution level) of the study area exceeded the maximum contamination level of $HEI > 20$. Thus, it can be concluded that this river is highly contaminated with heavy metals. The metals followed the decreasing order S-2 > S-10 > S-8 > S-1 > S-3 > S-7 > S-4 > S-6 > S-9 > S-5 (**Table 3-5**). The spatial distribution of *HEI* indicates that the north-western region of the study area is associated with a very high pollution pressure. There is extremely high pollution in the southern area (**Fig. 3-2b**).

The C_d shows the combined effects of water quality characteristics based on heavy metal pollution that is hazardous to human health. The range and average values of C_d were 10.4–188.0 and 57.1, respectively. From the calculated C_d , it can be stated that all sampling sites are highly contaminated by metals, as it exceeded the maximum contamination level of $C_d > 3$ (highly contaminated). The maximum and minimum contamination levels were found, at S-2 and S-5, respectively. The calculated values of C_d were in descending order S-2 > S-10 > S-8 > S-1 > S-3 > S-7 > S-4 > S-6 > S-9 > S-5 (**Table 3-5**). The spatial distribution of C_d is shown in **Fig. 3-2c**. It follows the same trend as for *HEI*. Again, the north-western region of the study area stands out as more polluted, and an extremely high pollution area was also found in the southern area. The spatial distribution of both *HEI* and C_d showed high similarity, including metal variables. Therefore, the contamination sources of this area are also like the *HEI*, and both are related to geogenic and anthropogenic sources.

The spatial distribution *WQI*, *HEI*, and C_d indicates that S-2, S-10, and S-8 are the most polluted areas of the study area. For water samples, TSS, COD, Fe, Pb, and Zn are the primary anthropogenic pollutants in the river water. Industries such as pharmaceutical, agrochemical, textile, edible oil, tea, and mineral water are located in the residential areas in the northern region. The south region (downstream) is influenced by processing and transport of industrial machinery, pulp, paper mills, Siddirganj Bazar, and agricultural areas. The middle-high polluted area is associated with the vegetable oil industry, pulp-paper and board mills, jute mill, and Taraba Bazar. Therefore, these adjacent industries together with urban and agricultural areas with massive landfill leachate from local bazars are responsible for water quality deterioration and high pollution pressure.

Table 3-5 Calculated value of Water Quality Index (*WQI*), Heavy metal Evaluation Index (*HEI*), and Degree of Contamination (*C_d*) with pollution level

Sample ID	Water Quality Index (<i>WQI</i>)	Heavy metal Evaluation Index (<i>HEI</i>)	Degree of Contamination (<i>C_d</i>)	Pollution Level
S-1	371.8	40.4	32.4	High
S-2	499.8	196.0	188.1	High
S-3	373.0	39.8	31.8	High
S-4	363.6	25.6	17.6	High
S-5	315.5	18.4	10.4	High
S-6	337.7	21.6	13.6	High
S-7	326.3	33.2	25.2	High
S-8	450.9	120.2	112.2	High
S-9	421.6	20.9	12.9	High
S-10	495.8	134.9	126.9	High
Average	395.6	65.1	57.1	High

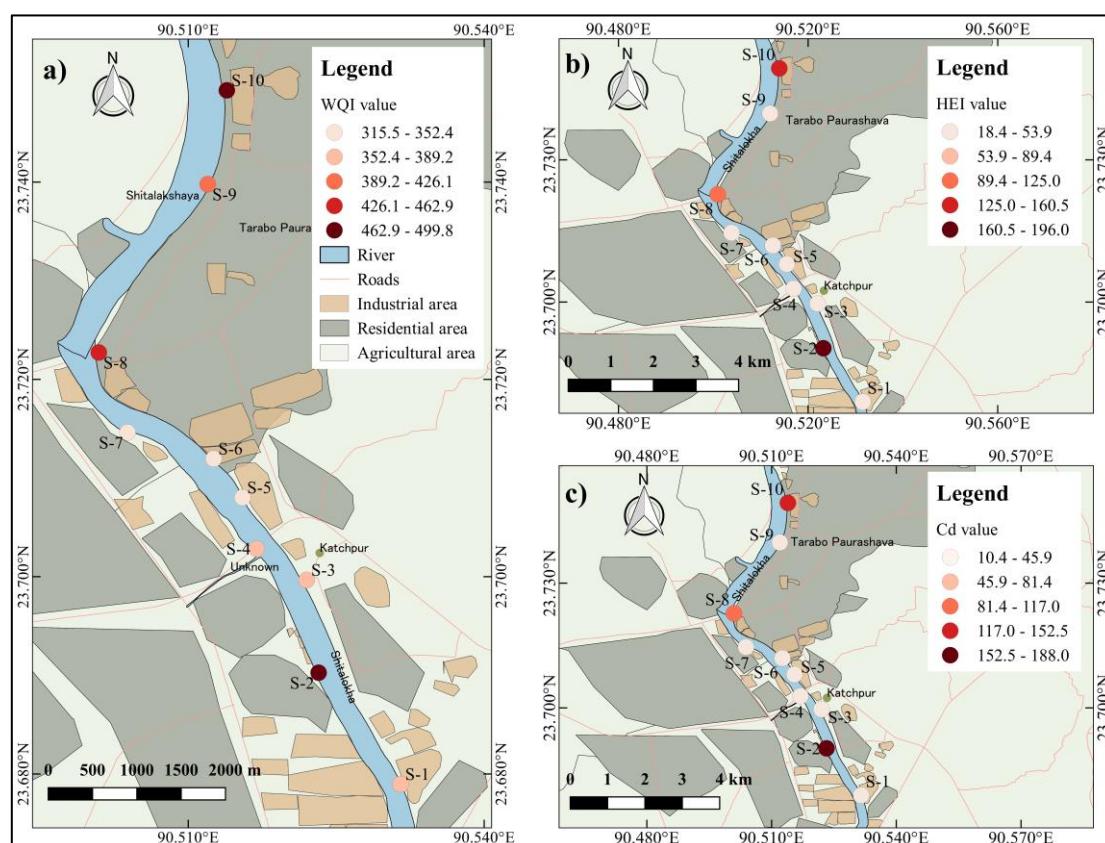


Fig. 3-2 Spatial distribution of a) *WQI*, b) *HEI*, and c) *C_d* for water sample.

3.5.3.2 Sediment pollution indices

I calculated sediment pollution indices (by considering BDL as zero) $PERI$, I_{geo} , EF , and PLI to evaluate heavy metal pollution in the Shitalakshaya River. As the natural background value of metals is not available in Bangladesh, we used ASVs (Average Shale Values) to calculate the sediment pollution indices. The calculated $PERI$ and E_f^i (PER) is shown in **Fig. 3-3a**. The $PERI$ value ranged from 12.7–134.0, indicating a low-risk level for all sampling sites. The ecological risk factor (E_f^i) for an individual metals in sediment followed the descending order $Pb > Cu > Co > Ni > Zn > Cr > Mn > Cd$. The E_f^i value for all metals (except Pb) remained below 40. Still, sediment at sampling location S-1 is at potential ecological risk with Pb ($80 \leq E_f^i < 160$). The $PERI$ decreased in the order S-1 (134.0) > S-5 (26.3) > S-9 (21.9) > S-3 (20.8) > S-7 (20.8) > S-2 (18.9) > S-10 (15.5) > S-6 (15.4) > S-8 (13.6) > S-4 (12.7). $PERI$ indicates that sediment at most of the sampling locations are in low-risk conditions ($PERI < 150$). The potential ecological risk at S-1 (downstream area) is much higher than in other locations.

EF values were used to analyze the influence of anthropogenic sources on heavy metal concentrations in the Shitalakshaya River sediments. The calculated EFs are shown in **Fig. 3-3b**. Average EFs for Pb, Cu, and Zn and hence the enrichment level are relatively high. For Cr it is moderate, and for Mn, Co, and Ni it is significant. Thus, the EFs for Mn, Cr, Pb, Co, Ni, Cu, and Zn indicate both natural and anthropogenic sources of pollution. The average EFs of Pb, Cu, and Zn are very high (> 40), indicating that the sediment of the study area is contaminated with these metals from anthropogenic sources. The mean EF decreases in the order Pb (277.9) > Cu (95.2) > Zn (91.8) > Co (33.7) > Ni (27.5) > Mn (21.3) > Cr (17.7). It shows that Pb, Cu, Zn contents in the sediments of the study area are very high due to anthropogenic activities.

The I_{geo} status is shown in **Fig. 3-3c**. The mean I_{geo} decreases in the following order Pb (0.46) > Zn (-0.45) > Cu (-0.89) > Co (-1.8) > Ni (-2.1) > Mn (-2.5) > Cr (-2.7) > Fe (-6.9). The calculations show that most sampling sites $I_{geo} \leq 0$ and hence is uncontaminated with heavy metals. The sediment at sampling point S-1, though, is heavily polluted with Pb ($3 < I_{geo} < 4$), moderate to heavily polluted with Cu ($2 < I_{geo} < 3$), and unpolluted to moderate contamination with Zn ($0 < I_{geo} < 1$). The sampling locations S-2, S-7, S-9 with Pb, and S-3, S-5 with Zn are uncontaminated to moderately contaminated. The S-5 is also moderately polluted with Pb ($1 < I_{geo} < 2$). Thus, Pb, Cu, and Zn represent higher contamination level in the study area. The heavy metal contamination factors CF and PLI are shown in **Fig. 3-3d**. The $PLIs$ are in the range 0.27–0.54. The $PLIs$ for all sample stations were < 1 , indicating baseline levels of contamination.

Depending on the PLI level, the contamination decreases in descending order: S-1 (0.54) > S-3 (0.42) > S-9 (0.36) > S-6 (0.35) > S-5 (0.34) > S-10 (0.33) > S-7 (0.32) > S-2 (0.31) > S-4 (0.29) > S-8 (0.27). The CFs for Fe, Mn, Cr, Co, and Ni indicate a low degree of contamination, as $CF < 1$.

The *CFs* of Pb for the sampling locations S-2, S-3, S-7, S-8, S-9, and S-10; Cu for S-3; Zn for all sampling stations except (S-4, S-7, S-8, and S-10) indicate moderate contamination ($1 < CF < 3$). The *CFs* of Pb for S-5 indicate considerable contamination ($3 < CF < 6$), whereas the *CFs* of Pb, and Cu for sampling point S-1 indicate very high contamination. The mean *CFs* of elements decrease in the order Pb (3.6) > Cu (1.2) > Zn (1.2) > Co (0.44) > Ni (0.36) > Mn (0.28) > Cr (0.23) > Fe (0.01).

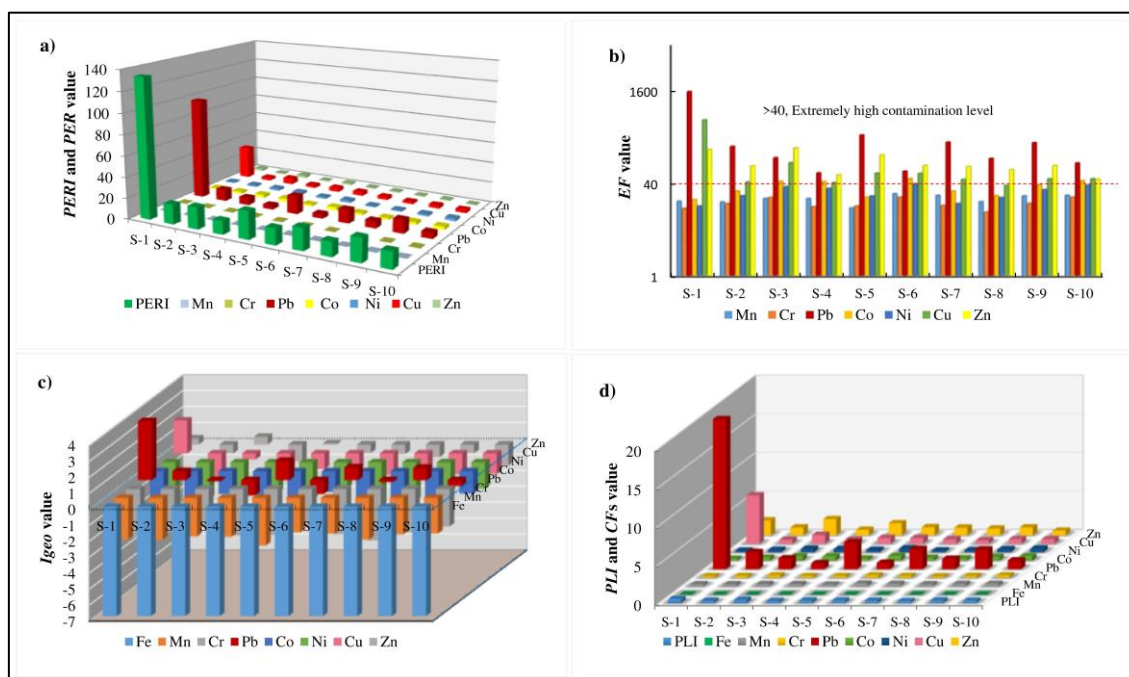


Fig. 3-3 a) Potential Ecological Risk Index (*PERI*), and Potential Ecological Risk (*PER*), b) Enrichment Factors (*EFs*), c) Geo-accumulation Index (*I_{geo}*), and d) Pollution Load Indices (*PLIs*) and Contamination Factors (*CFs*) for Shitalakshaya River shallow sediment

3.5.4 Pearson correlation

The relationships between the concentrations of different pollutants in water and sediment of the study area were analyzed by Pearson correlation. The correlation matrix for water samples shows a strong relationship between pH and temperature ($r = -0.89$, $p < 0.01$), EC and TDS ($r = 0.77$, $p < 0.01$), TDS with chloride ($r = 0.94$, $p < 0.01$), Fe and Mn ($r = 0.92$, $p < 0.01$), Co and Cu ($r = 0.80$, $p < 0.01$). Notably, no significant correlations were observed between alkalinity, total hardness, TSS, COD, Cr, and Zn (**Table 3-6**). Correlation analysis was also performed between the heavy metals of sediment samples (**Table 3-7**). Most metals showed strong positive correlation such as Fe-Cr ($r = 0.77$, $p < 0.01$), Fe-Co ($r = 0.80$, $p < 0.01$), Fe-Ni ($r = 0.78$, $p < 0.01$), Cr-Co ($r = 0.80$, $p < 0.01$), Cr-Ni ($r = 0.80$, $p < 0.01$), Pb-Cu ($r = 0.98$, $p < 0.01$), and Co-Ni ($r = 0.94$, $p < 0.01$). While moderate correlation was obtained between Fe-Pb ($r = -0.72$, $p < 0.05$), Mn-Co ($r = 0.74$, $p < 0.05$). Higher correlation

Table 3-6 Correlation matrix among the analyzed parameters in the water sample

	Temp.	pH	EC	TDS	TSS	Chloride	Alkalinity	TH	COD	Fe	Mn	Cr	Pb	Co	Ni	Cu	Zn
Temp.	1																
pH	-0.885**	1															
EC	0.117	-0.353	1														
TDS	0.656*	-0.666*	0.766**	1													
TSS	-0.079	-0.095	0.4	0.214	1												
Chloride	0.758*	-0.731*	0.609	0.935**	0.278	1											
Alkalinity	-0.317	0.542	-0.283	-0.376	-0.412	-0.48	1										
TH	-0.509	0.305	0.359	-0.05	0.347	-0.173	-0.127	1									
COD	0.15	-0.263	0.359	0.309	-0.048	0.234	-0.344	0.575	1								
Fe	0.541	-0.544	-0.189	0.128	-0.096	0.149	-0.166	-0.142	-0.091	1							
Mn	0.5	-0.521	-0.141	0.093	-0.21	0.147	-0.067	-0.174	-0.115	0.917**	1						
Cr	-0.234	0.352	0.119	0.038	-0.129	-0.056	0.581	0.159	-0.122	-0.251	-0.285	1					
Pb	0.355	-0.316	-0.447	-0.194	0.394	-0.021	-0.144	-0.3	-0.285	0.477	0.283	-0.232	1				
Co	0.646*	-0.444	-0.572	-0.036	-0.113	0.195	-0.232	-0.356	0.022	0.635*	0.552	-0.344	0.666*	1			
Ni	0.09	-0.17	-0.188	-0.178	0.227	-0.02	-0.111	0.036	-0.363	0.644*	0.764*	-0.246	0.371	0.397	1		
Cu	0.401	-0.244	-0.698*	-0.355	-0.369	-0.137	0.131	-0.484	-0.277	0.606	0.707*	-0.288	0.509	0.799**	0.603	1	
Zn	0.545	-0.553	0.054	0.183	-0.017	0.364	0.106	-0.31	-0.002	0.252	0.453	0.046	0.3	0.375	0.384	0.545	1

** . Correlation is significant at the 0.01 level (2-tailed).

* . Correlation is significant at the 0.05 level (2-tailed).

Table 3-7 Correlation matrix for heavy metals in river sediment

	Fe	Mn	Cr	Pb	Co	Ni	Cu	Zn
Fe	1							
Mn	0.422	1						
Cr	0.772**	0.598	1					
Pb	-0.715*	-0.298	-0.369	1				
Co	0.794**	0.739*	0.802**	-0.567	1			
Ni	0.779**	0.542	0.801**	-0.595	0.935**	1		
Cu	-0.607	-0.219	-0.253	0.982**	-0.435	-0.471	1	
Zn	-0.265	-0.398	0.03	0.559	-0.295	-0.26	0.602	1

** . Correlation is significant at the 0.01 level (2-tailed), * . Correlation is significant at the 0.05 level (2-tailed).

between variables may indicate common sources, similar or nearly identical metal accumulation properties, and mutual dependence of parameters with each other in surface water and sediment.

3.5.5 Principal component (PCA) and hierarchical cluster analysis (HCA)

PCA and HCA were used to analyze Fe, Mn, Ni, Cr, Co, Cu, Pb, and Zn for water and sediment and influencing physicochemical parameters TSS and COD for water. The data were standardized, and correlation between the quality parameters was used to find principal component scores, eigenvalues, and factor loadings. Based on the Kaiser criterion, the number of components in PCA was determined (Yu et al., 2018). According to this criterion, the component is acceptable when an eigenvalue is greater than 1. Thus, the first three components were obtained for water, and two components were extracted for the sediment samples. The first principal component is called Factor 1, the second Factor 2, and the third Factor 3, respectively. The obtained results of PCA for water and sediment sample are shown in **Table 3-8** and **Table 3-9**, respectively.

The eigenvalues for PCs for water samples ranged from 1.2 to 4.5, explaining 71.8% of the total variance. The three components explained 44.5, 15.0, and 12.3% of the total variance, respectively. Factor 1 had high positive loading for Fe, Mn, Pb, Co, Ni, and Cu ($r = 0.65-0.89$) and moderate loading for Zn ($r = 0.54$). Factor 2 had positive loading for TSS and Pb ($r = 0.55-0.93$). TSS was strongly associated, and Pb moderately associated with Factor 2. COD was only and strongly associated with Factor 3 ($r = 0.75$).

According to the Kaiser criterion, the sediment samples of the study area are a two-component system. The first two principal components accounted for 81.3% of the total variance. The eigenvalues ranged from 1.6–4.9. The selected two components explained 61.0, and 20.3%, respectively. Factor 1 had strong positive loading for Fe, Mn, Cr, Co, Ni ($r = 0.67-0.92$). This was also confirmed from the Pearson correlation matrix. Factor 2 was positively associated with Cr, Pb,

Cu, and Zn ($r = 0.52–0.65$). The positive relationship among the parameters indicates a similar source of origin that may be geogenic or anthropogenic such as industrial wastewater, agricultural run-off, and urban and municipal wastewater from the residential area.

Ward’s method with squared Euclidean distances was designated for HCA (e.g., Nakagawa et al., 2019). HCA for the water samples was performed based on the three PCs scores outlined above. Based on HCA, the sampling stations were classified into three different cluster groups as Cluster A, Cluster B, and Cluster C for water, and Cluster X, Cluster Y, Cluster Z for sediment sample, respectively. The average concentration of measured water and sediment quality parameters for each cluster group is shown in **Table 3-10a, b**.

Table 3-8 Principal component loadings and explained variance for the three components with Varimax normalized rotation in water sample

Parameters	Component 1	Component 2	Component 3
Total suspended solid (TSS)	-0.06	0.93	0.12
COD	-0.24	-0.32	0.75
Fe	0.85	-0.09	0.07
Mn	0.88	-0.24	-0.03
Cr	-0.37	-0.18	-0.67
Pb	0.65	0.55	0.06
Co	0.81	-0.06	0.29
Ni	0.78	0.23	-0.23
Cu	0.89	-0.25	-0.09
Zn	0.54	-0.12	-0.19
Eigen values	4.5	1.5	1.2
Explained variance (%)	44.5	15.0	12.3
Cumulative % of variance	44.5	59.5	71.8

According to **Table 3-10a**, cluster A is related to Fe, Mn, Co, Ni, Cu, Zn, and TSS; cluster B is related to TSS, COD, Fe, Pb, and Zn cluster C is related to COD and Cr. The calculated *WQI*, *HEI*, and *C_d* indicate that cluster A contained higher indices (*WQI*, *HEI*, *C_d*) than cluster B, and cluster C. Thus, cluster A represented the most polluted area. The decreasing order of indices and the hence contaminated area is Cluster A > Cluster B > Cluster C.

For sediment sample, Cluster X contained only one sample that was characterized by a relatively high concentration of Pb, Cu, and Zn. Cluster Y is associated with Cr, Pb, and Ni. Cluster Z is identified by a high Fe, Mn, and Zn concentration. The sediment quality indices PERI and PLI indicate that Cluster X is the most contaminated sediments of the study as shown in **Table 3-10b**.

The water and sediment sample principal component scatter plot are described by a. Factor 1 and 2, b. Factor 1 and 3, c. Factor 2 and 3 for water and d. Factor 1 and 2 for sediment. All water and sediment samples are classified into three clusters, as shown in **Fig. 3-4**. The components were not significantly affected by the water quality parameters at the site when a factor score is less than 0. Conversely, if a factor score is greater than 0, the water quality parameter characteristic influences

Table 3-9 Principal component loadings and explained variance for the two components with Varimax normalized rotation in sediment sample

Parameters	Component 1	Component 2
Fe	0.89	0.08
Mn	0.67	0.28
Cr	0.77	0.55
Pb	-0.81	0.52
Co	0.92	0.30
Ni	0.89	0.25
Cu	-0.72	0.64
Zn	-0.48	0.65
Eigen values	4.9	1.6
Explained variance (%)	61.0	20.3
Cumulative % of variance	61.0	81.3

Table 3-10 (a) Averaged concentrations of water quality parameters for each cluster group, **(b)** averaged concentrations of heavy metals in sediment for each cluster group

	Cluster A	Cluster B	Cluster C
(a)			
No. of samples	4	2	4
TSS (mg/L)	955.0	2063.0	573.0
COD (mg/L)	52.3	72.7	62.9
Fe (µg/L)	31150.5	3515.5	2199.5
Mn (µg/L)	44.9	13.5	16.8
Cr (µg/L)	0.0	0.0	82.3
Pb (µg/L)	182.5	185.0	155.0
Co (µg/L)	17.8	11.5	2.3
Ni (µg/L)	15.8	0.0	0.0
Cu (µg/L)	83.3	27.5	26.3
Zn (µg/L)	288.1	263.3	155.0
<i>WQI</i>	454.6	397.3	335.8
<i>HEI</i>	122.8	30.4	24.7
<i>C_d</i>	114.9	22.4	16.7
(b)	Cluster X	Cluster Y	Cluster Z
No. of samples	1	6	3
Fe (mg/kg)	607.2	611.3	614.6
Mn (mg/kg)	210.2	223.4	264.8
Cr (mg/kg)	16.8	18.5	26.4
Pb (mg/kg)	389.3	43.4	22.6
Co (mg/kg)	4.9	7.5	10.9
Ni (mg/kg)	13.9	22.0	32.3
Cu (mg/kg)	282.7	26.1	37.9
Zn (mg/kg)	184.9	98.3	118.4
<i>PERI</i>	133.6	19.1	17.3
<i>PLI</i>	0.54	0.32	0.37

TSS=Total suspended solid, COD= Chemical oxygen demand, *WQI*= Water quality index, *HEI*= Heavy metal evaluation index, *C_d*= Degree of contamination, *PERI*= Potential Ecological Risk Index, *PLI*= Pollution Load Index

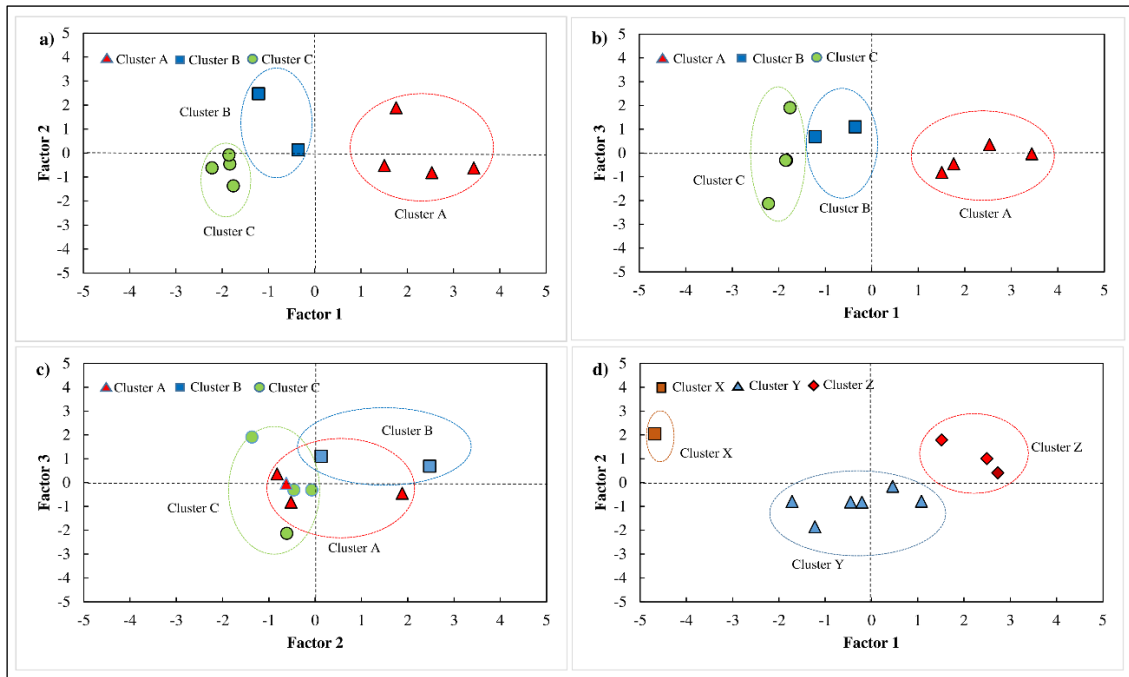


Fig. 3-4 Scatter plot for two principal components concerning cluster **a)** Factor 1 and Factor 2, **b)** Factor 1 and Factor 3, **c)** Factor 2 and Factor 3 for water, and **d)** Factor 1 and Factor 2 for sediment sample, respectively.

the component at the site (Nakagawa et al., 2016). The relationship between the water sample three factors (PCs) and two (PCs) of sediment samples is classified into three cluster groups shown in **Fig. 3-4**.

Cluster A for water samples is influenced by Factors 1 and 2 (**Fig. 3-4a**). Cluster B is to some extent affected by Factor 2. Cluster C shows smaller scores for both Factor 1 and Factor 2, indicating that this cluster contained less concentrations in water than Cluster A and B. Thus, it can be concluded that Cluster C was less contaminated than the other two clusters. **Fig. 3-4b, c** indicates that Cluster B is influenced by Factor 3. Factor 3 has less influence on Cluster C and A. Cluster A has higher Factor 1 scores than Cluster C and Cluster B, which has a positive score with Factor 2. Thus, samples of Cluster A have a higher concentration of pollutants from industrial, agricultural, and urban areas than clusters B and C and hence represent a more polluted zone in the study area. Factor 2 and Factor 3 scores show that Cluster B contained more pollutants from designated sources than Cluster C. Thus, Cluster B is more polluted than Cluster C. This was also confirmed by the *WQI*, *HEI*, and *C_d* values in **Table 3-10a**. Cluster X for sediments is influenced by Factor 2. Cluster Y is, to some extent, influenced by Factor 1. Cluster Z is affected by Factors 1 and 2 (**Fig. 3-4d**).

The spatial distribution of each cluster is shown in **Fig. 3-5** for both water and sediment. Cluster A is the most contaminated sample concerning physicochemical and toxicological parameters with high water quality indices (*WQI*, *HEI*, *C_d*) (**Fig. 3-5a**). The location of Cluster A is to the south

(downstream) and in the northern area (upstream). The southern area (downstream) associated with a large industrial and agricultural area, including a power plant industry and large local bazar, represented the highest pollution pressure. A highly polluted site is in the middle of the study area associated with the Tarabo Pourashava bazar. The northern area is associated with a high-density residential area. Therefore, the sources of pollution are not only from industrial wastewater and effluents but also from residential, municipal wastewater, and agricultural runoff. Cluster B is located in the southern and northern regions of the study area (**Fig. 3-5a**). The contamination of this area is lower than cluster A but higher than Cluster C. Cluster C is in the middle of the study area. Though all the sampling locations exceeded the maximum water quality evaluation indices, this cluster contained a lower pollution pressure than the other two Clusters, A and B.

The spatial distribution of each cluster for sediment in the study area is shown in **Fig. 3-5b**. This consisted of three clusters. Cluster X located in the southern area (downstream), is the most contaminated area concerning heavy metal contamination. The sediment analysis data showed that most of the metals were of geogenic sources, but the concentration of Pb, Cu, and Zn revealed that they have anthropogenic origin. The average Pb, Cu, and Zn concentration was higher in Cluster X than in Clusters Y and Z (**Table 3-10b**). Cluster Y is spread out along the entire study area. The sediment pollution pressure here is small regarding heavy metals. Cluster Z is located closer to the north. The medium polluted Cluster Z is situated to the north and southern area. The concentration of Cu and Zn in Cluster Z is higher than Cluster Y, attributed to anthropogenic sources.

The heavy metals' transport and fate are critical in the riverine system due to their toxicity, mobility, and reactivity with river water, sediment, and organisms. There was no regular correlation between water and sediment for the same sampling locations. Several processes (physical, hydrological, environmental, biological) and chemical reactivity (advection, dispersion, sorption/desorption, settling, sedimentation) are related to the transportation dynamics of heavy metals between water and sediment. The sediment is both a source and sink for heavy metals. The composition of sediments, such as their organic matter, size, and grain texture, is directly related to the association of heavy metals. The shallow sediment is responsible for the fate of heavy metals in the riverine system. It can act as a continuous source of contaminants that poses a severe risk to the health of an ecosystem.

The physical and chemical equilibrium, pH, state of elements, and organic matter contents control the distribution and accumulation of heavy metals in sediments. Generally, metal solubilization increases with lower pH, and dissolved heavy metals in the water adsorb to fine particles that settle in sediments (Debnath et al., 2021). Their high surface area facilitates the accumulation mechanism of heavy metals in sediments. Heavy metals are transported during the whole season, especially during the rainy monsoon period. They deposit on floodplains adjacent to river channels and assimilate into local biota. The study revealed that heavy metals such as Pb, Zn, Cu in sediment and Pb, Zn, Fe, TSS,

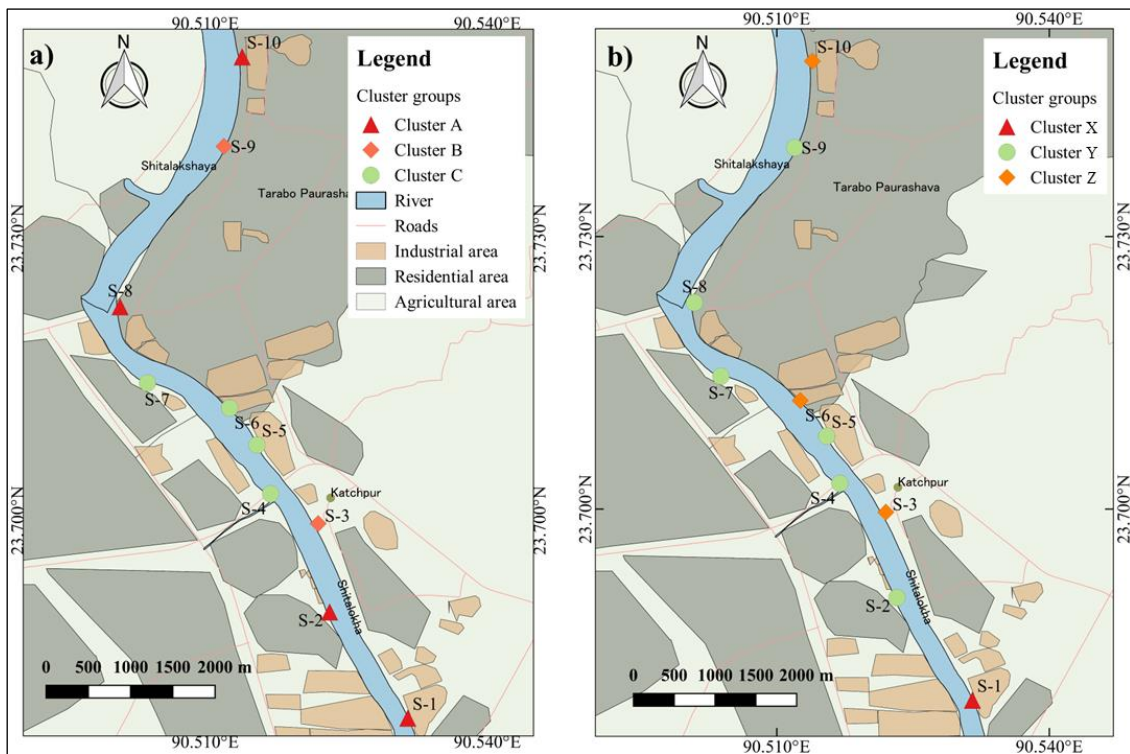


Fig. 3-5 Distribution of each cluster in the study area, **a)** water, **b)** sediment samples

COD, Cr, and Mn in water are at an alarming level in the investigated area.

The spatial analysis showed that the southern (downstream) and northern (upstream) area were the most polluted locations in the study area (**Fig. 3-5a**). These areas are associated with dense local industry, including power plants, residential areas, and local bazar. The bazar area is generally the most populated in Bangladesh with large waste generation. These areas represent loading and unloading of ships, barge transport, and transport and storage of different types of goods. Sometimes waste is discharged such as used oil and oily substances, coal, asbestos, and chemicals directly into the river. These are also possible sources of physicochemical and toxicological pollutants at this site. Again, **Fig. 3-5b** indicated the highest deposition of heavy metals in sediment in the southern area (downstream). This location is associated with large industries with many sewages outlet canals. Therefore, the pollutants attributed in this area are due to the loading of pollutants from upstream portions of the study area mixed with urban and industrial waste.

3.6 Conclusion

The present study assessed the physicochemical and toxicological contents of water and sediment of the Shitalakshaya River and compared them to standards of national and international quality guidelines. The analyses indicated that COD, TSS, Fe, Pb, Zn in water exceed the health-based guideline of DoE, WHO, USEPA, and CCME standard for aquatic life. Similarly, Pb, Co, Ni, Cu, Zn

(mainly Pb and Cu in sediment) exceeded the standards of ASV, TEC, CNEMC, CCMC for aquatic life. The environmental quality indices for water (*WQI*, *HEI*, *C_d*) and sediment (*PERI*, *EF*, *I_{geo}*, *PLI*) indicated that the water pollution level is higher than sediment pollution in the study area. As the concentrations of heavy metals such as Fe, Pb, Zn, Co, Ni, Cu are higher than the guideline values, further studies on their toxicity, bioaccumulation, and bio-magnification properties are needed.

As the river is an intensive fishing area and used for various domestic purposes, heavy metal pollution represents a significant threat to human health and other living organisms. The spatial distribution of different quality indices revealed that the urban area and the downstream region of the study area have a high pollution pressure. The multivariate analysis (Pearson correlation, principal component analysis, and cluster analysis) suggested Mn, Cd can be attributed to the release from natural sources, sources of COD, TSS, Pb, Zn, Cu are probably anthropogenic, and sources of Fe, Ni, and Co may be both geogenic and anthropogenic. The major inputs of anthropogenic sources of pollutants are industrial effluents, domestic and municipal wastewater, sewage, agricultural and stormwater runoff. The analytical data of the study area exposed that the concentration of Pb in water and sediment exceeded all national and international standards. Therefore, toxic metals need to be removed from the Shtalakshaya River to be a sustainable safe source of water and save the aquatic ecosystem. Promoting afforestation with phytoremediation plants along the riverbanks may reduce metal pollution. Agricultural runoff and leaching of toxic metals into the river system may be reduced by creating a buffer zone with strip grass around the irrigated agricultural area. However, some more recent remediation technologies such as by washing, dislodging, separation, immobilization, capping the sediments, micro-organism techniques might be used to remove heavy metals from the sediment. The findings of this study are expected to be of use to researchers and lawmakers in environmental management for controlling pollution and ecological remediation in similar riverine systems.

Chapter 4

Coprostanol adsorption behavior in agricultural soil, riverbed sediment, and sand

4.1 Introduction

The sterol coprostanol (5β -cholestan- 3β -ol) is formed in mammals by intestinal microorganisms. It is a derivative of cholesterol and aromatic compound in feces. Coprostanol comprises 40–60% of the total sterols in human fecal waste and is commonly used as a bio marker of sewage contamination in soil and watersheds (Alsalahi et al., 2015; Bachtiar et al., 2004; Lühe et al., 2013; Lyons et al., 2015; Nichols et al., 1993; Ren et al., 1996). The hydrogenation of the double bond between C-5 and C-6 in the second hexane ring of cholesterol (carnivore/omnivore) leads to production of coprostanol by enteric microbial reduction of cholesterol (Hussain et al., 2010). Due to the distribution of fecal sterols in human and animal feces, it is considered as a “fingerprint” of fecal pollution. Sterols such as dinosterol, cholesterol, campesterol, β -sitosterol, β -sitostanol, cholestanol, and stigmasterol may originate from natural sources, but coprostanol, cholestanol, and epicoprostanol are completely of fecal origin (Lu et al., 2016). Generally, cholesterol can be transformed into coprostanol by animals such as cats, pigs, cows, horses, sheep, and humans and the sterol profiles of humans and pigs are dominated by coprostanol (Leeming et al., 1996).

Coprostanol is hydrophobic in nature that is readily associated with particulate matter in sewage effluent and incorporated into sediments that bind to the soil matrix (Prost et al., 2017). Studies have demonstrated that coprostanol in sewage contaminated environments correlates well with coliform bacteria and no significant degradation was observed for 450 days at 15°C (Isobe et al., 2002). The coprostanol, once released into the environment from fecal pollution sources, is transported and distributed in soil, sediment, and water bodies. Coprostanol is a fecal contaminant marker that has been widely used as an indicator of fecal pollution in the water environment such as rivers, groundwater, lagoons, and estuaries. The fecal contaminants in water at elevated concentration cause toxic algal blooms, nutrient enrichment, and eutrophication problems that can lead to a decline in species diversity and hence instability of the ecosystem. Humans can be infected with waterborne diseases when water bodies are polluted by fecal materials. Bacterial and viral pathogen infected water that is consumed can lead to human diseases such as typhoid, cholera, diarrhea, polio, gastroenteritis, and hepatitis. Thus, degradation of water used for recreational, drinking, and aquaculture purposes fecal contamination is considered as a major environmental and health threat (e.g., Field and Samadpour, 2007; Vane et al., 2010).

Shimabara City with an area of 82.8 km² occupies 18% of the northeastern part of Shimabara Peninsula, Nagasaki, Japan. The city depends almost completely on groundwater for its public water supply. The livestock raised in the area is about 1000 milk cattle, 23,000 pigs, and 1,030,000 chicken (2015). Nakagawa et al., (2017; 2019; 2021) investigated the coprostanol content in soil, surface water, and groundwater system. The content in groundwater was up to 184.0 ng L⁻¹, and up 68,340 and 1247 ng L⁻¹ in surface water during winter and summer, respectively. The coprostanol content in water leached soil samples was about 4.6 ng g⁻¹. Coprostanol has been detected throughout the world in the range from < 4 up to 8,930 ng g⁻¹ of dry weight sediment (Frena et al., 2016a), 0.25 to 196 µg g⁻¹ in sediment (Froehner et al., 2009), 509 to 12,830 ng g⁻¹ in sediment (Melo et al., 2019), up to 39,428 ng g⁻¹ in sediment (Saeed et al., 2015), up to 5400 ng g⁻¹ in sediment (Tolosa et al., 2014), from 4.21 µg g⁻¹ to 8.32 µg g⁻¹ in dry sediment (Campos et al., 2012), up to 12.3 µg L⁻¹ and 70.6 µg g⁻¹ in suspended particles and sediments, respectively (Cordeiro et al., 2008), from 393.92 to 913.68 µg L⁻¹ in surface water (Furtula et al., 2012). These findings indicate that groundwater is not free from the risk of fecal pollution and can be affected by coprostanol.

The disposal of livestock waste from animal husbandry farms, manure applied as fertilizer, sewage contamination from urban areas is responsible for high concentrations that risk leaching coprostanol to the groundwater. An elevated level of coprostanol concentration can indicate serious environmental contamination risks due to fecal origin transport through soil, sediment, and sand and reach the groundwater. Coprostanol along with other fecal sterols is considered to be a more robust indicator of sewage contamination than fecal coliform bacteria. Basically, the contaminant ability of sorption to the solid fraction of soils, sediments, or sands is directly related to the fate of coprostanol in the environment. Therefore, it is important to study the sorption mechanisms of coprostanol for improving the knowledge regarding the transport, distribution, and fate of this chemical in the soil aquatic environment to help control and remediate water and soil from fecal pollution sources. Even though studies have focused on coprostanol contents in water, sediment, and soil (e.g., Bujagic et al., 2016; Machado et al., 2014), to the best of our knowledge, no previous studies on adsorption mechanisms of coprostanol have been conducted. In the present research, I used three different media (soil, sediment, and sand) to evaluate the adsorption capacity and leaching properties that can be used to predict where in the landscape this chemical marker of fecal contamination may affect the groundwater.

Adsorption is the basic process to understand the behavior of organic contaminants in soil and the characterization of mobility and distribution in environment (Lei et al., 2020; Qian et al., 2017). The physicochemical properties of organic pollutants (water solubility, K_D , K_{OC} , pKa), properties of soil media (pH, EC, CEC), soil texture (clay, silt, sand, organic matter), and environmental conditions (temperature) affect the sorption process. Pollutants that show low mobility in soil with strong or moderate sorption capacity, hence represent a small risk for leaching into the groundwater. Likewise,

pollutants with low sorption affinity show high mobility in soil and can represent an increased risk for groundwater contamination (Pavlovic et al., 2018). Recently, adsorption phenomena and dynamics of many organic pollutants including antibiotics have been studied (e.g., Alvarez-Esmorís et al., 2021; Conde-Cid et al., 2019b; Zhang et al., 2014). However, the distribution coefficients (K_D , K_L , and K_F) and sorption behavior of coprostanol in soil-water environmental systems are still to a major extent unknown and have not been investigated thoroughly yet.

In view of the above, the objective of this study was to experimentally determine the maximum adsorption capacity and distribution coefficients (K_D , K_L , and K_F) of coprostanol in soil, riverbed sediment, and sand as a function of soil particle size distribution (clay, silt, and sand), CEC, pH, EC, and organic matter content (OM). The experimental adsorption data of coprostanol were described by using three models: the Henry (linear) (K_D) (Mark et al., 2016; Zhou et al., 2020), Langmuir (K_L) (Álvarez-Esmorís et al., 2020a; Kaur et al., 2018), and Freundlich isotherm (K_F) (Conde-Cid et al., 2020; Zhang et al., 2011). The secondary objective was to assess the leaching properties of coprostanol and improve the understanding of transport processes in different geologic media. Thus, the migration pattern of coprostanol in the environment can be better described to reduce the risks of environmental and public health issues due to fecal pollutants.

4.2 Materials and methods

4.2.1 Samples

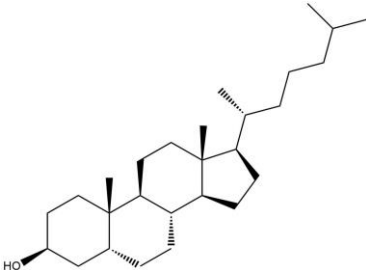
Three geologic media (soil, sediment, and sand) with different properties were selected for comparative sorption of coprostanol contaminant. Surface samples (0–20 cm depth) were collected from agricultural soils, riverbed sediments, and sandy soils using a soil sampling auger at different locations in Japan. Agricultural soil named Kuroboku (type: volcanic ash soil) was collected in Shimabara City (latitude: 32.75031666, longitude: 130.35076944). The riverbed sediment sample was collected from the riparian zone of the Urakami River (latitude: 32.793850, longitude: 129.877037) in Nagasaki City (near Bunkyo campus of Nagasaki university). The sand samples were collected from Arid Land Research Center of Tottori University near the sand dunes of Tottori City (latitude: 35.542003, longitude: 134.212468). In the laboratory, the samples were air dried, gently crushed, passed through a 2-mm sieve, homogenized, and stored in Ziplock polyethylene bags. Collected samples were characterized before the adsorption isotherm experiments.

4.2.2 Chemicals

The chemicals used in the experiment were all high purity either analytical grade or high-performance liquid chromatography grade. Before used, all glassware was three times successively washed and rinsed thoroughly with deionized water (resistivity $\sim 18 \text{ M}\Omega \text{ cm}$ at 25°C), deionized water

(resistivity ~15 MΩ cm at 25°C), acetone, methanol, and dichloromethane. The sterol coprostanol (5β-cholestan-3β-ol) with formula C₂₇H₄₈O and purity ≥ 95.0% was purchased from Cayman Chemical (Ann Arbor, MI 48108, USA). The basic chemical information of coprostanol is described in **Table 4-1**. Other used chemicals such as cholesterol d₇ (C₁₇H₃₉D₇O) with purity ≥ 98% was purchased from Toronto Research Chemicals (Canada), ethanol (purity 99.5%), PBS (phosphate buffer solution), pyridine (purity 99.5%), sodium sulfate (purity 99.0%), sodium pyrophosphate decahydrate (H₂₀Na₄O₁₇P₂) (purity 99.0%), were analytical grade, from Fujifilm Wako Pure Chemical Corporation (Osaka, Japan).

Table 4-1 Chemical properties of coprostanol

Target Compound	Coprostanol
IUPAC nomenclature	5β-cholestan-3β-ol
Molecular formula	C ₂₇ H ₄₈ O
Molecular weight	388.7
Solubility	Low water solubility (1.5×10 ⁻⁰⁵ g L ⁻¹)
Log <i>K</i> _{OW}	8.82
pKa	18.3
Chemical structure	

The acetone, methanol (purity ≥ 99.8%), strontium dichloride hexahydrate (Cl₂H₁₂O₆Sr) (purity 99.0%), potassium dichromate (K₂Cr₂O₇) (purity 99.5%), sulphuric acid (H₂SO₄) (purity 95.0%), ferrous ammonium sulfate hexahydrate (FeH₂₀N₂O₁₄S₂) (purity 99.0%), and oxalic acid dihydrate (C₂H₆O₆) (purity 99.5%) were analytical grade, from Nacalai Tesque, Inc. (Kyoto, Japan); dichloromethane (purity ≥ 99.5%) was HPLC grade, from Kanto Chemical Co., Inc. (Tokyo, Japan), and N,O-Bis(trimethylsilyl)trifluoroacetamide (C₈H₁₈F₃NOSi₂), purity (99.0%), was purchased from SUPELCO (Bellefonte, USA).

4.2.3 Methods

The electric conductivity and pH were measured by using EC meter (Model: HI 98311) and pH meter (Model: HI 98121), respectively, of HANNA instrument (Woonsocket RI USA, Romania). The

pH was measured in sample-water suspension at a ratio of 1:2.5 after 0.5 h of shaking by pH-electrode. The EC-meter was inserted into the water suspension after 1.0 h shaking at a ratio of 1:5 for the determination of EC (Brady and Well, 2008). CEC was determined by using Eco ion chromatography with 863 Compact Autosampler (Metrohm AG, CH-9100 Herisau, Switzerland). The CEC was determined after extraction of originally adsorbed cations with 0.0114 M $\text{Cl}_2\text{H}_{12}\text{O}_6\text{Sr}$ solution using Eco ion chromatography with 863 Compact Autosampler (Metrohm AG, CH-9100 Herisau Switzerland) (Nakagawa et al., 2022). Total organic carbon (OC) and organic matter (OM) content were analyzed by heating digestion with 0.4 N of chromic acid and analyzing the color of suspension by titration with 0.2 N ferrous ammonium sulfate (Mohr's salt) using the Tyulin method. The particle density was measured by the Pycnometer method. Particle size distribution (clay, silt, and sand) analysis was performed based on the integral suspension pressure method (ISP) by PARIO Soil Particle Analyzer using PARIO Plus mode. The coprostanol was quantified in adsorption experiments using Gas Chromatography Triple Quadrupole Mass Spectrometer (Agilent GC 7890A + MS 7000A).

4.2.4 Batch adsorption experiments

The solid-liquid equilibrium-batch method was used to determine the adsorption of coprostanol from an aqueous solution to soil (Brozni et al., 2021; Wang et al., 2020a; Xiang et al., 2019). Batch experiments were carried out to study coprostanol adsorption in equilibrium. For all experiments, air-dried soil, sediments, and sand (< 2 mm) were weighed in 50 mL glass containers. Coprostanol is sparingly soluble in aqueous buffers. It has a solubility of approximately 0.3 mg mL^{-1} in a 1:2 solution of ethanol:PBS (phosphate buffer solution) (pH 7.2). Using this method stock solutions of coprostanol compound was prepared in aqueous solution with deionized water (resistivity $\sim 18 \text{ M}\Omega \text{ cm}$ at 25°C). To exclude the decomposition of coprostanol and to prevent photo transformation all sample containers and prepared solutions were wrapped in aluminum foil.

All prepared samples and stock solutions were stored in a refrigerator at approximately -20°C before analysis. The sample preparation procedure was as follows: 1 g of each sample (particle size < 2 mm) was weighed in 50 mL centrifuge acryl glass tubes to reduce adsorption on the wall of tubes and suspended in 40 mL of individual solutions for soil, and 30 mL solutions for sediment and sand sample containing coprostanol using different concentrations. The individual five points concentration ranged were $1.5 - 4.0 \text{ mg L}^{-1}$ of coprostanol solution for soil sample and $1.0 - 3.0 \text{ mg L}^{-1}$ for sediment and sandy soil samples. The resulting suspensions were shaken in the dark for 48 h on a rotary shaker at laboratory temperature (25°C). Preliminary experiments showed that contact for 48 h under the above conditions was long enough for equilibrium to be reached. The soil suspension was separated by centrifugation at 3000 rpm for 20 min. All experiments were carried out at natural pH (soil = 5.84 ± 0.03 , sediment = 6.88 ± 0.01 , sandy soil = 7.17 ± 0.02).

Coprostanol (5 β (H)-Cholestan-3 β -ol) was extracted from the resulting supernatants in batch experiment according to Nakagawa et al. (2017), with some modification. At first, the supernatant samples were acidified with 1.0 N HCl to pH 2–3 and received 100 μ L of cholesterol d₇ reference solution. Then the samples were filtered through two series of filters: first an Oasis HLB Extraction Cartridge (Water Corporation, Milford, Massachusetts USA), then a PTFE non-sterile membrane filter (Toyo Roshi Kaisha. Ltd., Adventec, Japan) with 0.2 μ m. The coprostanol was extracted from supernatant samples by liquid–liquid extraction with dichloromethane in room temperature during three successive times. Pure nitrogen gas (purity > 99.99%) was blowing through the extract sample and concentrated to near dryness (< 1.0 mL). Then it was dehydrated by using anhydrous sodium sulfate. The extract was formed to trimethylsilyl using BSTFA (bis-trimethylsilyl trifluoroacetamide) and pyridine at 80°C for 60 min after concentration and dehydration, then quantified by using of Gas Chromatography Triple Quadrupole Mass Spectrometer (Agilent GC 7890A + MS 7000A). The batch equilibrium experimental study was performed in duplicate and the mean of these were used for further analyses.

The difference between initial concentrations added and those remaining in the equilibrium solution provided the amount of coprostanol adsorbed by soil, sediment, and sand. The concentration of coprostanol compound adsorbed in samples was calculated as (Franklin et al., 2022; Wang et al., 2020b):

$$q_e = \frac{(C_0 - C_e)}{m} V \quad (4-1)$$

where C_0 and C_e represent initial and equilibrium concentrations of coprostanol in the solution (mg L^{-1}), q_e refers to the amount of coprostanol adsorbed per gram of soil (mg g^{-1}), V is the solution volume (L), and m is the mass of soil (g).

4.2.5 Adsorption model and data analysis

The distribution of adsorbate molecules between liquid and solid phases at equilibrium of an adsorption process can be described by the adsorption isotherm. The adsorption process was described by adsorbate-adsorbent affinity, favorable adsorption, and adsorption mechanism using three adsorption isothermal equations namely, the Henry (linear), Langmuir, and Freundlich models. The interactions between adsorbate and adsorbent at equilibrium are demonstrated by the Henry equation (Álvarez-Esmorís et al., 2020b; Tang et al., 2022;) according to:

$$q_e = K_D C_e \quad (4-2)$$

where q_e is the equilibrium adsorption capacity ($\mu\text{g g}^{-1}$) of coprostanol into adsorbent, C_e is the equilibrium concentration (mg L^{-1}) of coprostanol in solution; K_D is the linear distribution coefficient (L kg^{-1}) of the coprostanol in the solid phase and the liquid phase.

The Langmuir adsorption isotherm (Ayub et al., 2020; Li et al., 2021) represents an adsorbent surface with homogeneous binding sites having equivalent sorption energies, and no interactions between adsorbed material:

$$q_e = \frac{q_{max}K_L C_e}{1+K_L C_e} \quad (4-3)$$

where C_e is the concentration of coprostanol in the supernatant solution (mg L^{-1}) at equilibrium, q_e is the quantity of coprostanol adsorbed onto the adsorbent at equilibrium ($\mu\text{g g}^{-1}$), q_{max} is the maximum monolayer adsorption capacity of adsorbent ($\mu\text{g g}^{-1}$), and K_L (L mg^{-1}) is the binding affinity between coprostanol and test adsorbent known as Langmuir adsorption constant.

For the Langmuir model, the favorable adsorption can be expressed in terms of a dimensionless constant separation factor or equilibrium parameter (R_L), that explains the favorability of adsorption process (Lei et al., 2013). This factor can be calculated from the Langmuir adsorption constant K_L using:

$$R_L = \frac{1}{1+C_0 \times K_L} \quad (4-4)$$

where C_0 represents the highest initial concentration of solution (mg L^{-1}), K_L is the Langmuir adsorption constant (L mg^{-1}), and the parameter R_L indicates the adsorption possibility favorable ($0 < R_L < 1$), unfavorable ($R_L > 1$), linear ($R_L = 1$), or irreversible ($R_L = 0$).

The Freundlich isotherm (Conde-Cid et al., 2019a; Inyinbor et al., 2016) is an empirical model that is not limited to monolayer adsorption but also describes multilayer processes:

$$q_e = K_F C_e^{\frac{1}{n}} \quad (4-5)$$

where q_e is the amount of coprostanol adsorbed at equilibrium ($\mu\text{g g}^{-1}$), C_e is the concentration (mg L^{-1}) of coprostanol in solution at equilibrium, and K_F is the Freundlich's constant. K_F can be used to measure the adsorption capacity, and $\frac{1}{n}$ is the adsorption intensity of the adsorption process. The magnitude of the exponent, $\frac{1}{n}$, gives an indication of the favorability of adsorption. When the value of $\frac{1}{n}$ is $0.1 \leq \frac{1}{n} \leq 0.9$, adsorption is favorable, and representing beneficial of adsorption (Hameed et al., 2008; Wei et al., 2017; Yardim et al., 2003).

The sorption capacity was evaluated by the soil-water distribution coefficient (K_D) and the organic carbon content normalized distribution coefficient ($\text{Log } K_{OC}$) as Xiang et al., (2018):

$$K_D = \frac{q_e}{C_e} \quad (4-6)$$

$$\text{Log } K_{OC} = \text{Log}\left[\left(\frac{K_D}{OM}\right) \times 100 \times 1.724\right] \quad (4-7)$$

where organic matter (OM) content to organic carbon (OC) content ratio is 1.724.

4.3 Results and discussion

4.3.1 Physicochemical characteristics of samples

The experimental findings of physicochemical variables are shown in **Table 4-2**. The pH of soil, sediment, and sand sample were 5.84 ± 0.03 , 6.88 ± 0.01 , 7.17 ± 0.02 , respectively. The soil and sediment were slightly acidic, and the sand was slightly alkaline. The EC for soil, sediment, and sand were 49.0 ± 2.0 , 39.3 ± 1.45 , and $24.3 \pm 0.33 \mu\text{S cm}^{-1}$, respectively. The CEC for soil, sediment, and sand was 6.56 ± 0.04 , 3.06 ± 0.09 , and $1.42 \pm 0.15 \text{ cmol}_e \text{ kg}^{-1}$, respectively. The OM content was 2.15 ± 0.02 , 0.52 ± 0.01 , and $0.09 \pm 0.004 \%$ for soil, sediment, and sand, respectively. Particle density for soil, sediment, and sand was 2.29, 2.63, and 2.60 g cm^{-3} , respectively. The particle size distribution for the soil was 62.1% sand, 28.3% silt, and 9.6% clay. The river sediment contained 95.4% sand, 4.1% silt, and 0.5% clay. The sand contained 98.0% sand, 2.0% silt, and 0.0% clay. Using a textural triangle, soil samples could be classified as sandy loam, whereas riverbed sediment and sand samples were classified as sand.

4.3.2 Adsorption isotherm

The adsorption isotherms were used for the determination of coprostanol mobility, fate, and transport in the soil-water system, by quantifying adsorption favorability, adsorption intensity, the maximum sorption capacity. The experiments were performed without pH variation. The isotherm data were fitted using the Henry (linear), Langmuir, and Freundlich models to describe the adsorption isotherm process (**Fig. 4-1**). The Henry model follows a linear isotherm containing slope equal to partition distribution coefficient of soil and water (K_D) (Rabelo et al., 2021; Wang et al., 2022). The Langmuir model involves a set of homogenous sorption sites of monolayer sorption with uniform energies (Dutta et al., 2022; Vimonses et al., 2009). The Langmuir model was developed to describe the adsorption of coprostanol on homogeneous sample surfaces. On the other hand, the Freundlich isotherm is an empirical equation. It is used to describe the sorption on heterogeneous and amorphous surfaces of the adsorbent (soil, sediment, and sand) varying in affinity and energy distribution (Deng et al., 2021; Prakathi et al., 2020).

The average results of the experimental adsorption isotherms of the study are shown in **Table 4-3**. The adsorption isothermal experimental curves with standard error bars are shown in **Fig. 4-1**. The Henry model generally fitted experimental data best as compared to the Langmuir and Freundlich models for soil and sediment samples. Similar results for organic pollutants were found by Álvarez-Esmorís et al., (2020b) and Wu et al., (2018). For the Henry model the determination coefficient (R^2) was 0.980 for soil, 0.978 for riverbed sediment, and 0.942 for the sand sample (**Fig. 4-1, Table 4-3**). Regression between q_e ($\mu\text{g g}^{-1}$) and C_e (mg L^{-1}) was performed for the modification of the Henry model to the sorption isotherm data that resulted in a higher determination coefficient for samples.

The Freundlich isotherms resulted in significant fits to analyzed soil ($R^2 = 0.865$) sample data. Meanwhile, the Langmuir model had a better fit for the adsorption process of coprostanol in the sediment ($R^2 = 0.974$), and sand ($R^2 = 0.988$) sample, as compared with the Freundlich model ($R^2 = 0.842, 0.875$, respectively) (**Fig. 4-1, Table 4-3**). Many organic pollutants such as toxins and anatoxina, 2,4-dichlorophenol, oxytetracycline, benzalkonium chlorides, and triclosan are best described by the Langmuir model (e.g., Batool et al., 2020; Khan et al., 2017; Klitzke et al., 2011; Lei et al., 2013; Li et al., 2021), and 17 β -estradiol-17-sulfate, bithionol and levamisole, and sulfadiazine have been shown to be best described by the Freundlich model (e.g., Bai et al., 2015; Ma et al., 2019; Rabelo et al., 2021). As the adsorption for soil sample was better described by the Freundlich model, the coprostanol adsorption may be interpreted as a multilayer type in heterogenous surface. Similarly, the sorption to sediment, and sand may be interpreted as monolayer type with homogenous surface due to the better fit of the Langmuir model as compared to the Freundlich model. For prediction of leaching properties and mobility to groundwater it is important to understand the connection between transport and natural decay of coprostanol concentration in different geologic media.

The batch experimental data were fitted by the models using a numerical solver to obtain the best fit. The mean of the absolute differences between model values and observations shows the goodness-of-fit. The observations of soil sample were closer to the model values for the Freundlich model whereas those of the sediment, sand samples were closer to the Langmuir isotherm model values. The simulation results further confirmed that the Freundlich isotherm was the best fit for soil sample and the Langmuir isotherm was best for the sediment, and sand. This indicates that the soil corresponds to an adsorption process of the multilayer type with heterogenous surface best described by the Freundlich model. In turn, this may be owing due to soil's higher organic matter and clay content as compared to sediment, and sand, and the subsequent high adsorption capacity.

The Henry absorption coefficients (K_D) were significantly different for each media type according to 193.7 L kg⁻¹ for soil, 120.8 L kg⁻¹ for riverbed sediment, and 94.8 L kg⁻¹ for sand. The Freundlich K_F is an empirical constant expressing sorption capacity (sorption isotherm slope) for a given range of concentration. In our study, the Freundlich adsorption constant (K_F) was 166.9 for soil, 89.2 for sediment, and 67.3 $\mu\text{g}^{1-\frac{1}{n}} \text{L}^{\frac{1}{n}} \text{kg}^{-1}$ for sand, respectively.

This suggests that the adsorption of coprostanol is different in soil, sediment, and sand. The highest K_F was obtained in soil samples with high organic matter content and low pH. In contrast, the minimum K_F was obtained for sediment, and sand with low organic matter content and high pH (**Table 4-2**). The K_D (94.8–193.7 L kg⁻¹) and K_F (67.3–166.9 $\mu\text{g}^{1-\frac{1}{n}} \text{L}^{\frac{1}{n}} \text{kg}^{-1}$) increased in the order of sand < sediment < soil, indicating that the sorption affinity of coprostanol in the various media exhibits a similar increasing trend. The lowest K_D , and K_F value for sediment, and sand indicates a higher mobility of coprostanol in and easier leaching than for soil.

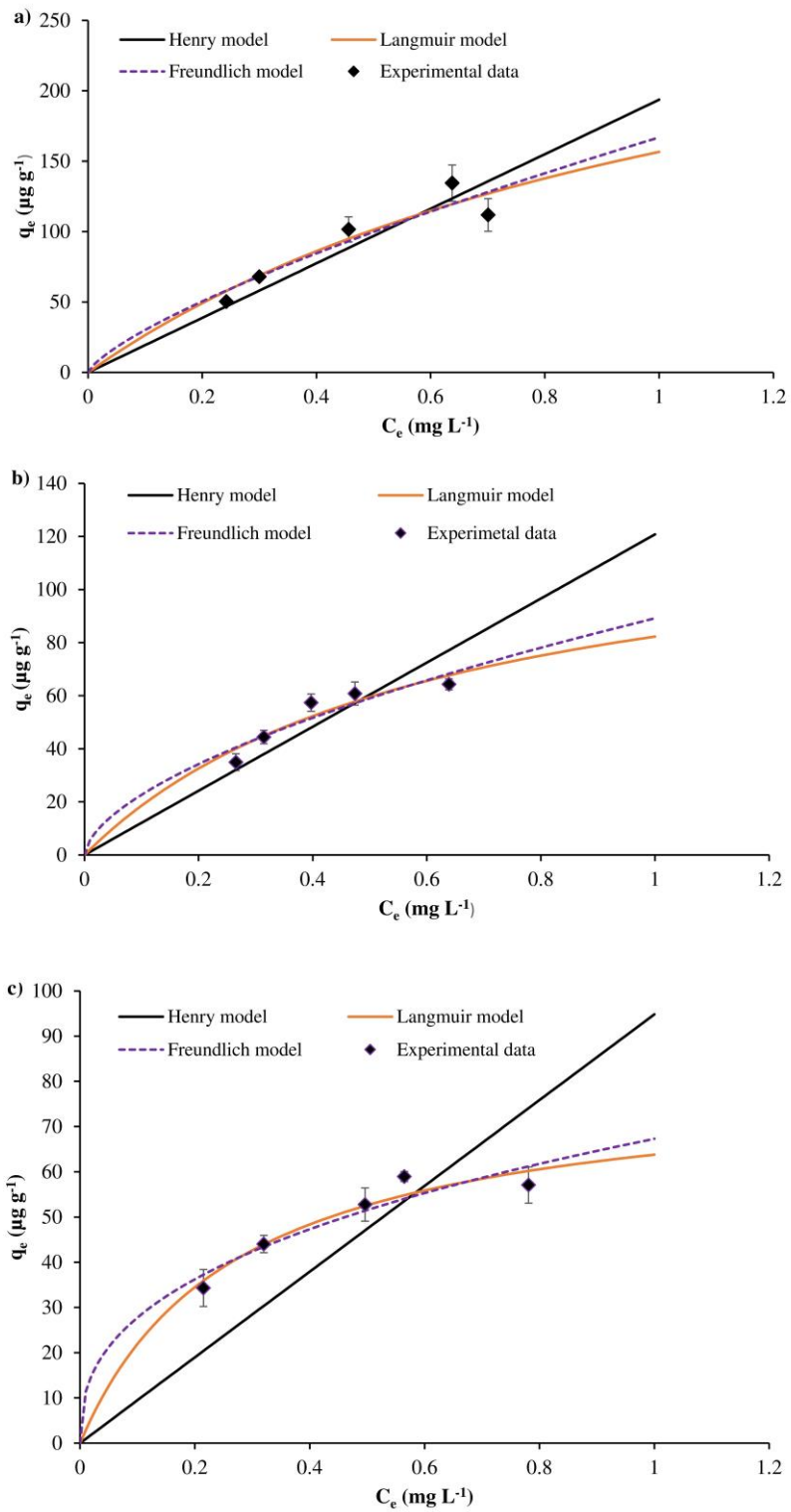


Fig. 4-1 Adsorption isotherm curves of coprostanol, in (a) soil, b) sediment, and (c) sand samples. Isothermal curves show error bars of adsorption concentration generated from the standard errors of the duplicate experiment. q_e , adsorption concentration at equilibrium; C_e , liquid-phase concentration at equilibrium.

Table 4-2 Basic physicochemical properties (mean \pm standard error) of the test samples

Sample	pH	EC	Particle size distribution			OC	OM	Particle density	CEC	Log K_{OC}
			Sand	Silt	Clay					
			(%)	(%)	(%)					
Soil	5.84 \pm 0.03	49.0 \pm 2.0	62.1	28.3	9.6	1.25 \pm 0.02	2.15 \pm 0.02	2.29	6.56 \pm 0.04	4.19
Sediment	6.88 \pm 0.01	39.3 \pm 1.45	95.4	4.1	0.5	0.30 \pm 0.01	0.516 \pm 0.01	2.63	3.06 \pm 0.09	4.60
Sand	7.17 \pm 0.02	24.3 \pm 0.33	98.0	2.0	0.0	0.05 \pm 0.004	0.086 \pm 0.004	2.60	1.42 \pm 0.15	5.28

EC = electrical conductivity ($\mu\text{S cm}^{-1}$), OC = organic carbon content (%), OM = organic matter content (%), CEC = cation exchange capacity ($\text{cmol}_c \text{kg}^{-1}$), K_{OC} = organic carbon (OC) normalized adsorption coefficient (L kg^{-1}).

Table 4-3 Sorption parameters showing mean values calculated with different isotherm models for coprostanol in soil, sediment, and sand

Sample type	Adsorbate	Type of Isotherm								
		Henry (linear)			Langmuir			Freundlich		
		Parameters			Parameters			Parameters		
		K_D	R^2	q_{\max}	K_L	R_L	R^2	K_F	$\frac{1}{n}$	R^2
Soil	Coprostanol	193.68	0.980	345.05	0.831	0.231	0.918	166.9	0.743	0.865
Sediment	Coprostanol	120.79	0.978	133.17	1.62	0.182	0.974	89.2	0.596	0.842
Sand	Coprostanol	94.81	0.942	80.99	3.71	0.088	0.988	67.3	0.385	0.875

K_D = linear distribution coefficient (L kg^{-1}), q_{\max} = maximum monolayer adsorption capacity of adsorbent ($\mu\text{g g}^{-1}$), K_L = Langmuir adsorption constant (L mg^{-1}), R_L = separation factor or equilibrium parameter, K_F = Freundlich's constant ($\mu\text{g}^{1-\frac{1}{n}} \text{L}^{\frac{1}{n}} \text{kg}^{-1}$), $\frac{1}{n}$ = adsorption intensity.

The soil presented higher sorption capacity than the sediment and sand as shown in **Table 4-3**. For the Langmuir model the maximum adsorption capacity (i.e., q_{\max} value) was 345.1 $\mu\text{g g}^{-1}$ for soil, 133.2 $\mu\text{g g}^{-1}$ for sediment, and 80.9 $\mu\text{g g}^{-1}$ for sand. Thus, sorption capacity of coprostanol followed the same order of soil > sediment > sand. The high adsorption capacity in soil might be attributed due to the relatively higher surface area compared to sediment and sand sample.

The separation factor R_L is a consistent indicator of adsorption intensity, representing that sorption is favorable ($0 < R_L < 1$), unfavorable ($R_L > 1$), or irreversible ($R_L = 0$). In the current study, the R_L values for soil, sediment, and sand suggested that coprostanol adsorption to the tested media was favorable under the present conditions. Thus, all three geologic media are effective adsorbents of coprostanol from an aqueous solution.

In the Freundlich model, the exponent $\frac{1}{n}$ is the slope, showing the variation of the adsorption with concentration. The value of $\frac{1}{n}$ demonstrates the intensity of adsorption. Generally, the larger the $\frac{1}{n}$, the stronger is the partitioning interaction (Lee and Park, 2016; Qian et al., 2017). The magnitude of $\frac{1}{n}$ parameter of the Freundlich model for soil sample was 0.743, suggesting that the adsorption is favorable for coprostanol, and the adsorption will increase with increasing amounts of coprostanol in the solution. Moreover, $\frac{1}{n}$ (dimensionless) is the Freundlich adsorption parameters as well as linearity index. As the $\frac{1}{n}$ value of sediment and sand was 0.596, and 0.385, this indicates a non-linear adsorption isotherm for the respective samples, whereas this value for the soil was 0.743 (nearer to 1), suggesting a nearer linear adsorption isotherm curve (**Fig. 4-1 a, b, c**).

The partitioning distribution (K_D) is a measure of the relative solubility of the organic molecules in both solid and solution phase. The highest K_D value for soil indicates that coprostanol sorption is directly influenced by soil characteristics. The organic carbon (OC) content was $1.25 \pm 0.02\%$, organic matter (OM) content $2.15 \pm 0.02\%$, clay content 9.6%, and cation exchange capacity (CEC) $6.56 \pm 0.04 \text{ cmol}_c \text{ kg}^{-1}$ for the soil. These values were higher than sediment and sand resulting in higher sorption capacity. Generally, clay and organic matter content tend to adsorb organic pollutants with different binding energies and the adsorption depends on the adsorbent-adsorbate interaction forces and sorption mechanisms (Dai et al., 2020; Higgins and Luthy, 2006; Oukali-Haouchine et al., 2013; Tang et al., 2009; Wu et al., 2015). Generally, at low pH humic acid may provide more adsorption sites and increase the adsorption capacity. In slightly acidic solutions like in my soil, some acidic functional groups of humic acid are dissociated, causing it to bear a negative charge, and humic acid has a closed or curly structure. This structure can provide more adsorption sites and may increase the adsorption capacity (Wei et al., 2021). Moreover, a higher CEC is favorable for high adsorption capacity. A high CEC indicates high organic matter content that is favorable for high adsorption capacity.

The Pearson correlation was used to estimate the relationship between adsorption isothermal parameters and physicochemical characteristics of the samples (**Table 4-4**). The correlation matrix showed a strong positive relation among K_D , q_{max} , and K_F , with EC ($r = 0.93, 0.86, 0.91$), silt ($r = 0.98; 0.99, p < 0.05; 0.99$), clay ($r = 0.98; 0.99, p < 0.05; 0.99$), OM ($r = 0.99, p < 0.05; 0.99; 1.00, p < 0.01$), and CEC ($r = 0.99, p < 0.05; 0.98, 0.99$), respectively. Similarly, the $\frac{1}{n}$ showed strong positive correlation with EC ($r = 1.00, p < 0.05$), silt ($r = 0.85$), clay ($r = 0.84$), OM ($r = 0.91$), and CEC ($r = 0.95$). The separation factor R_L showed a strong positive relation with EC ($r = 0.99$). The pH and sand content displayed strong negative correlation with K_D ($r = -0.99, p < 0.05; -0.98$), q_{max} ($r = -0.99; -0.99, p < 0.05$), K_F ($r = -1.0, p < 0.01; -0.99$). Based on the correlation, the main factors governing the coprostanol sorption are pH, OM, CEC, silt, and clay content as a high correlation between these indicates mutually high inter-dependence.

Table 4-4 Correlation matrix between adsorption media and model parameter

	Correlations												
	pH	EC	Sand	Silt	Clay	OM	CEC	K_D	q_{max}	K_L	R_L	K_F	$1/n$
pH	1												
EC	-0.91	1											
Sand	0.99	-0.84	1										
Silt	-0.99	0.84	-1.00**	1									
Clay	-0.99	0.83	-1.00*	1.00*	1								
OM	-1.00**	0.90	-0.99	0.99	0.99	1							
CEC	-0.99	0.95	-0.97	0.97	0.96	0.99	1						
K_D	-.99*	0.93	-0.98	0.98	0.98	.99*	.99*	1					
q_{max}	-0.99	0.86	-.99*	.99*	.99*	0.99	0.98	0.99	1				
K_L	0.84	-0.99	0.76	-0.76	-0.74	-0.84	-0.89	-0.87	-0.79	1			
R_L	-0.87	0.99	-0.79	0.79	0.77	0.86	0.92	0.89	0.81	-.99*	1		
K_F	-1.00**	0.91	-0.99	0.99	0.99	1.00**	0.99	.99*	0.99	-0.84	0.87	1	
$1/n$	-0.91	1.00*	-0.85	0.85	0.84	0.91	0.95	0.93	0.87	-0.99	0.99	0.92	1

**p < 0.01, *p < 0.05

Both clay minerals and organic matter contain weak electrical charges. In most soils the dominant charge is negative. Organic matter is charged due to the ionization of carboxyl and phenolic groups and thus organic matter can often contribute substantially to the CEC of a soil causing high adsorption capacity. The total specific surface area (SA) is controlled by a combination of the particle size distribution (primarily clay and fine silt contents), clay mineralogy, organic matter (OM) content, and iron and aluminum oxide contents. In general, the surface area available for sorption increases with increasing clay and fine silt content. According to Arthur et al., (2023), there was a significant positive contribution of organic carbon (OC) to surface area (13.9 m²/g per %C). In the current study, the soil contained a higher amount of OC than sediment and sand having higher surface area and hence

showed a high adsorption capacity of coprostanol to soil. Consequently, sediment and sand were found to have less sorption (**Table 4-3**). As mentioned above, this is explained by (i) the higher surface area of clay compared to sand, and (ii) the relatively small amount of reactive functional groups relevant to sorption in sand. As well, the sand surfaces become more negatively charged with increasing pH, leading to an increased repulsion of the anionic group (Klitzke et al., 2011). In a previous study, this mechanism explained observed high mobility of organic pollutants in column experiments with sandy sediments (Klitzke et al., 2010).

Hydrophobic interaction is the main adsorption mode of adsorbents on organic matter (Wei et al., 2021). Due to the strong hydrophobic nature of its molecules coprostanol has low affinity for the aqueous phase but great affinity for adsorption to high organic matter containing soil and sediment material via Van der Waals forces between coprostanol and humic acid substances in organic matter. The high affinity of coprostanol for the clay-rich soil material may reflect an ultrastructure of microaggregates of the low-charge smectites that facilitates the adsorption process in clay fractions of soils. Again, the coprostanol molecule has long hydrocarbon tails that allow dispersion forces to link the chains to one another. The weak energy associated with these individual atomic-scale interactions may facilitate clusters of coprostanol molecules sufficient to account for the high adsorption of coprostanol in the soil sample. I infer that these intermolecular forces between coprostanol molecules and humic acid substances in organic matter may contribute significantly to high adsorption of coprostanol to soil sample (**Fig. 4-2**).

According to Aristilde and Sposito, (2010); the interaction between ciprofloxacin ($C_{17}H_{18}FN_3O_3$) and organic matter is caused by intermolecular hydrogen bonding interactions (Aristilde et al., 2010). The soil organic matter retains abundant oxygen-containing functional groups including phenolic groups, carboxylate anions in polyphenols, alcohols, and carbohydrate residues. On the other hand, coprostanol contains the polar functional -OH group. Hence, there is a possibility for the formation of intermolecular hydrogen bonding between the oxygen-containing functional groups of humic substances on the clay surface and the polar functional -OH group of the coprostanol and subsequent increase in adsorption capacity of coprostanol in soil (**Fig. 4-2**). Therefore, the adsorption of coprostanol in soil is a physical adsorption that is reversible, but the adsorption capacity in sediment and sand is lower than for soil samples. Sediment and sand have a high leaching ability leading to high mobility and potential pollution migration to groundwater.

The experimental results of our study were analyzed with different approaches for a better understanding of the adsorption patterns of coprostanol and its leaching properties in the tested samples. This is, e.g., why the organic carbon normalized adsorption coefficient (K_{OC}) was calculated. The sorption behavior of coprostanol is significantly influenced by organic matter (OM) content. The leaching potential of organic pollutants and the potential risk to groundwater contamination are determined by organic carbon content normalized sorption coefficient ($\log K_{OC}$) that was obtained

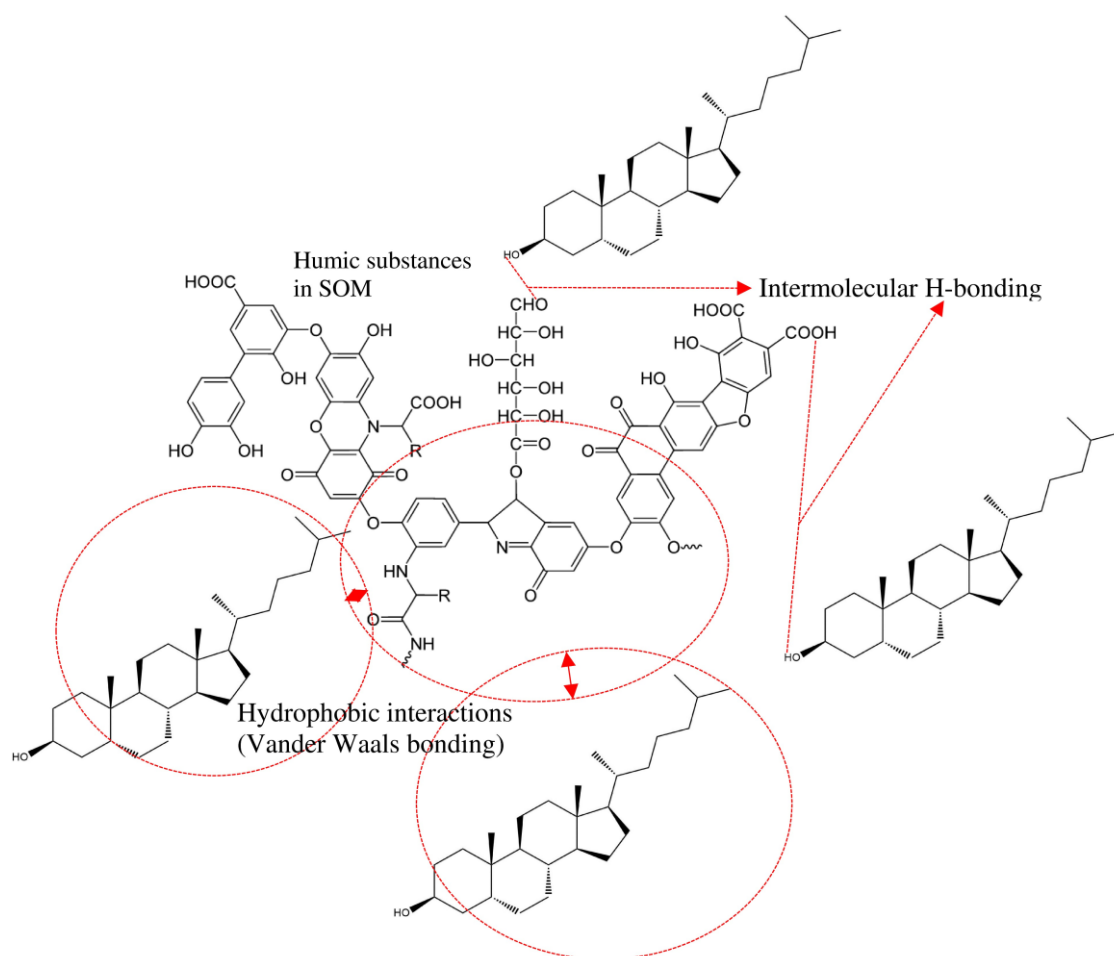


Fig. 4-2 Schematic diagram illustrating possible adsorption mechanism of coprostanol in humic substances of organic matter in adsorbents (possible intermolecular H-bonding and hydrophobic interactions between coprostanol and humic substances) (humic acid structure source: Yikrazauul, 2009).

from OM content and the K_D . Organic pollutants with $K_{OC} < 50$, 150-500, and $K_{OC} > 2000$ may be considered as highly mobile, moderately mobile, and slightly mobile compounds, respectively.

In the present study, the K_{OC} values indicated slight mobility for the studied cases. Based on the test guidelines of the Environmental Safety Assessment for Chemical Pesticides in China, organic pollutants are classified into the following categories: $\log K_{OC} > 4.30$ indicate high adsorbed compounds; $3.70 < \log K_{OC} \leq 4.30$ sub-high adsorbed compounds; $3.00 < \log K_{OC} \leq 3.70$ medium adsorbed compounds; $2.30 < \log K_{OC} \leq 3.00$, sub-hardly adsorbed compounds, and $\log K_{OC} < 2.30$ hardly adsorbed compounds. According to the guideline (Xiang et al., 2018; Kaur et al., 2018; Pal et al., 2015), coprostanol belongs to sub-high adsorbed and slightly mobile compounds category to soil sample (**Table 4-2**). This indicates that agricultural soils could serve as a sink of coprostanol from sewage wastewater. The coprostanol is slightly mobile compound and groundwater pollution is now

continuing, it may migrate to groundwater system, and we can detect the potential fecal pollution risks in the groundwater system only after a long time. The adsorption parameters (K_D , q_{\max} , and K_F) indicated that the fecal pollution risks may be more severe in riverbed sediments and sands than in soil due to low content of adsorption influencing parameters.

4.4 Conclusions

This study focused on the adsorption properties of coprostanol in soil, sediment, and sand and the potential for migration to the groundwater system. The comparative study of adsorption isotherms of three geologic media revealed that coprostanol has a higher affinity to soil ($q_{\max} = 345.1 \mu\text{g g}^{-1}$, $K_D = 193.7 \text{ L kg}^{-1}$, $K_F = 166.9 \mu\text{g}^{1-\frac{1}{n}} \text{ L}^{\frac{1}{n}} \text{ kg}^{-1}$) than sediment ($q_{\max} = 133.2 \mu\text{g g}^{-1}$, $K_D = 120.8 \text{ L kg}^{-1}$, $K_F = 89.0 \mu\text{g}^{1-\frac{1}{n}} \text{ L}^{\frac{1}{n}} \text{ kg}^{-1}$), and sand ($q_{\max} = 80.9 \mu\text{g g}^{-1}$, $K_D = 94.8 \text{ L kg}^{-1}$, $K_F = 67.3 \mu\text{g}^{1-\frac{1}{n}} \text{ L}^{\frac{1}{n}} \text{ kg}^{-1}$). The Henry and Freundlich adsorption isotherms described best the experimental data for soil and a sorption behavior as a multilayer type on heterogeneous surfaces. The Langmuir model fitted sediment, and sand best and may be described as homogeneous type adsorption. This study suggests that coprostanol was adsorbed via hydrogen bond and hydrophobic interaction to the soil organic matter. The Pearson correlation coefficient showed that pH, OM, silt, and clay content were the most influencing parameters for the coprostanol adsorption. Soil with high organic matter contents showed highest adsorption affinity. The clay content also had a positive effect on the adsorption of coprostanol due to the high specific surface area.

The normalized organic carbon content sorption coefficient (K_{OC}) indicated that coprostanol is a sub-high adsorbed to high adsorbed compound and has a slightly leaching property that may indicate potential risks of fecal origin for the groundwater system after a long period. These risks are accentuated for geologic media with high fractions of sand where the adsorption of coprostanol is limited due to lower clay and organic matter contents. The results are of importance for ways to protect the environment and public health by considering coprostanol as an emerging bio marker. Finally, due to heterogeneity of potentially adsorbing components in the studied samples, it is difficult to interpret mechanisms at a finer scale. Thus, additional research and characterizations are needed to test possible hypotheses and to interpret the mechanisms at a finer spatial scale. However, the presented results provide a useful starting point for further investigations and offer some guidelines that will be helpful for future research in understanding the adsorption behavior of coprostanol in different geological media. Future studies need to address comparative studies of column experiments for adsorption mechanisms of coprostanol in different geologic media with batch experiments including kinetics and finer-scale desorption mechanisms.

Chapter 5

Summary and conclusions

In the present research, I have predominantly discussed three topics based on the preservation and sustainable utilization of urban river environment related to surface and groundwater resources. The first two topics are how the urban riverine system is influenced by unplanned rapid urbanization, industrialization and agricultural activities based on different land-used types. In the third topic, I evaluated for the first-time sorption behavior of a fecal pollution indicator named coprostanol in urban riverbed sediment, soil, and sand sample, and an estimation of its fate, potential bioavailability, and transport mechanism through it. Then, I compared the results of agricultural soil with those of sand, and riverbed sediment sample to estimate which geologic media is more responsible for leaching the fecal pollutants that migrate to groundwater and posing potential risks to the groundwater system. The research contents, background information, results, and discussions were described in chapter 2, 3, and 4. The summary and conclusions of this study are presented in chapter 5.

In chapter 1, I described the existing problems with urban river environment by rapid unplanned urbanization, industrialization, and agricultural activities. Meanwhile, measuring the quality parameters is not only sufficient to control these situations, but also need to identify the sources of pollutants. There are many methods, techniques, and measures that have been performed to solve this problem in many countries throughout the world. Then, the contents of our research were simply illustrated.

In chapter 2, I investigated the water quality parameters and source identification of pollutants in the Pasur River, a vital reservoir of surface water in the Sundarbans mangrove area in Bangladesh. This study concluded that pH, iron, manganese, total suspended solids, and chloride at some locations had much higher concentrations in the river water than recommended by WHO and Bangladesh environmental standards (DoE) and thus are not safe for household use or aquatic ecosystems. I used water quality indices, spatial distribution, and multivariate statistical analyses to evaluate the pollution level and source determination. Multivariate analysis was used to improve the knowledge regarding the source of pollution. There was obtained four distinct groups of clusters by HCA. The concentration of different water quality parameters was different regarding land use and the importance of the three PC scores. The cluster groups for water samples revealed that the sample of cluster C was most polluted, and the samples of cluster A were the least polluted in the study area. The severe enrichment of pollutants in this area is primarily due to anthropogenic sources related to industrial, agricultural, urbanization, and fishing activities.

Monitoring of coastal activities is essential to save the coastal ecosystems. This monitoring system can give policymakers and stakeholders an interest in the coastal environment and resources.

A systematic and periodic inspection of each industry located beside the river should be performed before certificates of compliances are issued by the Department of Environment (DoE), Bangladesh. Short- and long-term scientific studies should be immediately started to assess the impacts of industrial activities on coastal water, soil, and fishery resources, as well as human health. Thus, this study recommends that continuous monitoring and modern remediation technologies for reducing the pollution level of the Pasur River as well as adjoining agricultural areas should be implemented regarding the risk for human health and ecosystems in the vicinity of the river. To avoid and alleviate environmental contamination, effective approaches for extracting harmful heavy metals from sewage and industrial effluents are urgently needed before the effluent is released into the environment. As well, traditional treatment techniques such as chlorination, boiling, filtration, sedimentation, long storage, and solar radiation are necessary for water used for domestic purposes. Finally, public awareness of the impacts and remedies of pollution should be raised so that they can play a key role in pollution reduction.

In the chapter 3, I assessed the physicochemical and toxicological contents of water and sediment of the Shitalakshaya River, Bangladesh, and compared them to standards of national and international quality guidelines. The analyses indicated that COD, TSS, Fe, Pb, Zn in water exceed the health-based guideline of DoE, WHO, USEPA, and CCME standard for aquatic life. Similarly, Pb, Co, Ni, Cu, Zn (mainly Pb and Cu in sediment) exceeded the standards of ASV, TEC, CNEMC, CCMC for aquatic life. The environmental quality indices for water (*WQI*, *HEI*, *C_d*) and sediment (*PERI*, *EF*, *I_{geo}*, *PLI*) indicated that the water pollution level is higher than sediment pollution in the study area. As the concentrations of heavy metals such as Fe, Pb, Zn, Co, Ni, Cu are higher than the guideline values, further studies on pollution remediation techniques are needed.

As the river is an intensive fishing area and used for various domestic purposes, heavy metal pollution represents a significant threat to human health and other living organisms. The spatial distribution of different quality indices revealed that the urban area and the downstream region of the study area have a high pollution pressure. The multivariate analysis (Pearson correlation, principal component analysis, and cluster analysis) suggested Mn, Cd can be attributed to the release from natural sources, sources of COD, TSS, Pb, Zn, Cu are probably anthropogenic, and sources of Fe, Ni, and Co may be both geogenic and anthropogenic. The major inputs of anthropogenic sources of pollutants are industrial effluents, domestic and municipal wastewater, sewage, agricultural and stormwater runoff. The analytical data of the study area exposed that the concentration of Pb in water and sediment exceeded all national and international standards. Therefore, toxic metals need to be removed from the Shtalakshaya River to be a sustainable safe source of water and save the aquatic ecosystem. Promoting afforestation with phytoremediation plants along the riverbanks may reduce metal pollution. Agricultural runoff and leaching of toxic metals into the river system may be reduced by creating a buffer zone with strip grass around the irrigated agricultural area. However, some more

recent remediation technologies such as by washing, dislodging, separation, immobilization, capping the sediments, micro-organism techniques might be used to remove heavy metals from the sediment. The findings of this study are expected to be of use to researchers and lawmakers in environmental management for controlling pollution and ecological remediation in similar riverine systems.

Finally, in chapter 4, I focused on the adsorption behavior of coprostanol in urban riverbed sediment, soil, and sand, and the potential for migration to the groundwater system. The comparative study of adsorption isotherms of three geologic media revealed that coprostanol has a higher affinity to soil ($q_{\max} = 345.1 \mu\text{g g}^{-1}$, $K_D = 193.7 \text{ L kg}^{-1}$, $K_F = 166.9 \mu\text{g}^{1-\frac{1}{n}} \text{ L}^{\frac{1}{n}} \text{ kg}^{-1}$) than sediment ($q_{\max} = 133.2 \mu\text{g g}^{-1}$, $K_D = 120.8 \text{ L kg}^{-1}$, $K_F = 89.0 \mu\text{g}^{1-\frac{1}{n}} \text{ L}^{\frac{1}{n}} \text{ kg}^{-1}$), and sand ($q_{\max} = 80.9 \mu\text{g g}^{-1}$, $K_D = 94.8 \text{ L kg}^{-1}$, $K_F = 67.3 \mu\text{g}^{1-\frac{1}{n}} \text{ L}^{\frac{1}{n}} \text{ kg}^{-1}$). The Henry and Freundlich adsorption isotherms described best the experimental data for soil and a sorption behavior as a multilayer type on heterogeneous surfaces. The Langmuir model fitted sediment, and sand best and may be described as homogeneous type adsorption. This study suggests that coprostanol was adsorbed via hydrogen bond and hydrophobic interactions to the soil organic matter. The Pearson correlation coefficient showed that pH, OM, silt, and clay content were the most influencing parameters for the coprostanol adsorption. Soil with high organic matter contents showed highest adsorption affinity. The clay content also had a positive effect on the adsorption of coprostanol due to the high specific surface area.

The normalized organic carbon content sorption coefficient (K_{OC}) indicated that coprostanol is a sub-high adsorbed compound and has a slightly leaching property that may indicate potential fecal pollution risks for the groundwater system after a long period. These risks are accentuated for geologic media with high fractions of sand where the adsorption of coprostanol is limited due to lower clay and organic matter contents. Finally, due to heterogeneity of potentially adsorbing components in the studied samples, it is difficult to interpret mechanisms at a finer scale. Thus, additional research and characterizations are needed to test possible hypotheses and to interpret the mechanisms at a finer spatial scale. However, the presented results provide a useful starting point for further investigations and offer some guidelines that will be helpful for future research in understanding the adsorption behavior of coprostanol in different geological media. Future studies need to address comparative studies of column experiments for adsorption mechanisms of coprostanol in different geologic media with batch experiments including kinetics and finer-scale desorption mechanisms.

References

- Aditya, S.K., Krishnakumar, A., AnoopKrishnan, K., 2023. Influence of COVID-19 lockdown on river water quality and assessment of environmental health in an industrialized belt of southern Western Ghats, India. *Environmental Science and Pollution Research*. <https://doi.org/10.1007/s11356-023-27397-0>
- Ahsan, M.A., Satter, F., Siddique, M.A.B., Akbor, M.A., Ahmed, S., Shajahan, M., Khan, R., 2019. Chemical and physicochemical characterization of effluents from the tanning and textile industries in Bangladesh with multivariate statistical approach. *Environmental Monitoring and Assessment* 191:575. <https://doi.org/10.1007/s10661-019-7654-2>
- Ahsan, M.A., Siddique, M.A.B., Munni, M.A., Akbor, M.A., Bithi, U.H., Mia, M.Y., 2018. Analysis of major heavy metals in the available fish species of the Dhaleshwari River, Tangail, Bangladesh. *International Journal of Fisheries and Aquatic Studies* 6, 349-354. <https://www.fisheriesjournal.com/archives/?year=2018&vol=6&issue=4&part=E&ArticleId=1650>
- Alam, M.M., Zahan, M.K.E., Rahman, M.H., Zahid, A.A.S.M., 2020. Water quality assessment of Shitalakhya River. *Asian Journal of Fisheries and Aquatic Research* 6, 9-20. <https://doi.org/10.9734/AJFAR/2020/v6i130086>
- Algul, F., Beyhan, M., 2020. Concentrations and sources of heavy metals in shallow sediments in Lake Bafa, Turkey. *Scientific Reports* 10, 11782. <https://doi.org/10.1038/s41598-020-68833-2>
- Ali, M.M., Ali, M.L., Islam, M.S., Rahman, M.Z., 2016. Preliminary assessment of heavy metals in water and sediment of Karnaphuli River, Bangladesh. *Environmental Nanotechnology, Monitoring & Management* 5, 27-35. <https://doi.org/10.1016/j.enmm.2016.01.002>
- Ali, M.M., Ali, M.L., Islam, M.S., Rahman, M.Z., 2018. Assessment of toxic metals in water and sediment of Pasur River in Bangladesh. *Water Science and Technology* 77, 1418-1430. <https://doi.org/10.2166/wst.2018.016>
- Ali, M.M., Rahman, S., Islam, M.S., Rakib, M.R.J., Hossen, S., Rahman, M.Z., Kormoker, T., Idris, A.M., Phoungthong, K., 2022. Distribution of heavy metals in water and sediment of an urban river in a developing country: A probabilistic risk assessment. *International Journal of Sediment Research* 37, 173-187. <https://doi.org/10.1016/j.ijsrc.2021.09.002>
- Ali, M.M., Ali, M.L., Islam, M.S., Rahman, M.Z., 2018. Assessment of toxic metals in water and sediment of Pasur River in Bangladesh. *Water Sci. Technol.* 77, 1418–1430. <https://doi.org/10.2166/wst.2018.016>.
- Ali, M.M., Ali, M.L., Islam, M.S., Rahman, M.Z., 2016. Preliminary assessment of heavy metals in water and sediment of Karnaphuli River, Bangladesh. *Environ. Nanotechnol. Monit. Manag.* 5, 27–35. <https://doi.org/10.1016/j.enmm.2016.01.002>

- Alomary, A.A., Belhadj, S. 2007. Determination of heavy metals (Cd, Cr, Cu, Fe, Ni, Pb, Zn) by ICP-OES and their speciation in Algerian Mediterranean Sea sediments after a five-stage sequential extraction procedure. *Environmental Monitoring and Assessment* 135, 265-280. <https://doi.org/10.1007/s10661-007-9648-8>
- Alrabie, N.A., Yusuff, F.M., Hashim, R., Zulkeflee, Z., Arshad, A., Amal, M.N.A. 2019. Heavy metals concentrations in stormwater and tilapia fish (*Oreochromis niloticus*) in Kuala Lumpur holding and storage SMART ponds. *Pertanika Journal of Tropical Agricultural Science* 42, 225-236. <http://psasir.upm.edu.my/id/eprint/67334>
- Alsalahi, M. A., Latif, M. T., Ali, M. M., Dominick, D., Khan, M. F., Mustaffa, N. I. H., Nadzir, M. S. M., Nasher, E., Zakaria, M. P., 2015. Sterols as biomarkers in the surface microlayer of the estuarine areas. *Marine Pollution Bulletin* 93, 278–283. <http://dx.doi.org/10.1016/j.marpolbul.2015.01.011>
- Álvarez-Esmorís, C., Conde-Cid, M., Fernández-Calviño, D., Fernández-Sanjurjo, M. J., Núñez-Delgado, A., Álvarez-Rodríguez, E., Arias-Estévez, M., 2020a. Adsorption-desorption of doxycycline in agricultural soils: Batch and stirred-flow-chamber experiments. *Environ. Res.* 186, 109565. <https://doi.org/10.1016/j.envres.2020.109565>.
- Álvarez-Esmorís, C., Conde-Cid, M., Ferreira-Coelho, G., Fernández-Sanjurjo, M.J., Núñez-Delgado, A., Álvarez-Rodríguez, E., Arias-Estévez, M., 2020b. Adsorption/desorption of sulfamethoxypyridazine and enrofloxacin in agricultural soils. *Sci. Total Environ.* 706, 136015. <https://doi.org/10.1016/j.scitotenv.2019.136015>.
- Alvarez-Esmorís, C., Conde-Cid, M., Fernandez-Sanjurjo, M. J., Núñez-Delgado, A., Alvarez-Rodríguez, E., Arias-Estevéz, M., 2021. Environmental relevance of adsorption of doxycycline, enrofloxacin, and sulfamethoxypyridazine before and after the removal of organic matter from soils. *J. Environ. Manage.* 287, 112354. <https://doi.org/10.1016/j.jenvman.2021.112354>.
- Amankwaa, G., Yin, X., Zhang, L., Huang, W., Cao, Y., Ni, X., Gyimah, E., 2021. Spatial distribution and eco-environmental risk assessment of heavy metals in surface sediments from a crater lake (Bosomtwe/Bosumtwi). *Environmental Science and Pollution Research* 28, 19367-19380. <https://doi.org/10.1007/s11356-020-12112-0>
- Amano, H., Nakagawa, K., Berndtsson, R., 2018. Surface water chemistry and nitrate pollution in Shimabara, Nagasaki, Japan. *Environmental Earth Sciences* 77, 354. <https://doi.org/10.1007/s12665-018-7529-9>
- Amin, N., Rahman, M., Raj, S., Ali, S., Green, J., Das, S., Doza, S., Mondol, M.H., Wang, Y., Islam, M.A., Alam, M., Huda, T.M.N., Haque, S., Unicomb, L., Joseph, G., Moe, C.L., 2019. Quantitative assessment of fecal contamination in multiple environmental sample types in urban communities in Dhaka, Bangladesh using SaniPath microbial approach. *PLoS ONE* 14, e0221193. <https://doi.org/10.1371/journal.pone.0221193>

- Anwar, E.A.A.E., 2019. Assessment of heavy metal pollution in soil and bottom sediment of Upper Egypt: comparison study. *Bulletin of the National Research Centre* 43, 180. <https://doi.org/10.1186/s42269-019-0233-4>
- APHA, 2017. Standard methods for the examination of water and wastewater. 23rd ed. Washington DC: American Public Health Association. <http://dl.mozh.org/upload/StandardMethods23RD.pdf> (accessed on 1 April 2022).
- Apollaro, C., Di Curzio, D., Fuoco, I., Buccianti, A., Dinelli, E., Vespasiano, G., Castrignano, A., Rusi, S., Barca, D., Figoli, A., Gabriele, B., Rosa, R.D., 2022. A multivariate non-parametric approach for estimating probability of exceeding the local natural background level of arsenic in the aquifers of Calabria region (Southern Italy). *Sci. Total Environ.* 806, 150345. <https://doi.org/10.1016/j.scitotenv.2021.150345>
- Aradpour, S., Noori, R., Naseh, M.R.V., Hosseinzadeh, M., Safavi, S., Rozegar, F.G., Maghrebi, M., 2021. Alarming carcinogenic and non-carcinogenic risk of heavy metals in Sabalan dam reservoir, Northwest of Iran. *Environ. Pollut. Bioavail.* 33, 278–291. <https://doi.org/10.1080/26395940.2021.1978868>.
- Aradpour, S., Noori, R., Tang, Q.; Bhattarai, R., Hooshyaripor, F., Hosseinzadeh, M., Haghghi, A.T., Klove, B., 2020. Metal contamination assessment in water column and surface sediments of a warm monomictic man-made lake: Sabalan Dam Reservoir, Iran. *Hydrol. Res.* 51, 799–814. <https://doi.org/10.2166/nh.2020.160>.
- Arefin, M.A., Mallik, A., 2018. Sources and causes of water pollution in Bangladesh: A technical overview. *Bibechana* 15, 97-112. <https://doi.org/10.3126/bibechana.v15i0.18688>
- Aristilde, L., Sposito, G., 2010. Binding of ciprofloxacin by humic substances: A molecular dynamics study. *Environ. Toxicol. Chem.* 29, 90-98. <https://doi.org/10.1002/etc.19>.
- Arthur, E., Tuller, M., Norgaard, T., Moldrup, P., Chen, C., Rehman, H.U., Weber, P.L., Knadel, M., Jonge, L.W.D., 2023. Contribution of organic carbon to the total specific surface area of soils with varying clay mineralogy. *Geoderma* 430, 116314. <https://doi.org/10.1016/j.geoderma.2022.116314>
- Astatkie, H., Ambelu, A., Mengistie, E., 2021. Contamination of Stream Sediment with Heavy Metals in the Awetu Watershed of Southwestern Ethiopia. *Front. Earth Sci.* 9, 668737. <https://doi.org/10.3389/feart.2021.658737>
- Ayub, A., Raza, Z. A., Majeed, M. I., Tariq, M. R., Irfan, A., 2020. Development of sustainable magnetic chitosan biosorbent beads for kinetic remediation of arsenic contaminated water. *Int. J. Biol. Macromol.* 163, 603-617. <https://doi.org/10.1016/j.ijbiomac.2020.06.287>.
- Bachtiar, T., Radjasa, O. K., Sabdono, A., 2004. Natural biodegradation of coprostanol in an experimental system of three environmental conditions of Jakarta waters, Indonesia. *J. Coast. Dev.*

- 8, 17-25. <https://media.neliti.com/media/publications/136588-EN-natural-biodegradation-of-coprostanol-in.pdf>
- Bahloul, M., Baati, H., Amdouni, R., Azri, C., 2018. Assessment of heavy metals contamination and their potential toxicity in the surface sediments of Sfax Solar Saltern, Tunisia. *Environmental Earth Sciences* 77, 27. <https://doi.org/10.1007/s12665-018-7227-7>
- Bai, X., Casey, F. X. M., Hakk, H., DeSutter, T. M., Oduor, P. O. G., Khan, E., 2015. Sorption and degradation of 17 β -estradiol-17-sulfate in sterilized soil–water systems. *Chemosphere* 119, 1322–1328. <http://dx.doi.org/10.1016/j.chemosphere.2014.02.016>
- Bakan, G., Ozkoc, H.B., Tulek, S., Cuce, H., 2010. Integrated environmental quality assessment of Kızılırmak River and its coastal environment. *Turk. J. Fish. Aquat. Sci.* 10, 453–462. <https://doi.org/10.4194/trjfas.2010.0403>.
- Batool, S., Idrees, M., Ahmad, M., Ahmad, M., Hussain, Q., Iqbal, A., Kong, J., 2020. Design and characterization of a biomass template/SnO₂ nanocomposite for enhanced adsorption of 2,4-dichlorophenol. *Environ. Res.* 181, 108955. <https://doi.org/10.1016/j.envres.2019.108955>.
- Bawa-Allah, K.A., 2023. Assessment of heavy metal pollution in Nigerian surface freshwaters and sediment: A meta-analysis using ecological and human health risk indices. *Journal of Contaminant Hydrology* 256, 104199. <https://doi.org/10.1016/j.jconhyd.2023.104199>
- Bawa-Allah, K.A., 2023. Assessment of heavy metal pollution in Nigerian surface freshwaters and sediment: A meta-analysis using ecological and human health risk indices. *Journal of Contaminant Hydrology* 256, 104199. <https://doi.org/10.1016/j.jconhyd.2023.104199>
- Bhuyan, M.S., Bakar, M.A., Nabi, M.R.U., Senapathi, V., Chung, S.Y., Islam, M.S., 2019. Monitoring and assessment of heavy metal contamination in surface water and sediment of the Old Brahmaputra River, Bangladesh. *Applied Water Science* 9, 125. <https://doi.org/10.1007/s13201-019-1004-y>
- Bhuyan, M.S., Bakar, M.A., Nabi, M.R.U., Senapathi, V., Chung, S.Y., Islam, M.S., 2019. Monitoring and assessment of heavy metal contamination in surface water and sediment of the Old Brahmaputra River, Bangladesh. *Appl. Water Sci.* 9, 125. <https://doi.org/10.1007/s13201-019-1004-y>.
- Bi, S.; Wang, L., Li, Y., Zhang, Z., Wang, Z., Ding, X., Zhou, J. A., 2021. Comprehensive Method for Water Environment Assessment considering Trends of Water Quality. *Adv. Civ. Eng.* 2021, 5548113. <https://doi.org/10.1155/2021/5548113>.
- Brady, N.C., Well, R.R., 2008. In: *The Nature and Properties of Soils*, fourteenth ed. Peason Prentice Hall, Upper Saddle River, New Jersey, Columbus, Ohio.
- Brown, R.M., McClelland, N.I., Deininger, R.A., O'Connor, M.F., 1972. A Water Quality Index—Crashing the Psychological Barrier. *Indic Environ Quality* 15, 173-182. https://doi.org/10.1007/978-1-4684-2856-8_15

- Brozni, D., Didovi, M. P., Rimac, V., Marinic, J., 2021. Sorption and leaching potential of organophosphorus insecticide dimethoate in Croatian agricultural soils. *Chemosphere* 273, 128563. <https://doi.org/10.1016/j.chemosphere.2020.128563>.
- Bujagic, I. M., Grujic, S., Jaukovic, Z., Lausevic, M., 2016. Sterol ratios as a tool for sewage pollution assessment of river sediments in Serbia. *Environ. Pollut.* 213, 76-83. <http://dx.doi.org/10.1016/j.envpol.2015.12.036>.
- Cai, Y., Mao, L., Deng, X., Zhou, C., Zhang, Y., 2023. Trace elements in surface sediments from Xinyanggang River of Jiangsu Province, China: Spatial distribution, risk assessment and source appointment. *Marine Pollution Bulletin* 187, 114550. <https://doi.org/10.1016/j.marpolbul.2022.114550>
- Calmuc, V.A., Calmuc, M., Arseni, M., Topa, C.M., Timofti, M., Burada, A., Iticescu, C., Georgescu, L.P., 2021. Assessment of heavy metal pollution levels in sediments and of ecological risk by quality indices, applying a case study: The lower Danube River, Romania. *Water* 13, 1801. <https://doi.org/10.3390/w13131801>
- Campos, V., Fraca'cio, R., Fraceto, L. F., Rosa, A. H., 2012. Fecal Sterols in Estuarine Sediments as Markers of Sewage Contamination in the Cubataõ Area, Saõ Paulo, Brazil. *Aquat Geochem* 18, 433–443. <https://doi.org/10.1007/s10498-012-9167-2>.
- Canadian Council of Ministers of the Environment, 2007. Canadian Water Quality Guidelines for the Protection of Aquatic Life. <https://ccme.ca/en/resources/water-aquatic-life> (accessed on 5 January 2022).
- Chowdhury, R.M., Muntasir, S.Y., Hossain, M.M., 2012. Water quality index of water bodies along Faridpur-Barisal Road in Bangladesh. *Glob. Eng. Technol. Rev.* 2, 1–8. <https://citeseerx.ist.psu.edu/viewdoc/download?doi=10.1.1.681.1779&rep=rep1&type=pdf> (accessed on 13 June 2021).
- Colla, N.S.L., Bott, S.E., Ronda, A.C., Menendez, M.C., Arias, A.H., Vitale, A.J., Piccolo, M.C., 2023. Insights on metal pollution of a Patagonia watershed: A case study in the lower course of the Negro River, Argentina. *Chemosphere* 323, 138234. <https://doi.org/10.1016/j.chemosphere.2023.138234>
- Conde-Cid, M., Fernández-Calviño, D., Fernández-Sanjurjo, M.J., Núñez-Delgado, A., Álvarez-Rodríguez, E., Arias-Estévez, M., 2019a. Adsorption/desorption and transport of sulfadiazine, sulfachloropyridazine, and sulfamethazine, in acid agricultural soils. *Chemosphere* 234:978-986. <https://doi.org/10.1016/j.chemosphere.2019.06.121>.
- Conde-Cid, M., Fernández-Calviño, D., Nóvoa-Muñoz, J. C., Núñez-Delgado, A., Fernández-Sanjurjo, M. J., Arias-Estévez, M., Álvarez-Rodríguez, E., 2019b. Experimental data and model prediction of tetracycline adsorption and desorption in agricultural soils. *Environ. Res.* 177, 108607. <https://doi.org/10.1016/j.envres.2019.108607>.

- Conde-Cid, M., Fernández-Calviño, D., Núñez-Delgado, A., Fernández-Sanjurjo, M. J., Arias-Estévez, M., Álvarez-Rodríguez, E., 2020. Estimation of adsorption/desorption Freundlich's affinity coefficients for oxytetracycline and chlortetracycline from soil properties: Experimental data and pedotransfer functions. *Ecotoxicol. Environ. Saf.* 196, 110584. <https://doi.org/10.1016/j.ecoenv.2020.110584>.
- Cordeiro, L. G. S. M., Carreira, R. S., Wagener, A. L. R., 2008. Geochemistry of fecal sterols in a contaminated estuary in southeastern Brazil. *Org. Geochem.* 39, 1097-1103. <https://doi.org/10.1016/j.orggeochem.2008.02.022>.
- Dai, Y., Zhuang, J., Chen, X., 2020. Synergistic effects of unsaturated flow and soil organic matter on retention and transport of PPCPs in soils. *Environ. Res.* 191, 110135. <https://doi.org/10.1016/j.envres.2020.110135>.
- Debnath, A., Singh, P.K., Sharma, Y.C., 2021. Metallic contamination of global river sediments and latest developments for their remediation. *Journal of Environmental Management* 298, 113378. <https://doi.org/10.1016/j.jenvman.2021.113378>
- Deng, Y., Yan, C., Nie, M., Ding, M., 2021. Bisphenol A adsorption behavior on soil and biochar: impact of dissolved organic matter. *Environ. Sci. Pollut. Res.* 28, 32434–32445. <https://doi.org/10.1007/s11356-021-12723-1>.
- Department of Environment, 1997. Peoples' Republic of Bangladesh. Environmental Conservation Rules. <https://www.elaw.org/system/files/Bangladesh+-+Environmental+Conservation+Rules,+1997.pdf> (accessed on 30 December 2021).
- Ding, H., Niu, X., Zhang, D., Lv, M., Zhang, Y., Lin, Z., Fu, M., 2023. Spatiotemporal analysis and prediction of water quality in Pearl River, China, using multivariate statistical techniques and data-driven model. *Environmental Science and Pollution Research* 30, 63036–63051. <https://doi.org/10.1007/s11356-023-26209-9>
- Duncan, A.E., Vries, N.D., Nyarko, K.B., 2018. Assessment of heavy metal pollution in the sediments of the River Pra and its tributaries. *Water Air Soil Pollut* 229, 272. <https://doi.org/10.1007/s11270-018-3899-6>
- Duodu, G.O., Goonetilleke, A., Ayoko, D.A., 2016. Comparison of pollution indices for the assessment of heavy metal in Brisbane River sediment. *Environmental Pollution* 219, 1077-1091. <http://dx.doi.org/10.1016/j.envpol.2016.09.008>
- Dutta, S. K., Amin, M. K., Ahmed, J., Elias, M., Mohiuddin, M., 2022. Removal of toxic methyl orange by a cost-free and eco-friendly adsorbent: Mechanism, phytotoxicity, thermodynamics, and kinetics. *S. Afr. J. Chem. Eng.* 40, 195-208. <https://doi.org/10.1016/j.sajce.2022.03.006>.
- El-Hamid, H.T.A., Hegazy, T.A. 2017. Evaluation of Water Quality Pollution Indices for Groundwater Resources of New Damietta, Egypt. *MOJ Ecology and Environmental Science* 2, 263-266. <http://doi.org/10.15406/mojes.2017.02.00045>

- El-Sorogy, A.S., Youssef, M., 2021. Pollution assessment of the Red Sea Gulf of Aqaba seawater, northwest Saudi Arabia. *Environ. Monit. Assess.* 193, 141. <https://doi.org/10.1007/s10661-021-08911-8>.
- Environment Review Report, 2014. Mongla Economic Zone, Bangladesh Export Zone Authority: Mongla, Bagerhat, pp. 1–33. <https://www.beza.gov.bd/wp-content/uploads/2015/10/ERR-of-Mongla-EZ.pdf> (accessed on 13 June 2021).
- EPA, 2001. Methods for collection, storage, and manipulation of sediments for chemical and toxicological analyses. Technical manual. <https://www.epa.gov/ocean-dumping/methods-collection-storage-and-manipulation-sediments-chemical-and-toxicological> (accessed on 2 April 2022)
- Fang, X., Peng, B., Wang, X., Song, Z., Zhou, D., Wang, Q., Qin, Z., Tan, C., 2019. Distribution, contamination and source identification of heavy metals in bed sediments from the lower reaches of the Xiangjiang River in Hunan province, China. *Science of The Total Environment* 689, 557-570. <https://doi.org/10.1016/j.scitotenv.2019.06.330>
- Fatema, K., Begum, M., Zahid, M.A., Hossain, M.E., 2018. Water quality assessment of the river Buriganga, Bangladesh. *J. Biodivers. Conserv. Bioresour. Manag.* 4, 47–53. <http://dx.doi.org/10.3329/jbcbm.v4i1.37876>.
- Fentahun, A., Mechal, A., Karuppanan, S., 2023. Hydrochemistry and quality appraisal of groundwater in Birr River Catchment, Central Blue Nile River Basin, using multivariate techniques and water quality indices. *Environ Monit Assess* 195, 655. <https://doi.org/10.1007/s10661-023-11198-6>
- Field, K. G., Samadpour, M., 2007. Fecal source tracking, the indicator paradigm, and managing water quality. *Water Res.* 41 (16), 3517-3538. <https://doi.org/10.1016/j.watres.2007.06.056>.
- Franklin, A. M., Williams, C., Andrews, D. M., Watson, J. E., 2022. Sorption and desorption behavior of four antibiotics at concentrations simulating wastewater reuse in agricultural and forested soils. *Chemosphere* 289, 133038. <https://doi.org/10.1016/j.chemosphere.2021.133038>.
- Frena, M., Bataglioni, G.A., Tonietto, A.E., Eberlin, M.N., Alexandre, M.R., Madureira, L.A.S., 2016a. Assessment of anthropogenic contamination with sterol markers in surface sediments of a tropical estuary (Itajaí-Açu, Brazil). *Science of the Total Environment* 544, 432–438. <http://dx.doi.org/10.1016/j.scitotenv.2015.11.137>
- Frena, M., Souza, M.R.R., Damasceno, F.C., Madureira, L.A.S., Alexandre, M.R., 2016b. Evaluation of anthropogenic contamination using sterol markers in a tropical estuarine system of northeast Brazil. *Marine Pollution Bulletin* 109, 619–623. <http://dx.doi.org/10.1016/j.marpolbul.2016.05.022>
- Froehner, S., Martins, R. F., Errera, M. R., 2009. Assessment of fecal sterols in Barigui River sediments in Curitiba, Brazil. *Environ. Monit. Assess.* 157, 591–600.

<http://dx.doi.org/10.1007/s10661-008-0559-0>.

- Furtula, V., Liu, J., Chambers, P., Osachoff, H., Kennedy, C., Harkness, J., 2012. Sewage Treatment Plants Efficiencies in Removal of Sterols and Sterol Ratios as Indicators of Fecal Contamination Sources. *Water Air Soil Pollut* 223, 1017–1031. <https://doi.org/10.1007/s11270-011-0920-8>.
- Gad, M., Safa, M.M.A.E., Farouk, M., Hussein, H., Alnemari, A.M., Elsayed, S., Khalifa, M.M., Moghanm, F.S., Eid, E.M., Saleh, A.H., 2021. Integration of water quality indices and multivariate modeling for assessing surface water quality in Qaroun Lake, Egypt. *Water* 13, 2258. <https://doi.org/10.3390/w13162258>
- Gaonkar, C.V., Nasnodkar, M.R., Matta, V.M., 2021. Assessment of metal enrichment and contamination in surface sediment of Mandovi estuary, Goa, West coast of India. *Environmental Science and Pollution Research* 28, 57872-57887. <https://doi.org/10.1007/s11356-021-14610-1>
- Geen, A.V., Ahmed, K.M., Akita, Y., Alam, M.J., Culligan, P.J., Emch, M., Escamilla, V., Feighery J., Ferguson, A.S., Knappett, P., Layton, A.C., Mailloux, B.J., McKay, L.D., Mey, J.L., Serre, M.L., Streatfield, P.K., Wu, J., Yunusz, M., 2011. Fecal Contamination of Shallow Tubewells in Bangladesh Inversely Related to Arsenic. *Environ. Sci. Technol.* 45, 1199–1205. <https://doi.org/10.1021/es103192b>
- Ghaderpoori, M., kamarehie, B., Jafari, A., Ghaderpoury, A., Karami, M., 2018. Heavy metals analysis and quality assessment in drinking water-Khorramabad city, Iran. *Data in Brief* 16, 685-692. <https://doi.org/10.1016/j.dib.2017.11.078>
- Goher, M.E., Hassan, A.M., Abdel-Moniem, I.A., Fahmy, A.H., El-sayed, S.M., 2014. Evaluation of surface water quality and heavy metal indices of Ismailia Canal, Nile River, Egypt. *Egypt. J. Aquat. Res.* 40, 225–233. <http://dx.doi.org/10.1016/j.ejar.2014.09.001>
- Guo, R., He, X., 2013. Spatial variations and ecological risk assessment of heavy metals in surface sediments on the upper reaches of Hun River, northeast China. *Environmental Earth Sciences* 70, 1083-1090. <https://doi.org/10.1007/s12665-012-2196-8>
- Hakanson, L., 1980. An ecological risk index for aquatic pollution control, A sedimentological approach. *Water Research* 14, 975-1001. [https://doi.org/10.1016/0043-1354\(80\)90143-8](https://doi.org/10.1016/0043-1354(80)90143-8)
- Hameed, B.H., Mahmoud, D.K., Ahmad, A.L., 2008. Equilibrium modeling and kinetic studies on the adsorption of basic dye by a low-cost adsorbent: Coconut (*Cocos nucifera*) bunch waste. *Journal of Hazardous Materials* 158, 65–72. <https://doi.org/10.1016/j.jhazmat.2008.01.034>
- Haque, M.M., Niloy, N.M., Nayna, O.K., Fatema, K.J., Quraishi, S.B., Park, J.H., Kim, K.W., Tareq, S.M. 2020. Variability of water quality and metal pollution index in the Ganges River, Bangladesh. *Environmental Science and Pollution Research* 27, 42582-42599. <https://doi.org/10.1007/s11356-020-10060-3>
- Hasan, M.K., Shahriar, A., Jim, K.U., 2019. Water pollution in Bangladesh and its impact on public health. *Heliyon* 5, e02145. <https://doi.org/10.1016/j.heliyon.2019.e02145>

- Higgins, C. P., Luthy, R. G., 2006. Sorption of Perfluorinated Surfactants on Sediments. *Environ. Sci. Technol.* 40, 7251-7256. <https://doi.org/10.1021/es061000n>.
- Horton, R.K., 1965. An index number system for rating water quality. *J. Water Pollut. Control Fed.* 373, 303–306.
- Hossain, M.N., Rahaman, A., Hasan, M.J., Uddin, M.M., Khatun, N., Shamsuddin, S.M., 2021. Comparative seasonal assessment of pollution and health risks associated with heavy metals in water, sediment and fish of Buriganga and Turag River in Dhaka City, Bangladesh. *SN Applied Sciences* 3, 509. <https://doi.org/10.1007/s42452-021-04464-0>
- Hossain, F., Islam, M.A., Al-Mamun, A., Naher, K., Khan, R., Das, S., Tamim, U., Hossain, S.M., Nahid, F., Islam, M.A., 2016. Assessment of Trace Contaminants in Sediments of the Poshur River Nearby Mongla Port of Bangladesh. *Nucl. Sci. Appl.* 25, 7–11. http://baec.portal.gov.bd/sites/default/files/files/baec.portal.gov.bd/page/1f00cd0e_737d_4e2e_ab9f_08183800b7a2/2=2504-F.pdf (accessed on 15 October 2021).
- Hossain, M.B., Shanta, T.B., Ahmed, A.S.S., Hossain, M.K., Semme, S.A., 2019. Baseline study of heavy metal contamination in the Sangu River estuary, Chattogram, Bangladesh. *Mar. Pollut. Bull.* 140, 255–261. <https://doi.org/10.1016/j.marpolbul.2019.01.058>.
- Hossain, M.J., Chowdhury, M.A., Jahan, S., Zzaman, R.U., Islam, S.L.U., 2021. Drinking Water Insecurity in Southwest Coastal Bangladesh: How Far to SDG 6.1? *Water* 13, 3571. <https://doi.org/10.3390/w13243571>
- Howladar, M.F., Hossain, M.N., Anju, K.A., Das, D., 2021. Ecological and health risk assessment of trace metals in water collected from Haripur gas blowout area of Bangladesh. *Sci. Rep.* 11, 15573. <https://doi.org/10.1038/s41598-021-94830-0>
- Huang, Z., Zheng, S., Liu, Y.; Zhao, X., Qiao, X.; Liu, C., Zheng, B., Yin, D., 2021. Distribution, toxicity load, and risk assessment of dissolved metal in surface and overlying water at the Xiangjiang River in southern China. *Sci. Rep.* 11, 109. <https://doi.org/10.1038/s41598-020-80403-0>
- Hussain, M. A., Ford, R., Hill, J., 2010. Determination of fecal contamination indicator sterols in an Australian water supply system. *Environ. Monit. Assess.* 165, 147–157. <https://doi.org/10.1007/s10661-009-0934-5>
- Inyinbor, A.A., Adekola, F.A., Olatunji, G.A., 2016. Kinetics, isotherms and thermodynamic modeling of liquid phase adsorption of Rhodamine B dye onto *Raphia hookeri* fruit epicarp. *Water Resour. Ind.* 15, 14-27. <https://doi.org/10.1016/j.wri.2016.06.001>
- Islam, J.B., Sarkar, M., Rahman, A.K.M.L., Ahmed, K.S. 2015. Quantitative assessment of toxicity in the Shitalakkhya River, Bangladesh. *Egyptian Journal of Aquatic Research* 41, 25-30. <https://doi.org/10.1016/j.ejar.2015.02.002>
- Islam, M.A., Das, B., Quraishi, SB., Khan R, Naher, K., Hossain, S.M., Karmaker, S., Latif, A.S.,

- Hossen, M.B., 2020. Heavy metal contamination and ecological risk assessment in water and sediments of the Halda river, Bangladesh: A natural fish breeding ground. *Marine Pollution Bulletin* 160, 111649. <https://doi.org/10.1016/j.marpolbul.2020.111649>
- Islam, M.S., Ahmed, M.K., Raknuzzaman, M., Mamun, M.H.A., Islam, M.K., 2015. Heavy metal pollution in surface water and sediment: A preliminary assessment of an urban river in a developing country. *Ecological Indicators* 48, 282-291. <https://doi.org/10.1016/j.ecolind.2014.08.016>
- Islam, M.S., Nakagawa, K., Abdullah-Al-Mamun, M., Siddique, M.A.B., Berndtsson, R. 2022. Is road-side fishpond water in Bangladesh safe for human use? An assessment using water quality indices. *Environmental Challenges* 6:100434. <https://doi.org/10.1016/j.envc.2021.100434>
- Islam, M.M.M., Hofstra, N., Islam, M.A., 2017. The Impact of Environmental Variables on Faecal Indicator Bacteria in the Betna River Basin, Bangladesh. *Environ. Process.* 4, 319–332. <https://doi.org/10.1007/s40710-017-0239-6>
- Isobe, K.O., Tarao, M., Zakaria, M.P., Chiem, N.H., Minh, L.Y., Takada, H., 2002. Quantitative application of fecal sterols using gas chromatography–mass spectrometry to investigate fecal pollution in tropical waters: Western Malaysia and Mekong delta, Vietnam. *Environ. Sci. Technol.* 36, 4497-4507. <https://doi.org/10.1021/es020556h>
- Jahan, S., Strezov, V., 2017. Water quality assessment of Australian ports using water quality evaluation indices. *PLoS ONE* 12, e0189284. <https://doi.org/10.1371/journal.pone.0189284>
- Kabir, M.H., Islam, M.S., Tusher, T.R., Hoq M.E., Mamun S.A., 2020. Changes of heavy metal concentrations in shitalakhya river water of Bangladesh with seasons. *Indonesian Journal of Science & Technology* 5:395-409. <https://doi.org/10.17509/ijost.v5i3.25007>
- Kalipci, E., Cüce, H., Ustaoglu, F., Dereli, M.L., Türkmen, M., 2023. Toxicological health risk analysis of hazardous trace elements accumulation in the edible fish species of the Black Sea in Türkiye using multivariate statistical and spatial assessment. *Environmental Toxicology and Pharmacology* 97, 104028. <https://doi.org/10.1016/j.etap.2022.104028>
- Kang, Z., Wang, S., Qin, J., Wu, R., Li, H., 2020. Pollution characteristics and ecological risk assessment of heavy metals in paddy fields of Fujian province, China. *Scientific Reports* 10, 12244. <https://doi.org/10.1038/s41598-020-69165-x>
- Karunanidhi, D., Aravinthasamy, P., Subramani, T., Chandrajith, R., Raju, N.J., Antunese, I.M.H.R. 2022. Provincial and seasonal influences on heavy metals in the Noyyal River of South India and their human health hazards. *Environmental Research* 204, 111998. <https://doi.org/10.1016/j.envres.2021.111998>
- Kaur, P., Makkar, A., Kaur, P., Shilpa, 2018. Temperature Dependent Adsorption–Desorption Behaviour of Pendimethalin in Punjab Soils. *Bull. Environ. Contam. Toxicol.* 100, 167–175. <https://doi.org/10.1007/s00128-017-2235-y>

- Kaushik, H., Ranjan, R., Ahmad, R., Kumar, A., Prashant, Kumar, N., Ranjan, R.K., 2021. Assessment of trace metal contamination in the core sediment of Ramsar wetland (Kabar Tal), Begusarai, Bihar (India). *Environmental Science and Pollution Research* 28, 18686-18701. <https://doi.org/10.1007/s11356-020-11775-z>
- Khadija, D., Hicham, A., Rida, A., Hicham, E., Nordine, N., Najlaa, F., 2021. Surface water quality assessment in the semi-arid area by a combination of heavy metal pollution indices and statistical approaches for sustainable management. *Environmental Challenges* 5, 100230. <https://doi.org/10.1016/j.envc.2021.100230>
- Khan, R., Saxena, A., Shukla, S., Sekar, S., Senapathi, V., Wu, J., 2021. Environmental contamination by heavy metals and associated human health risk assessment: a case study of surface water in Gomti River Basin, India. *Environmental Science and Pollution Research* 28, 56105-56116. <https://doi.org/10.1007/s11356-021-14592-0>
- Khan, A. H., Macfie, S. M., Ray, M. B., 2017. Sorption and leaching of benzalkonium chlorides in agricultural soils. *J. Environ. Manage.* 196, 26-35. <https://doi.org/10.1016/j.jenvman.2017.02.065>.
- Khan, M.H., Nafees, M., Muhammad, N., Ullah, U., Hussain, R., Bilal, M., 2021. Assessment of Drinking Water Sources for Water Quality, Human Health Risks, and Pollution Sources: A Case Study of the District Bajaur, Pakistan. *Arch. Environ. Contam. Toxicol.* 80, 41–54. <https://doi.org/10.1007/s00244-020-00801-3>.
- Khan, M.H.R., Liu, J.; Liu, S., Li, J.; Cao, L., Rahman, A., 2020. Anthropogenic effect on heavy metal contents in surface sediments of the Bengal Basin River system, Bangladesh. *Environ. Sci. Pollut. Res.* 27, 19688–19702. <https://doi.org/10.1007/s11356-020-08470-4>.
- Kibria, G., Hossain, M.M., Mallick, D., Lau, T.C., Wu, R., 2016. Monitoring of metal pollution in waterways across Bangladesh and ecological and public health implications of pollution. *Chemosphere* 165, 1-9. <http://dx.doi.org/10.1016/j.chemosphere.2016.08.121>
- Klitzke, S., Apelt, S., Weiler, C., Fastner, J., Chorus, I., 2010. Retention and degradation of the cyanobacterial toxin cylindrospermopsin in sediments-The role of sediment preconditioning and DOM composition. *Toxicon* 55, 999-1007. <https://doi.org/10.1016/j.toxicon.2009.06.036>.
- Klitzke, S., Beusch, C., Fastner, J., 2011. Sorption of the cyanobacterial toxins cylindrospermopsin and anatoxin-a to sediments. *Water Res.* 45, 1338-1346. <https://doi.org/10.1016/j.watres.2010.10.019>.
- Krishna, A.K., Satyanarayanan, M., Govil, P.K., 2009. Assessment of heavy metal pollution in water using multivariate statistical techniques in an industrial area: A case study from Patancheru, Medak District, Andhra Pradesh, India. *J. Hazard. Mater.* 167, 366–373. <https://doi.org/10.1016/j.jhazmat.2008.12.131>
- Kumar, P., Hama, S., Abbass, R.A., Nogueira, T., Brand, V.S., Abhijit, K.V., Andrade, M.D.F., Asfaw, A., Aziz, K.H., Cao, S.J., Gendy, A.E., Khare, M., Muula, A.S., Nagendra, S.M.S., Ngow, A.V.,

- Omer, K., Olaya, Y., Salam, A., 2021. Potential health risks due to in-car aerosol exposure across ten global cities. *Environment International* 155, 106688. <https://doi.org/10.1016/j.envint.2021.106688>
- Kumar, S., Islam, A.R.M.T., Hasanuzzaman, M., Salam, R., Khan, R., Islam, M.S., 2021. Preliminary assessment of heavy metals in surface water and sediment in Nakuvadra-Rakiraki river, Fiji using indexical and chemometric approaches. *Journal of Environmental Management* 298, 113517. <https://doi.org/10.1016/j.jenvman.2021.113517>
- Kumar, A., Mishra, S., Taxak, A.K., Pandey, R., Yu, Z.G., 2020. Nature rejuvenation: Long term (1989–2016) vs short-term memory approach-based appraisal of water quality of the upper part of Ganga River, India. *Environ. Technol. Innov.* 20, 101164. <https://doi.org/10.1016/j.eti.2020.101164>.
- Lee, S. C., Park, S., 2016. Removal of furan and phenolic compounds from simulated biomass hydrolysates by batch adsorption and continuous fixed-bed column adsorption methods. *Bioresour. Technol.* 216, 661-668. <https://doi.org/10.1016/j.biortech.2016.06.007>.
- Leeming, R., Ball, A., Ashbolt, N., Nichols, P., 1996. Using faecal sterols from humans and animals to distinguish faecal pollution in receiving waters. *Water Res.* 30, 2893-2900. [https://doi.org/10.1016/S0043-1354\(96\)00011-5](https://doi.org/10.1016/S0043-1354(96)00011-5).
- Lei, C., Hu, Y. Y., He, M. Z., 2013. Adsorption characteristics of triclosan from aqueous solution onto cetylpyridinium bromide (CPB) modified zeolites. *Chem. Eng. J.* 219, 361-370. <https://doi.org/10.1016/j.cej.2012.12.099b>
- Lei, W., Tang, X., Zhou, X., 2020. Biochar amendment effectively reduces the transport of 3,5,6-trichloro-2-pyridinol (a main degradation product of chlorpyrifos) in purple soil: Experimental and modeling. *Chemosphere* 245, 125651. <https://doi.org/10.1016/j.chemosphere.2019.125651>
- Li, J., Guo, K., Cao, Y., Wang, S., Song, Y., Zhang, H., 2021. Enhance in mobility of oxytetracycline in a sandy loamy soil caused by the presence of microplastics. *Environ. Pollut.* 269, 116151. <https://doi.org/10.1016/j.envpol.2020.116151>
- Lin, Y., Gritsenko, D., Feng, S., Teh, Y.C., Lu, X., Xu, J., 2016. Detection of heavy metal by paper-based microfluidics. *Biosens. Bioelectron.* 83, 256–266. <https://doi.org/10.1016/j.bios.2016.04.061>
- Ling, T.Y., Gerunsin, N., Soo, C.L., Nyanti, L., Sim, S.F., Grinang, J., 2017. Seasonal Changes and Spatial Variation in Water Quality of a Large Young Tropical Reservoir and Its Downstream River. *J. Chem.* 2017, 8153246. <https://doi.org/10.1155/2017/8153246>
- Lipy, E.P., Hakim, M., Mohanta, L.C., Islam, D., Lyzu, C., Roy, D.C., Jahan, I., Akhter, S., Raknuzzaman, M., Sayed, M.A. 2021. Assessment of heavy metal concentration in water, sediment and common fish species of Dhaleshwari river in Bangladesh and their health implications. *Biological Trace Element Research* 199, 4295-4307.

<https://doi.org/10.1007/s12011-020-02552-7>

- Lu, Y., Philp, R. P., Biache, C., 2016. Assessment of Fecal Contamination in Oklahoma Water Systems through the Use of Sterol Fingerprints. *Environments* 3, 28. <https://doi.org/10.3390/environments3040028>.
- Lühe, B. D., Dawson, L. A., Mayes, R. W., Forbes, S. L., Fiedler, S., 2013. Investigation of sterols as potential biomarkers for the detection of pig (*S. s. domesticus*) decomposition fluid in soils. *Forensic Sci. Int.* 230, 68-73. <https://doi.org/10.1016/j.forsciint.2013.03.030>.
- Luo, M., Yu, H., Liu, Q., Lan, W., Ye, Q., Niu, Y., Niu, Y., 2021. Effect of river-lake connectivity on heavy metal diffusion and source identification of heavy metals in the middle and lower reaches of the Yangtze River. *Journal of Hazardous Materials* 416, 125818. <https://doi.org/10.1016/j.jhazmat.2021.125818>
- Lyons, B. P., Devlin, M. J., Hamid, S. A. A., Al-Otiabi, A. F., Al-Enezi, M., Massoud, M. S., Al-Zaidan, A. S., Smith, A. J., Morris, S., Bersuder, P., Barber, J. L., Papachlimitzou, A., Al-Sarawi, H. A., 2015. Microbial water quality and sedimentary faecal sterols as markers of sewage contamination in Kuwait. *Mar. Pollut. Bull.* 100 (2), 689–698. <https://doi.org/10.1016/j.marpolbul.2015.07.043>
- Ma, X., Liu, X., Ding, S., Su, S., Gan, Z., 2019. Sorption and leaching behavior of bithionol and levamisole in soils. *Chemosphere* 224, 519-526. <https://doi.org/10.1016/j.chemosphere.2019.02.170>
- Machado, S. K., Froehner, s., Sáñez, J., Figueira, R. C. L., Ferreira, P. A. L., 2014. Assessment of historical fecal contamination in Curitiba, Brazil, in the last 400 years using fecal sterols. *Sci. Total Environ.* 493, 1065–1072. <http://dx.doi.org/10.1016/j.scitotenv.2014.06.104>.
- Mahmoud, E.K., Ghoneim, A.M., 2016. Effect of polluted water on soil and plant contamination by heavy metals in El-Mahla El-Kobra, Egypt. *Solid Earth* 7, 703–711. <https://doi.org/10.5194/se-7-703-2016>
- Malsiu, A., Shehu, I., Stafilov, T., Faiku, F., 2020. Assessment of heavy metal concentrations with fractionation method in sediments and waters of the Badovci Lake (Kosovo). *Journal of Environmental and Public Health* 2020, 3098594. <https://doi.org/10.1155/2020/3098594>
- Mark, N., Arthur, J., Dontsova, K., Brusseau, M., Taylor, S., 2016. Adsorption and attenuation behavior of 3-nitro-1,2,4-triazol-5-one (NTO) in eleven soils. *Chemosphere* 144, 1249–1255. <http://dx.doi.org/10.1016/j.chemosphere.2015.09.101>.
- Mekuria, D.M., Kassegne, A.B., Asfaw, S.L., 2021. Assessing pollution profiles along Little Akaki River receiving municipal and industrial wastewaters, Central Ethiopia: implications for environmental and public health safety. *Heliyon* 7, e07526. <https://doi.org/10.1016/j.heliyon.2021.e07526>

- Melo, M. G., Silva, B. A., Costa, G. D. S., Neto, J. C. A. S., 2019. Patrícia Kaori Soares, Adalberto Luis Val, Jamal da Silva Chaar, Hector Henrique Ferreira Koolen, Giovana Anceski Bataglion, Sewage contamination of Amazon streams crossing Manaus (Brazil) by sterol biomarkers. *Environ. Pollut.* 244, 818-826. <https://doi.org/10.1016/j.envpol.2018.10.055>.
- Molekoa, M.D., Avtar, R., Kumar, P., Minh, H.V.T., Dasgupta, R., Johnson, B., Sahu, N., Verma, R.L., Yunus, A.P. 2021. Spatio-temporal analysis of surface water quality in Mokopane area, Limpopo, South Africa. *Water* 13, 220. <https://doi.org/10.3390/w13020220>
- Mongla Municipality in Khulna Division, 2011. <https://www.citypopulation.de/en/bangladesh/khulna/admin/bagerhat/015899> (accessed on 20 June 2021).
- Mookan, V.P., Machakalai, R.K., Srinivasan, S., Sigamani, S., Kolandhasamy, P., Gnanamoorthy, P., Moovendhan, M., Srinivasan, R., Hatamleh, A.A., AI-Dosary, M.A., 2023. Assessment of metal contaminants along the Bay of Bengal — Multivariate pollution indices. *Marine Pollution Bulletin* 192, 115008. <https://doi.org/10.1016/j.marpolbul.2023.115008>
- Muller, J., 1981. Determination of the residence times of aerosol constituents. *Journal of Aerosol Science* 12, 202-203. [https://doi.org/10.1016/0021-8502\(81\)90096-3](https://doi.org/10.1016/0021-8502(81)90096-3)
- Nakagawa, K., Amano, H., Asakura, H., Berndtsson, R., 2016. Spatial trends of nitrate pollution and groundwater chemistry in Shimabara, Nagasaki, Japan. *Environmental Earth Sciences* 75, 234. <https://doi.org/10.1007/s12665-015-4971-9>
- Nakagawa, K., Amano, H., Berndtsson, R., Takao, Y., Hosono, T., 2019. Use of sterols to monitor surface water quality change and nitrate pollution source. *Ecological Indicator* 107, 105534. <https://doi.org/10.1016/j.ecolind.2019.105534>
- Nakagawa, K., Amano, H., Persson, M., Berndtsson, R., 2021. Spatiotemporal variation of nitrate concentrations in soil and groundwater of an intensely polluted agricultural area. *Sci. Rep.* 11, 2598. <https://doi.org/10.1038/s41598-021-82188-2>
- Nakagawa, K., Amano, H., Takao, Y., Hosono, T., Berndtsson, R., 2017. On the use of coprostanol to identify source of nitrate pollution in groundwater. *J. Hydrol.* 550, 663–668. <https://doi.org/10.1016/j.jhydrol.2017.05.038>
- Nakagawa, K., Imura, T., Berndtsson, R., 2022. Distribution of heavy metals and related health risks through soil ingestion in rural areas of western Japan. *Chemosphere*, 290, 133316. <https://doi.org/10.1016/j.chemosphere.2021.133316>
- Nakagawa, K., Amano, H., Asakura, H., Berndtsson, R., 2016. Spatial trends of nitrate pollution and groundwater chemistry in Shimabara, Nagasaki, Japan. *Environ. Earth Sci.* 75, 234. <https://doi.org/10.1007/s12665-015-4971-9>

- Nakagawa, K., Amano, H., Berndtsson, R., Takao, Y., Hosono, T., 2019. Use of sterols to monitor surface water quality change and nitrate pollution source. *Ecol. Indic.* 107, 105534. <https://doi.org/10.1016/j.ecolind.2019.105534>
- Nasiruddin, M., Islam, A.R.M., Siddique, M.A.B., Hasanuzaman, M., Hassan, M.M., Akbor, M.A., Hasan, M., M.A., Islam, M.S., Khan, R., Amin, M.A., Pal, S.C., Idris, A.M., Kumar, S., 2023. Distribution, sources, and pollution levels of toxic metal(loid)s in an urban river (Ichamati), Bangladesh using SOM and PMF modeling with GIS tool. *Environmental Science and Pollution Research* 30, 20934–20958. <https://doi.org/10.1007/s11356-022-23617-1>
- Nazneen, S., Singh, S., Raju, N.J., 2018. Heavy metal fractionation in core sediments and potential biological risk assessment from Chilika lagoon, Odisha state, India. *Quaternary International* 507, 370-388. <https://doi.org/10.1016/j.quaint.2018.05.011>
- Ndondo, G.R.N., Boum, S.N., Song, F., Eyong, G.E.T., Komba, D.E., Nlend, B., Etame, J., 2021. Hydrogeochemical characteristics and quality assessment of surface water in an agricultural area in equatorial Africa: The Mungo River Basin, Southwest Cameroon, Central Africa. *Journal of Geoscience and Environment Protection* 9, 164-181. <https://doi.org/10.4236/gep.2021.93010>
- Nichols, P. D., Leeming, R., Rayner, M. S., Latham, V., Ashbolt, N. J., Turner, C., 1993. Comparison of the abundance of the fecal sterol coprostanol and fecal bacterial groups in inner-shelf waters and sediments near Sydney, Australia. *J. Chromatogr. A* 643 (1-2), 189-195. [https://doi.org/10.1016/0021-9673\(93\)80552-J](https://doi.org/10.1016/0021-9673(93)80552-J)
- Nkinda, M.S., Rwiza, M.J., Ijumba, J.N., Njau, K.N. 2021. Heavy metals risk assessment of water and sediments collected from selected river tributaries of the Mara River in Tanzania. *Discover Water* 1, 3. <https://doi.org/10.1007/s43832-021-00003-5>
- Noori, R., Berndtsson, R., Hosseinzadeh, M., Adamowski, J.F., Abyaneh, M.R., 2019. A critical review on the application of the National Sanitation Foundation Water Quality Index. *Environ. Pollut.* 244, 575–587. <https://doi.org/10.1016/j.envpol.2018.10.076>
- Ojekunle, O.Z., Ojekunle, O.V., Adeyemi, A.A., Taiwo, A.G., Sangowusi, O.R., Taiwo, A.M., Adekitan, A.A., 2016. Evaluation of surface water quality indices and ecological risk assessment for heavy metals in scrap yard neighborhood. *Springerplus* 5, 560. <https://doi.org/10.1186/s40064-016-2158-9>
- Omeka, M.E., Egbueri, J.C., 2023. Hydrogeochemical assessment and health-related risks due to toxic element ingestion and dermal contact within the Nnewi-Awka urban areas, Nigeria. *Environ Geochem Health* 45, 2183–2211. <https://doi.org/10.1007/s10653-022-01332-7>
- Omwene, P.I., Oncel, M.S., Çelen, M., Kobya, M., 2018. Heavy metal pollution and spatial distribution in surface sediments of Mustafakemalpas, a stream located in the world's largest borate basin (Turkey). *Chemosphere* 208,782-792. <https://doi.org/10.1016/j.chemosphere.2018.06.031>

- Oukali-Haouchine, O., Barriuso, E., Mayata. Y., Moussaoui, K. M., 2013. Factors affecting metribuzin retention in Algerian soils and assessment of the risks of contamination. *Environ. Monit. Assess.* 185, 4107–4115. <https://doi.org/10.1007/s10661-012-2853-0>
- Pal, R., Megharaj, M., Kirkbride, K. P., Naidu, R., 2015. Adsorption and desorption characteristics of methamphetamine, 3,4-methylenedioxymethamphetamine, and pseudoephedrine in soils. *Environ. Sci. Pollut. Res.* 22, 8855–8865. <https://doi.org/10.1007/s11356-014-2940-6>.
- Parvin, F., Haque, M.M., Tareq, S.M., 2022. Recent status of water quality in Bangladesh: A systematic review, meta-analysis and health risk assessment. *Environmental Challenges* 6, 100416. <https://doi.org/10.1016/j.envc.2021.100416>
- Pavlidou, A., Anastasopoulou, E., Dassenakis, M., Hatzianestis, I., Paraskevopoulou, V., Simboura, N., Rousselak, E., Drakopoulou, P., 2014. Effects of olive oil wastes on river basins and an oligotrophic coastal marine ecosystem: A case study in Greece. *Sci. Total Environ.* 497–498, 38–49. <https://doi.org/10.1016/j.scitotenv.2014.07.088>
- Pavlovic, D. M., Glavac, A., Gluhak, M., Runje, M., 2018. Sorption of albendazole in sediments and soils: Isotherms and kinetics. *Chemosphere* 193, 635-644. <https://doi.org/10.1016/j.chemosphere.2017.11.025>
- Peluso, J., Coll, C.S.P., Cristos, D., Rojas, D.E., Aronzon, C.M., 2021. Comprehensive assessment of water quality through different approaches: Physicochemical and ecotoxicological parameters. *Sci. Total. Environ.* 800, 149510. <https://doi.org/10.1016/j.scitotenv.2021.149510>
- Persits, F.M., Wandrey, C.J., Milici, R.C., Manwar, A., 2001. Digital geologic and geophysical data of Bangladesh. U.S. Geol. Surv. Open-File Rep. <https://doi.org/10.3133/ofr97470H> (accessed 25 June, 2021)
- Pia, H.I., Akhter, M., Sarker, S., Hassan, M., Rayhan, A.B.M.S., Islam, M.M., Hassan, M.A., 2018. Contamination Level (Water Quality) Assessment and Agro-ecological Risk Management of Shitalakshya River of Dhaka, Bangladesh. *Hydro Current Res* 9, 1. <https://doi.org/10.4172/2157-7587.1000292>
- Pichtel, J., 216. Oil and Gas Production Wastewater: Soil Contamination and Pollution Prevention. *Appl. Environ. Soil Sci.* 2016, 2707989. <https://doi.org/10.1155/2016/2707989>
- Piroozfar, P., Alipour, S., Modabberi, S., Cohen, D., 2021. Using multivariate statistical analysis in assessment of surface water quality and identification of heavy metal pollution sources in Sarough watershed, NW of Iran. *Environ. Monit. Assess.* 193, 564. <https://doi.org/10.1007/s10661-021-09363-w>
- Prakathi, J., Mahanty, B., Lhamo, P., 2020. Adsorption, Bioavailability and Microbial Toxicity of Diclofenac in Agricultural Soil. *Bull. Environ. Contam. Toxicol.* 105, 490–495. <https://doi.org/10.1007/s00128-020-02955-1>
- Proshad, R., Zhang, D., Idris, A.M., Islam, M.S., Kormoker, T., Sarker, M.N.I., Khadka, S., Sayeed,

- A., Islam, M., 2021. Comprehensive evaluation of chemical properties and toxic metals in the surface water of Louhajang River, Bangladesh. *Environmental Science and Pollution Research* 28, 49191-49205. <https://doi.org/10.1007/s11356-021-14160-6>
- Proshad, R., Dey, H.C., Khan, M.S.U., Kumar, A.B.S., Idris, A.M., 2023. Source-oriented risks apportionment of toxic metals in river sediments of Bangladesh: a national wide application of PMF model and pollution indices. *Environ Geochem Health*. <https://doi.org/10.1007/s10653-022-01455-x>
- Proshad, R., Zhang, D., Idris, A.M., Islam, M.S., Kormoker, T., Sarker, M.N.I., Khadka, S., Sayeed, A., Islam, M., 2021. Comprehensive evaluation of chemical properties and toxic metals in the surface water of Louhajang River, Bangladesh. *Environ. Sci. Pollut. Res.* 28, 49191–49205. <https://doi.org/10.1007/s11356-021-14160-6>
- Prost, K., Birk, J., J., Lehndorff, E., Gerlach, R., Amelung, W., 2017. Steroid Biomarkers Revisited – Improved Source Identification of Faecal Remains in Archaeological Soil Material. *PLoS ONE* 12 (1), e0164882. <https://doi.org/10.1371/journal.pone.0164882>
- Qian, J., Shen, M., Wang, P., Wang, C., Hou, J., Ao, Y., Liu, J., Li, K., 2017. Adsorption of perfluorooctane sulfonate on soils: Effects of soil characteristics and phosphate competition. *Chemosphere* 168, 1383-1388. <https://doi.org/10.1016/j.chemosphere.2016.11.114>.
- Qin, G., Liu, J., Xu, S., Wang, T., 2020. Water quality assessment and pollution source apportionment in a highly regulated river of Northeast China. *Environ Monit Assess* 192, 446. <https://doi.org/10.1007/s10661-020-08404-0>
- Rabelo, A. E. C. D. G. D. C., Neto, S. M. D. S., Coutinho, A. P., Antonino, A. C. D., 2021. Sorption of sulfadiazine and flow modeling in an alluvial deposit of a dry riverbed in the Brazilian semiarid. *J. Contam. Hydrol.* 241, 103818. <https://doi.org/10.1016/j.jconhyd.2021.103818>
- Rahman, M.S., Ahmed, Z., Seefat, S.M., Alam, R., Islam, A.R.M.T., Choudhury, T.R., Begum, B.A., Idris, A.M., 2022. Assessment of heavy metal contamination in sediment at the newly established tannery industrial Estate in Bangladesh: A case study. *Environmental Chemistry and Ecotoxicology* 4, 1-12. <https://doi.org/10.1016/j.enceco.2021.10.001>
- Rahman, M.S., Saha, N., Molla, A.H., 2014. Potential ecological risk assessment of heavy metal contamination in sediment and water body around Dhaka Export Processing Zone, Bangladesh. *Environmental Earth Sciences* 71, 2293-2308. <https://doi.org/10.1007/s12665-013-2631-5>
- Rajesh, K.S., Liu, Y., Zhang, X., Ravi, K.B., Bai, G., Li, X., 2018. Studies on seasonal pollution of heavy metals in water, sediment, fish and oyster from the Meiliang Bay of Taihu Lake in China. *Chemosphere* 191, 626-638. <https://doi.org/10.1016/j.chemosphere.2017.10.078>
- Ram, A., Tiwari, S.K., Pandey, H.K., Chaurasia, A.K., Singh, S., Singh, Y.V., 2021. Groundwater quality assessment using water quality index (WQI) under GIS framework. *Applied Water Science* 11, 46. <https://doi.org/10.1007/s13201-021-01376-7>

- Ramachandra, T.V., Bhat, S.P., Mahapatra, D.M., Krishnadas, G., 2012. Impact of indiscriminate disposal of untreated effluents from thermal power plants on water resources. *Indian J. Environ. Prot.* 32, 705–718. http://wgbis.ces.iisc.ernet.in/energy/water/paper/ijep_water_resources/ijep_water_resources.pdf (accessed on 7 October 2021)
- Rampley, C.P.N., Whitehead, P.G., Softley, L., Hossain, M.A., Jin, L., David, J., Shawal, S., Das, P., Thompson, I.P., Huang, W.E., Peters, R., Holdship, P., Hope, R., Alabaster, G., 2020. River toxicity assessment using molecular biosensors: Heavy metal contamination in the Turag-Baluburiganga River systems, Dhaka, Bangladesh. *Science of the Total Environment* 703, 134760. <https://doi.org/10.1016/j.scitotenv.2019.134760>
- Ren, D., Li, L., Schwabacher, A. W., Young, J. W., Beitz, D. C., 1996. Mechanism of cholesterol reduction to coprostanol by *Eubacterium coprostanoligenes* ATCC 51222. *Steroids* 61, 33-40. [https://doi.org/10.1016/0039-128X\(95\)00173-N](https://doi.org/10.1016/0039-128X(95)00173-N)
- Saeed, T., Al-Shimmari, F., Al-Mutairi, A., Abdullah, H., 2015. Spatial assessment of the sewage contamination of Kuwait's marine areas. *Mar. Pollut. Bull.* 94, 307-317. <https://doi.org/10.1016/j.marpolbul.2015.01.030>
- Salati, S., Moore, F., 2010. Assessment of heavy metal concentration in the Khoshk River water and sediment, Shiraz, Southwest Iran. *Environmental Monitoring and Assessment* 164, 677-689. <https://doi.org/10.1007/s10661-009-0920-y>
- Sangaré, L.O., Diallo, S.B.O., Sanogo, D., Zheng, T., 2023. Assessment of potential health risks from heavy metal pollution of surface water for drinking in a multi-industry area in Mali using a multi-indices approach. *Environ Monit Assess* 195, 700. <https://doi.org/10.1007/s10661-023-11258-x>
- Sarkar, A. M., Rahman, A. K. M. L., Samad, A., Bhowmick, A. C., Islam, J. B., 2019. Surface and Ground Water Pollution in Bangladesh: A Review. *Asian Review of Environmental and Earth Sciences*, 6, 47–69. <https://doi.org/10.20448/journal.506.2019.61.47.69>
- Sarker, K.K., Bristy, M.S., Alam, N., Baki, M.A., Shojib, F.H., Quraishi, S.B., Khan, M.F., 2020. Ecological risk and source apportionment of heavy metals in surface water and sediments on Saint Martin's Island in the Bay of Bengal. *Environmental Science and Pollution Research* 27, 31827-31840. <https://doi.org/10.1007/s11356-020-09384-x>
- Sharma, G., Lata, R., Thakur, N., Bajala, V., Kuniyal, J.C., Kumar, K., 2021. Application of multivariate statistical analysis and water quality index for quality characterization of Parbati River, Northwestern Himalaya, India. *Discov. Water* 1, 5. <https://doi.org/10.1007/s43832-021-00005-3>
- Shirani, M., Afzali, K.N., Jahan, S., Strezov, V., Sardo, M.S. 2020. Pollution and contamination assessment of heavy metals in the sediments of Jazmurian Playa in Southeast Iran. *Scientific*

- Reports 10, 4775. <https://doi.org/10.1038/s41598-020-61838-x>
- Siddique, M.A.B., Alam, M.K., Islam, S., Diganta, M.T.M., Akbor, M.A., Bithi, U.H., Chowdhury, A.I., Ullah, A.K.M.A., 2020. Apportionment of some chemical elements in soils around the coal mining area in northern Bangladesh and associated health risk assessment. *Environmental Nanotechnology, Monitoring & Management* 14, 100366. <https://doi.org/10.1016/j.enmm.2020.100366>
- Singh, H., Pandey, R., Singh, S.K., Shukla, D.N., 2017. Assessment of heavy metal contamination in the sediment of the River Ghaghara, a major tributary of the River Ganga in Northern India. *Applied Water Science* 7, 4133-4149. <https://link.springer.com/article/10.1007/s13201-017-0572-y>
- Smedley, P.L., Kinniburgh, D.G., 2002. A review of the source, behaviour and distribution of arsenic in natural waters. *Appl. Geochem.* 17, 517–568. [https://doi.org/10.1016/S0883-2927\(02\)00018-5](https://doi.org/10.1016/S0883-2927(02)00018-5)
- Son, C.T., Giang, N.T.H., Thao, T.P., Nui, N.H., Lam, N.T., Cong, V.H., 2020. Assessment of Cau River water quality assessment using a combination of water quality and pollution indices. *Journal of Water Supply: Research and Technology-Aqua* 69, 160-172. <https://doi.org/10.2166/aqua.2020.122>
- Sorlini, S., Palazzini, D., Sieliechi, J.M., Ngassoum, M.B., 2013. Assessment of Physical-Chemical Drinking Water Quality in the Logone Valley (Chad-Cameroon). *Sustainability* 5, 3060–3076. <https://doi.org/10.3390/su5073060>
- Sultana, M.S., Islam, M.S., Saha, R., Mansur, M.A. 2009. Impact of the Effluents of Textile Dyeing Industries on the Surface Water Quality inside D.N.D Embankment, Narayanganj, Bangladesh *Journal of Scientific and Industrial Research* 44, 65-80. <https://doi.org/10.3329/bjsir.v44i1.2715>
- Sultana, N., Muktedir, M.A.H., Chowdhury, H., Baten, M.A., 2016. Assessment of the Quality of Industrial Wastewater in Three Metropolitan Cities in Bangladesh. *J. Environ. Sci. & Natural Resources*, 9, 21-25. <http://dx.doi.org/10.3329/jesnr.v9i2.32145>
- Tabrez, S., Zughaibi, T.A., Javed, M., 2022. Water quality index, Labeo rohita, and Eichhornia crassipes: Suitable bio-indicators of river water pollution. *Saudi. J. Biol. Sci.* 29, 75–82. <https://doi.org/10.1016/j.sjbs.2021.10.052>
- Tang, X., Cao, A., Zhang, Y., Chen, X., Hao, B., Xu, J., Fang, W., Yan, D., Li, Y., Wang, Q., 2022. Soil properties affect vapor-phase adsorption to regulate dimethyl disulfide diffusion in soil. *Sci. Total Environ.* 825, 154012. <https://doi.org/10.1016/j.scitotenv.2022.154012>.
- Tang, Z., Zhang, W., Chen, Y., 2009. Adsorption and desorption characteristics of monosulfuron in Chinese soils. *J. Hazard. Mater.* 166, 1351-1356. <https://doi.org/10.1016/j.jhazmat.2008.12.052>.

- Tolosa, I., Mesa, M., Alonso-Hernandez, C. M., 2014. Steroid markers to assess sewage and other sources of organic contaminants in surface sediments of Cienfuegos Bay, Cuba. *Mar. Pollut. Bull.* 86, 84-90. <https://doi.org/10.1016/j.marpolbul.2014.07.039>.
- Tylmann, W., Łysek, K., Kinder, M., Pempkowiak, J., 2011. Regional pattern of heavy metal content in lake sediments in northeastern Poland. *Water, Air, & Soil Pollution* 216, 217-228. <https://doi.org/10.1007/s11270-010-0529-3>
- U.S. Department of Health and Human Services, 2012. Public Health Service, Agency for Toxic Substances and Disease Registry. Toxicological Profile for Manganese. Available online: <https://www.atsdr.cdc.gov/toxprofiles/tp151.pdf> (accessed on 18 July 2021).
- Uddin, M.J., Jeong, Y., 2021. Urban river pollution in Bangladesh during last 40 years: potential public health and ecological risk, present policy, and future prospects toward smart water management. *Heliyon* 7, e06107. <https://doi.org/10.1016/j.heliyon.2021.e06107>
- United Nations, 2023. <https://www.un.org/sustainabledevelopment/water-and-sanitation/>. (accessed 25 may, 2023)
- USEPA, 2009. National Primary Drinking Water Regulation Table, EPA 816-F-09- 004. The United States Environmental Protection Agency. https://www.epa.gov/sites/default/files/2016-06/documents/npwdr_complete_table.pdf (accessed on 4 January 2022)
- Vane, C. H., Kim, A. W., McGowan, S., Leng, M. J., Heaton, T.H.E., Kendrick, C. P., Coombs, P., Yang, H., Swann, G.E.A. 2010. Sedimentary records of sewage pollution using faecal markers in contrasting peri-urban shallow lakes. *Science of the Total Environment* 409, 345–356. <http://dx.doi.org/10.1016/j.scitotenv.2010.09.033>.
- Vane, C.H., Kim, A.W., McGowan, S., Leng, M.J., Heaton, T.H.E., Kendrick, C.P., Coombs, P., Yang, H., Swan, G.E.A., 2010. Sedimentary records of sewage pollution using faecal markers in contrasting peri-urban shallow lakes. *Science of the Total Environment* 409, 345–356. <http://dx.doi.org/10.1016/j.scitotenv.2010.09.033>
- Varol, M., Karakaya, G., Alpaslan, K., 2022. Water quality assessment of the Karasu River (Turkey) using various indices, multivariate statistics and APCS-MLR model. *Chemosphere* 308, 136415. <https://doi.org/10.1016/j.chemosphere.2022.136415>
- Vimonses, V., Lei, S., Jin, B., Chow, C. W. K., Saint, C., 2009. Kinetic study and equilibrium isotherm analysis of Congo Red adsorption by clay materials. *Chem. Eng. J.* 148, 354-364. <https://doi.org/10.1016/j.cej.2008.09.009>.
- Wang, F., Dong, W., Zhao, Z., Wang, H., Li, W., Chen, G., Wang, F., Zhao, Y., Huang, J., Zhou, T., 2021. Heavy metal pollution in urban river sediment of different urban functional areas and its influence on microbial community structure. *Science of the Total Environment* 778, 146383. <https://doi.org/10.1016/j.scitotenv.2021.146383>

- Wang, B., Li, M., Zhang, H., Zhu, J., Chen, S., Ren, D., 2020a. Effect of straw-derived dissolved organic matter on the adsorption of sulfamethoxazole to purple paddy soils. *Ecotoxicol. Environ. Saf.* 203, 110990. <https://doi.org/10.1016/j.ecoenv.2020.110990>
- Wang, T., Yu, C., Chu, Q., Wang, F., Lan, T., Wang, J., 2020b. Adsorption behavior and mechanism of five pesticides on microplastics from agricultural polyethylene films. *Chemosphere* 244, 125491. <https://doi.org/10.1016/j.chemosphere.2019.125491>
- Wang, W., Rhodes, G., Zhang, W., Yu, X., Teppen, B. J., Li, H., 2022. Implication of cation-bridging interaction contribution to sorption of perfluoroalkyl carboxylic acids by soils. *Chemosphere* 290:133224. <https://doi.org/10.1016/j.chemosphere.2021.133224>
- Wei, C., Song, X., Wang, Q., Hu, Z., 2017. Sorption kinetics, isotherms and mechanisms of PFOS on soils with different physicochemical properties. *Ecotoxicol. Environ. Saf.* 142, 40-50. <http://dx.doi.org/10.1016/j.ecoenv.2017.03.040>
- Wei, M., Lv, D., Cao, L. H., Zhou, K., Jiang, K., 2021. Adsorption behaviours and transfer simulation of levofloxacin in silty clay, *Environ. Sci. Pollut. Res.* 28, 46291–46302. <https://doi.org/10.1007/s11356-021-13955-x>.
- Whaley-Martin, K.J., Mailloux, B.J., Geen, A.V., Bostick, B.C., Ahmed, K.M., Choudhury, I., Slater, G.F., 2017. Human and livestock waste as a reduced carbon source contributing to the release of arsenic to shallow Bangladesh groundwater. *Science of the Total Environment* 595, 63–71. <http://dx.doi.org/10.1016/j.scitotenv.2017.03.234>
- WHO, 1984. Guidelines for Drinking-water Quality. <https://apps.who.int/iris/bitstream/handle/10665/252072/9241541687eng.pdf?sequence=1&isAllowed=y> (accessed on 30 December 2021)
- WHO, 2011. Guidelines for Drinking-Water Quality, 4th ed. Available online: http://apps.who.int/iris/bitstream/handle/10665/44584/9789241548151_eng.pdf (accessed on 2 January 2022).
- Withanachchi, S.S., Ghambashidze, G., Kunchulia, I., Urushadze, T., Ploeger, A., 2018. Water Quality in Surface Water: A Preliminary Assessment of Heavy Metal Contamination of the Mashavera River, Georgia. *Int. J. Environ. Res. Public Health* 15, 621. <https://doi.org/10.3390/ijerph15040621>
- Wu, H., Yang, W., Yao, R., Zhao, Y., Zhao, Y., Zhao, Y., Zhang, Y., Yuan, Q., Lin, A., 2021. Evaluating surface water quality using water quality index in Beiyun River, China. *Environ. Sci. Pollut. Res.* 27, 35449–35458. <https://doi.org/10.1007/s11356-020-09682-4>
- Wu, W., Sheng, H., Gu, C., Song, Y., Willbold, S., Qiao, Y., Liu, G., Zhao, W., Wang, Y., Jiang, X., Wang, F., 2018. Extraneous dissolved organic matter enhanced adsorption of dibutyl phthalate in soils: Insights from kinetics and isotherms. *Sci. Total Environ.* 631–632, 1495-1503. <https://doi.org/10.1016/j.scitotenv.2018.02.251>

- Wu, Y., Si, Y., Zhou, D., Gao, J., 2015. Adsorption of diethyl phthalate ester to clay minerals. *Chemosphere* 119, 690-696. <https://doi.org/10.1016/j.chemosphere.2014.07.063>
- Xiang, L., Wang, X. D., Chen, X. H., Mo, C. H., Li, Y. W., Li, H., Cai, Q. Y., Zhou, D. M., Wong, M. H., Li, Q. X., 2019. Sorption Mechanism, Kinetics, and Isotherms of Di-n-butyl Phthalate to Different Soil Particle-Size Fractions. *J. Agric. Food Chem.* 67, 4734-4745. <https://doi.org/10.1021/acs.jafc.8b06357>
- Xiang, L., Xiao, T., Mo, C. H., Zhao, H. M., Li, Y. W., Li, H., Cai, Q. Y., Zhou, D. M., Wong, M. H., 2018. Sorption kinetics, isotherms, and mechanism of aniline aerofloat to agricultural soils with various physicochemical properties. *Ecotoxicol. Environ. Saf.* 154, 84-91. <https://doi.org/10.1016/j.ecoenv.2018.01.032>
- Xie, Q., Qian, L., Liu, S., Wang, Y., Zhang, Y., Wang, D., 2020. Assessment of long-term effects from cage culture practices on heavy metal accumulation in sediment and fish. *Ecotoxicology and Environmental Safety* 194, 110433. <https://doi.org/10.1016/j.ecoenv.2020.110433>
- Xiong, B., Li, R.; Johnson, D., Luo, Y., Xi, Y., Ren, D., Huang, Y., 2021. Spatial distribution, risk assessment, and source identification of heavy metals in water from the Xiangxi River, Three Gorges Reservoir Region, China. *Environ. Geochem. Health* 2021, 43, 915-930. <https://doi.org/10.1007/s10653-020-00614-2>
- Yan, C.A., Zhang, W., Zhang, Z., Liu, Y., Deng, C., Nie, N., 2015. Assessment of Water Quality and Identification of Polluted Risky Regions Based on Field Observations & GIS in the Honghe River Watershed, China. *PLoS ONE* 10, e0119130. <https://doi.org/10.1371/journal.pone.0119130>
- Yardim, M.F., Budinova, T., Ekinci, E., Petrov, N., Razvigorova, M., Minkov, V., 2003. Removal of mercury (II) from aqueous solution by activated carbon obtained from furfural. *Chemosphere* 52, 835-841. [https://doi.org/10.1016/S0045-6535\(03\)00267-4](https://doi.org/10.1016/S0045-6535(03)00267-4)
- Yeh, G., Lin, C., Nguyen, D.H., Hoang, H.G., Shern, J.C., Hsiao, P.J., 2021. A five-year investigation of water quality and heavy metal mass flux of an industrially affected river. *Environ. Sci. Pollut. Res.* 29, 12465-12472. <https://doi.org/10.1007/s11356-021-13149-5>
- Yikrazuul, 2009. File: Humic acid.svg. https://commons.wikimedia.org/wiki/File:Humic_acid.svg (accessed 10 March 2023)
- Yu, Z.Q., Amano, H., Nakagawa, K., Berndtsson, R., 2018. Hydrogeochemical evolution of groundwater in a quaternary sediment and cretaceous sandstone unconfined aquifer in Northwestern China. *Environmental Earth Sciences* 77, 629. <https://doi.org/10.1007/s12665-018-7816-5>
- Zereen, F., Islam, F., Habib, M.A., Begum, D.A., Zaman, M.S., 2011. Inorganic pollutants in the Padma River, Bangladesh. *Environ. Geol.* 39, 1059-1062. <https://doi.org/10.1007/s002549900098>

- Zhang, H., Li, H., Gao, D., Yu, H., 2022. Source identification of surface water pollution using multivariate statistics combined with physicochemical and socioeconomic parameters. *Science of the Total Environment* 806, 151274. <https://doi.org/10.1016/j.scitotenv.2021.151274>
- Zhang, Y. L., Lin, S. S., Dai, C. M., Shi, L., Zhou, X. F., 2014. Sorption–desorption and transport of trimethoprim and sulfonamide antibiotics in agricultural soil: effect of soil type, dissolved organic matter, and pH. *Environ. Sci. Pollut. Res.* 21, 5827–5835. <https://doi.org/10.1007/s11356-014-2493-8>
- Zhang, Z., Sun, K., Gao, B., Zhang, G., Liu, X., Zhao, Y., 2011. Adsorption of tetracycline on soil and sediment: Effects of pH and the presence of Cu (II). *J. Hazard. Mater.* 190, 856–862. <https://doi.org/10.1016/j.jhazmat.2011.04.017>
- Zhou, B., Zhang, Z., Wang, S., Wu, Y., Hu, S., Sun, R., 2020. Batch Adsorption and Column Leaching Studies of Aniline in Chinese Loess Under Different Hydrochemical Conditions. *Bull. Environ. Contam. Toxicol.* 104, 511–519. <https://doi.org/10.1007/s00128-020-02830-z>

Acknowledgements

All praises for Almighty Allah who guides me in the darkness and helps me in difficulties.

It is a great honor for me to express my sincere appreciation and deepest sense of gratitude to my respected supervisor **Professor Nakagawa Kei**, Department of Environmental Sciences, Nagasaki University, for his highly valued guidance, encouragement, scientific suggestions, and constant monitoring throughout the whole research work. He constantly inspired me and steered me in the right direction whenever I needed it.

I would like to acknowledge Professor Nishiyama Masaya, Professor Asakura Hiroshi, and Professor Yuji Takao who provided me with many valuable advice and comments. These helped me to improve the quality of this dissertation. Meanwhile, I would also like to thank Professor Ronny Berndtsson who helped me in many admirations of this research. I also feel great pleasure to convey profound veneration and deep appreciation to all respected teachers in my whole life during my prolonged period of study. I am thankful to the researchers of my research group, Zhiqiang Yu, Li Zhuolin, Shabbar Shah, for their co-operation, fruitful discussion, and support in many respects during my research work.

In addition, I would like to express gratitude to my parents, all teachers, and my beloved wife Faria Jeba, for providing great support and spiritual encouragement during my PhD program. I am also thankful to my brothers and sisters, Md. Ashraful Alam, Arin, Anan, Arnob, Bushra, Mahin, Vasa, and Barno for their wholehearted support and all sorts of encouragement throughout my life. Finally, my sincere gratitude is specially extended to all my relatives for their inspiration, prayer, and encouragement during my study life.

In fine, my heart full thanks to all my well-wishers in home and aboard.

Md. Shahidul Islam
Nagasaki, March 2024.